ANALYZING THE PREDICTIVE CAPACITY OF A PHYSICALLY-BASED DEBRIS FLOW MODEL: A CASE STUDY FOR DEBRIS FLOW IN THE POST-2008 WENCHUAN EARTHQUAKE AREA.

YI XIAO

August 2020

SUPERVISORS:

Prof. dr.C.J.van Westen
Dr.B.van den Bout BSc

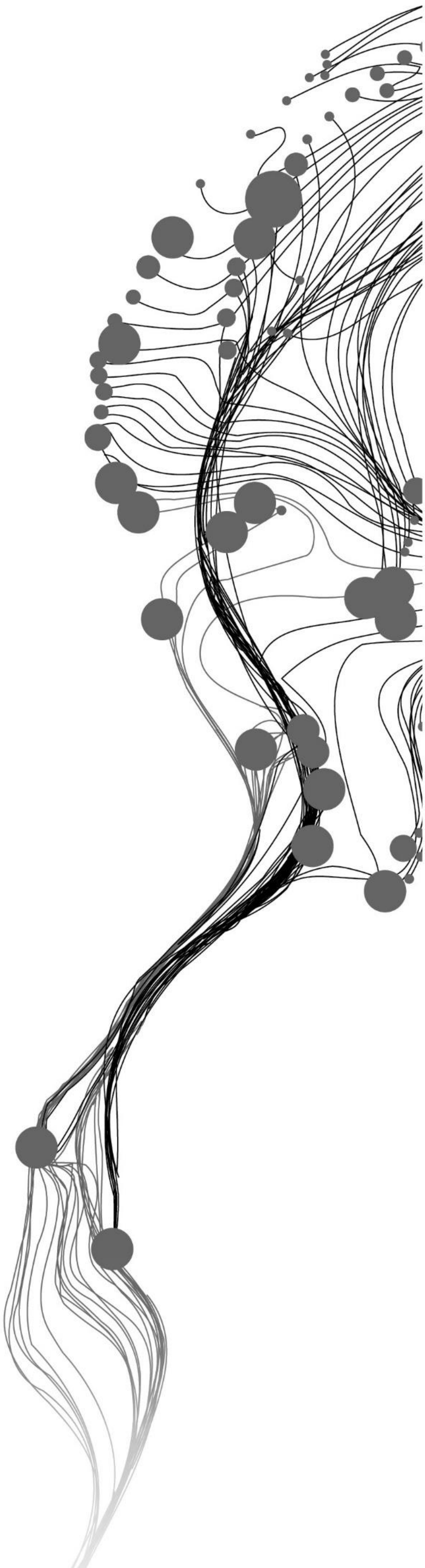

ANALYZING THE PREDICTIVE CAPACITY OF A PHYSICALLY-BASED DEBRIS FLOW MODEL: A CASE STUDY FOR DEBRIS FLOW IN THE POST-2008 WENCHUAN EARTHQUAKE AREA.

YI XIAO
Enschede, The Netherlands, August, 2020

Thesis submitted to the Faculty of Geo-Information Science and Earth Observation of the University of Twente in partial fulfilment of the requirements for the degree of Master of Science in Geo-information Science and Earth Observation.
Specialization: [4-D earth]

SUPERVISORS:
Prof. dr.C.J.van Westen
Dr.B.van den Bout BSc

THESIS ASSESSMENT BOARD:
Prof. Norman Kerle (Chair)
Dr. Rens van Beek (University of Utrecht) (External Examiner)
etc

ABSTRACT

Post-seismic debris flows are one of the most destructive post-earthquake secondary hazards. The threats posed by them can last decades. One of the most effective methods of risk mitigation is debris flow early warning. Physically-based models are widely used to reproduce historical debris flows, and they performed excellently. It is believed that the physically-based models are capable of high feasibility on debris flow prediction. And the transferability of such models in space and time has been widely assumed that specific calibration is required specific calibration in general. To investigate the predictive capacity of physically-based models, an integrated debris flow physically-based model (*OpenLISEM Hazard*) was applied to the earthquake-stricken area in Wenchuan, China. In order to evaluate the spatial transferability, the model was calibrated for three catchments separately based on debris flow inventory. After that, cross-validations of calibrated models were operated between the three watersheds. Results show that the model performed well in simulating occurrence and scale of debris flows, the prediction of the precise arrival time of debris flow is a bit problematic. Cohen's kappa of spatial transferability regarding accuracy volume and time are 0.02 and 0.38 separately. The volume accuracy is affected by the transferred calibrated parameters in space, while the prediction of the exact arrival time is impacted less. Besides, the sensitivity of parameters is not only model-specific but also catchment-specific. To evaluate the temporal transferability, four variables that change over time were considered, and the calibrated models were run with different rainfall events from 2010 to 2013. The temporal transferability was investigated from three aspects. Two aspects are to test whether the model underpredicts the occurrence of debris flows and whether the calibrated models can produce the exact arrival time of debris flows over time. For these purposes, the calibrated models were run with the rainfalls that triggered debris flows. The results state that the model does not have the problem of low prediction of occurrence. However, in two watersheds, the arrival times were given at similar model-running times every year. Another aspect is to investigate whether the model overpredicts the occurrence of debris flows. In this case, the calibrated models were run with the rainfalls that did not trigger debris flows. The results show that the model is a little overproduce processes of debris flows. This study, therefore, suggests that the calibrated parameters of *OpenLISEM Hazard* can be spatially and temporally transferred between similar catchments and within at least five years in the earthquake-stricken area to predict the scale and occurrence of debris flows. The predictive capacity of the exact time is required to be improved. The integrated physically-based model is worth being expected to be applied for early warning in the broad region over time.

Keywords: physically-based model; transferability; predictive capacity; post-seismic debris flow; earthquake-stricken area

ACKNOWLEDGEMENTS

I sincerely present my appreciation to my first supervisor professor Cees Van Westen. It is my good luck that I can have such a patient, kind, responsible supervisor, who never feels disappointed with me and support me with insightful comments and suggestions for the research processes and the structure of this thesis. His great help is not only about the thesis, but also about the attitude towards research and life. I appreciate that I can know such a teacher like you during the master period.

I would also like to thank dr. B.van den Bout BSc, who took time from his schedule to be my second supervisor. He helped me tremendously with understanding the model and always spent time to help address the technique problems. This study could not have been completed without him.

I am also grateful to prof.dr.V.G.Jetten, who gave me a lot of significant suggestions at the beginning of this study. And prof. xuanmei Fan from SKLGP, who gave me a chance to do the fieldwork in the Wenchuan area. The open-source data published by prof. Fan ensured the feasibility of this study. I would also thank dr. chenxiao Tang from IMHE, CAS, who provided me with important data and gave me suggestions about the selection of study sites.

Many special thanks to Drs. Nanette Kingma, Ir. Bart Krol, prof. Norman Kerle, Dr. Janneke Ettema, and other staff in the ESA department. Thanks for the great help when I first came to ITC, and thanks for the consolations you gave me when I met some difficulties. It is a pity that I could not say goodbye to you face to face. During the two years, I learned a lot in ITC, and I will not forget the pleasant time.

Lastly, I would like to thank my family, my friends, who support me during this research and my entire study. Especially my family, I am very grateful to them for accompanying and taking care of me during the horrible three-month lockdown period in Wuhan.

TABLE OF CONTENTS

LIST OF FIGURES

LIST OF TABLES

1. INTRODUCTION

1.1. Background

Major endogenic hazardous events such as earthquakes pose threats to life, health, economy, and environment, leading to direct and indirect loss (UNDRR, 2019). The impact of the disaster event can last for decades, particularly when it alters the conditions of the landscape and increases the likelihood of other hazardous processes (Cui et al., 2011; Xu et al., 2014; Fan et al.,2018). In a mountainous earthquake-stricken region, post-seismic debris flow is a common secondary hazard. A severe quake alters the susceptibility to debris flows due to its impact on the vegetation, soil properties, and availability of loose materials (Cui et al., 2011; Fan et al.,2018). Climate factors, such as extreme rainstorm and rapid snowmelt, are primary triggers for post-seismic debris flows occurrence (Wieczorek & Glade, 2005). It is commonly observed that the governing factors and critical rainfall thresholds change over time until a new equilibrium in the geo-environment is established (Shieh et al., 2009; Guo et al., 2016; Zhang & Zhang, 2017; Fan et al., 2018; Tang 2019). Thus, the extent and frequency of post-seismic debris flows are changing with time. Enhanced risk management efforts are required in earthquake-stricken areas by reducing the adverse impacts of these frequent post-seismic debris flows on humans and the economy. Early warning plays an important role in debris flow risk reduction. It provides timely and valid information to allow people to take action in advance to avoid or mitigate the risk and make effective decisions (ISDR, 2004). Early warning can be implemented through real-time monitoring, empirical-, and physically-based models (Capparelli & Versace, 2011).

Real-time monitoring systems can be applied to either observe or detect the occurrence of debris flows directly. For instance, human observation, video cameras, acoustic flow sensors, laser measurements, and destructive methods (chains, bars, etc. that are hit by moving debris) have been utilized for real-time monitoring. Although these methods can provide direct and unequivocal information on processes of debris flows, enough observation points, and appropriate locations for the equipment are required, which is not feasible in inaccessible areas. Besides, these methods are easily affected by visibility and unexpected events. More importantly, the lead time is relatively short. Immediate action should be taken, and the system needs to be linked with a good disaster preparedness campaign. Also, it is only effective if events happened with a certain frequency. If nothing has happened for years is not likely that these systems keep functioning properly. Although these methods are the most direct, they are costly and labor-intensive and required substantial maintenance, which limits the widespread application in the early warning (Lahusen, 2005).

The empirical method mostly relies on the comparison between accumulative real-time or predicted rainfall and rainfall threshold for debris flow occurrence, which are derived from statistical analysis of historical precipitation and debris flow occurrence records at a regional scale (Alfieri et al., 2012). Often the same threshold applies for a large area, and the simplified assumptions which may be different for specific watershed limit this accuracy of this method (Capparelli & Versace, 2011).

Critical rainfall thresholds vary substantially in space (Hong & Adler, 2007). Hence, this method is suited for national and regional levels as a simple alternative for in situ monitoring (Alfieri et al., 2012). Another relevant limitation is that this method ignores the distinctions between different rainfall patterns (Capparelli & Versace, 2011). These different rainfall patterns initiate debris flows through different triggering conditions. It is generally believed that an intense but short-duration storm, can cause erosion of loose material due to high surface runoff with insufficient infiltration (Iverson, 2000; Zhou et al., 2014). Conversely, low-intensity rainstorms lasting few days may build a perched groundwater level (Iverson, 2000; Zhou et al., 2014), which can result in soil saturation and a sharp rise in pore-water pressure resulting in slope failures (Iverson, 2000; Zhou et al., 2014). Thus, It may not be possible to ensure the accuracy of early warning based on statistics-based rainfall thresholds for every event (Zhang et al., 2014). Besides, It has been observed that rainfall thresholds after an earthquake first decrease sharply, then gradually increase to pre-earthquake level due to so-called “landscape healing” processes (Shieh et al., 2009; Guo et al., 2016; Zhang & Zhang, 2017). While the rainfall threshold method assumes that the conditions that have induced previous debris flows will work so in the future (Westen, 2004; Chae et al., 2017), these rainfall thresholds may be invalid for new post-seismic debris flow. This method is not flexible and accurate enough for post-seismic debris flow early warning over time.

Physically-based models aim at reproducing the physical debris flow processes and can be used for early warning, but they require detailed information on terrain data, soil properties (soil cohesion, internal friction angle, soil depth, hydrological parameters), land use, etc. (Guimarães et al., 2003). Based on the simulated hydrological and erosion processes, physically-based models can mimic the initiation of debris flows. Applying physically-based models for early warning is a relatively objective, flexible, low-cost, and efficient approach at either the watershed or the regional scale (Alfieri et al., 2012; Raia et al., 2014; Salvatici et al., 2018; Naidu et al., 2018). However, debris flows are extreme events that occur within a short time but are influenced by long-term processes, which are complicated and interacting. The complexities surrounding the dynamics of debris flows and the varying geological characteristics, hydraulic regime, and pluviometric factors are difficult to quantify (Franzi & Bianco, 2001), and the limited theoretical understanding of debris flow give difficulties in the simulation of debris flow. Besides, the insufficient understanding of the spatial variability of input parameters limits the application scale of the models (Tofani et al., 2017). They may behave differently for debris flow simulation in different catchments due to changes of initiation mechanisms and controlling factors. In terms of post-seismic debris flows, the critical triggering conditions change with the recovery of governing factors over time. Substantial volumes of loose deposits on the hillslopes were transported to the channels due to erosion and mass movements. Hence, channel bed erosion and entrainment increasingly dominated the initiation of debris flows rather than the failure of shallow landslides (Zhang & Zhang, 2017). Besides, grain coarsening plays a vital role in the reduction of post-seismic debris flows activity as it increased the hydraulic conductivity and resistance to bed erosion (Hu et al., 2017; Zhang & Zhang, 2017; Domènech et al., 2019). Revegetation increases root cohesion, thereby decreases erosion rate and runoff while increasing infiltration capacity (Hales, 2018). Hence, the application of physically-based models has uncertainties over time because some original cases have changed. Event- and site- specific calibration is required for debris flow simulation. However, physically-based models can be used to support quantitative projections of some controlling factors over time (Salciarini et al., 2019). Besides, the spatial variability of parameters is uncertain in similar catchments. Therefore, the model applicability for early warning should be verified by application in other similar watersheds and a more extended period of applications in the same watershed. And evaluating the factors that affect the spatial-temporal transferability would promote the physically based models to become more applicable for early warning.

OpenLISEM Hazard is an integrated physically-based model, including the hydrological phase, slope phase, and sediment phase (Bout et al., 2018a). This model has been applied for debris flow simulation in different regions, even in the earthquake-stricken area, and performed with good accuracy (Bout et al., 2018a; Bout et al., 2018b; Bout et al., n.d.).

This research aims to implement a quantitative analysis of:
(1) the transferability of the physically-based model *OpenLISEM Hazard* in similar watersheds
(2) the transferability of the physically-based model in one watershed over time.

1.2. Research objectives and research questions

1.2.1. General objective

To analyze the temporal and spatial transferability of the physically-based debris flow model *OpenLISEM Hazard* for post-earthquake debris flow Early Warning in the epicenter of the 2008 Wenchuan earthquake in Sichuan province, China.

1.2.2. Sub-objectives and research questions

Sub-objective 1: To analyze the similarity of debris flow watersheds in terms of controlling factors and debris flow characteristics.

Associated research questions:

- What are the criteria for watershed selection (e.g., a large number of co-seismic landslides happened, post-seismic debris flows frequently occurred within a number of years)?
- How to measure the degree of similarity between watersheds, e.g., a procedure?
- What are the debris flow characteristics that can be used for analysis transferability?

Sub-objective 2: To determine the spatial transferability of the physically-based model.

Associated research questions:

- With what accuracy can we predict debris flow occurrence times, debris flow volumes, and runout, with a model that is calibrated in another similar watershed?
- To which parameter is the model most sensitive and how do the parameter changes affect the early warning indicators of debris flow (warning time, volume, and runout).
- What is the best way to represent the transferability success (e.g., Cohens Kappa)?
- What are the limitations and uncertainties that affect spatial transferability?

Sub-objectives 3: To determine the temporal transferability of the physically-based model.

Associated research questions:

- With what accuracy can we predict debris flow occurrence times, with a model that is calibrated in another rainfall scenario in the same catchment?
- Which of the possible changes that occur over time in a watershed affected by previous debris flows?
- What are the limitations and uncertainties that affect temporal transferability?

1.3. The organization of the thesis and workflow

This thesis consists of six chapters:

This first chapter describes the research background, research objectives, and research questions. The second chapter reviews the methods used for debris flow detection and application of rainfall thresholds and physically-based models on debris flow analysis. Chapter three introduces the study area and the selected watersheds with information on the climate, geology, lithology, mass movement hazard history, and human engineering activities. Chapter four introduces *OpenLISEM Hazard* in detail and explains the input data for model running and the model parameters set up of the three catchments. It also contains the methods used for parameter sensitivity analysis and calibration. This fifth chapter assesses the results of parameter sensitivity, calibration, spatial transferability, and temporal transferability. The last chapter presents the main limitations of this study, as well as significant findings and recommendations in this study.

2. METHODS USED FOR DEBRIS FLOW EARLY WARNING, A LITERATURE REVIEW

This chapter focus on the methods used for debris flow early warning. First, various monitoring methods, such as visual observation, camera, and multiple sensors, will be listed. After that, methods used for early warning such as rainfall threshold, physically-based modeling will be introduced.

2.1. Methods for the detection of debris flow

It is essential to monitor debris flows for event warnings and the validation of the modeling (Itakura, Inaba, & Sawada, 2005). Many methods have been applied for the detection of debris flows. Direct visual observation and video cameras are the most straightforward methods to monitor debris flow torrents. The visual observation method requires that observers continuously observe the collapse condition on slopes and the surface runoff in the channels when intense-prolonged rainfall occurs in the upstream area (Zhou et al., 2004). The warning highly relies on the observer's judgment and the length of the period needed for observation. Video cameras act as fixed eyes used for recording debris flow and estimating the flow velocity later. They are limited by the low visibility during some rainfall, fog, and night conditions, they only observe from a fixed position, and they only can deliver a warning after the movement of material is detected either visually or automatically through change detection tools (Lahusen, 2005). Pendulums and photocells are also simple debris flow detectors (Massimo Arattano & Marchi, 2008). Except for the above, more monitoring methods and devices have been developed: for example, laser scanning monitors debris flows by surface change detection (Schürch et al., 2011). Ground vibration sensors, such as seismometer, or acoustic flow sensors can be used for detection and discharge estimation (e.g., Zhang, 1993; Arattano, 1999; Itakura, Fujii, & Sawada, 2000). The combination of infrasonic and seismic sensors can be used for event warning (Schimmel & Hübl, 2015). Ultrasonic range finders sense the changes of flow stage to detect debris flow (Arattano & Marchi, 2008). Radar similarly estimates the possibility of debris flow occurrence through monitoring the change of underground water content (Jin & Xu, 2011). The use of wire sensors, pressure sensors, and imagery-based methods allow short response time for evacuation after the debris flow observation (Cho et al., 2008). Some of these devices are contact detectors that need restoration after activation. Besides, the risk of false alarms exists because of bad weather, e.g., heavy rainfall, fog, snow, darkness, and accidental circumstances, the passage of trains and birds, falling trees, background noise and many other cases (LaHusen, 2005; Massimo Arattano & Marchi, 2008). Based on a review of Itakura et al. (2005), Table 2-1 summarizes the devices and methods employed for debris flow detection, which are distinguished by their function and performance. The explanation of the symbols and proxies in the table are as follows: ○: "useful", has been applied to the field monitoring; ◊: "possible", signifies that is only useful in the laboratory only so far; 一: "to be investigated"; ×: "impossible"; C means the devices need to contact the flow while NC means non-contact; limitation1 means the methods or tools are useless in bad weathers; limitation2 means the devices can be affected by various accidental circumstances.

These are direct methods for debris flow monitoring without processes of data collection and complex evaluation. They are the first selections in the areas with scarcity data and urgent hazard-prone areas. However, some of the methods are costly as they require regular maintenances and reinstallation after the debris flows. Some of them suffer from many false positives due to the impacts of visibility and external interferences. And the warning is given after the sediments already moved, so the reaction time to take action that depends on the location of these devices is short, or there is no time to respond in advance.

Table 2-1. Monitoring devices and methods function, performance, and operation

Devices and methods	Function		Performance			Operation
	observation	early warning	C or NC	Limitation 1	Limitation 2	
Man observation	○	○	/	Yes	Yes	Human visual observation
Video camera	○	○	C & NC	Yes	Yes	Change detection algorithm, Vision detection, Recognition of debris flow
Pendulums	×	◊	C	No	Yes	Detection from the tilting of the pendulum
Photocell (infrared photobeams etc.)	×	○	NC	No	Yes	Detector for debris-flow passage
Laser scanning	×	◊	NC	Yes	Yes	Surface change detection
Radar	–	◊	NC	No	Yes	Flow stage detection Measurement of fine movement
Ultrasonic sensor	×	○	NC	No	Yes	Measurement of the flow stage
Ground vibration (e.g., seismometers, moving-coil geophones, etc.)	×	◊	NC	No	Yes	Ground vibration detection through seismic waves
Infrasonic sensor	×	○	NC	Yes	Yes	Seismic signals detection
Wire sensor	×	○	C	No	Yes	Detection from wire breaking
Pressure sensor	×	◊	C	No	Yes	Measurement of forces

○: useful, ◊: possible, –: to be investigated, ×: impossible

C: contact, NC: non-contact

Limitation1: limited by bad weather, Limitation2: affected by accidental circumstances

2.2. Methods based on rainfall thresholds

Debris flows are highly correlated with the rainfall intensity, rainfall duration, and rainfall amount. Rainfall patterns affect the debris flow both in terms of their occurrence as well as their development (Zhou et al., 2014; Pan et al., 2018). Abundant observational data proved that the initial time of debris flow is closely related to the rainfall pattern, and both of intensive rainfall and prolonged antecedent rainfall can initiate debris flows (Rianna, Pagano, & Urciuoli, 2014). Roughly the rainfall patterns can be classified into two types, the flat pattern and the peak pattern (Pan et al., 2013). The former one is characterized by slight variations in rainfall intensity and no peak in the duration-hourly rainfall graph, and the latter one shows a prominent peak and peaks might appear more than once (Pan et al., 2013). Rainfall thresholds are minimum rainfall conditions at which debris flows are likely triggered (Guzzetti et al., 2008). The well-calibrated rainfall threshold supported by sufficient historical data is one of the most common implementations for debris flow early warning. However, in many hazard-prone watersheds, limited data on rainfall and debris flow occurrences can be obtained to extract reliable critical thresholds (Zhou et al., 2004; Pan et al., 2018). Rainfall thresholds also can be physically determined, for example, using process-based thresholds and conceptual thresholds (Segoni, Piciullo, & Gariano, 2018). Either for improving the accuracy or compensating the shortcomings of the database, multiple methods have been applied for threshold analysis, such as various statistical analysis methods, grey forecast, related models, and neural networks (Zhou et al., 2004). Roughly, rainfall thresholds can be classified into three categories: (1) intensity-duration (I-D) thresholds, (2) thresholds considering antecedent rainfall, (3) hydro-meteorological thresholds.

The rainfall intensity-duration (I-D) threshold curve is objectively extracted based on the rainfall data from multiple rainfall events using statistical approaches. In 1980, Caine firstly proposed a global rainfall intensity-duration equation based on an extensive database. This database is comprised of 73 rainfall events that had triggered debris flows in different climatic regions. And this relationship is best defined during the rainfall duration from 10 minutes to 10 days (Caine, 1980). After this landmark work, information on the intensity and duration conditions of successful triggering rainfalls was collected worldwide. All kinds of I-D thresholds were concluded in different scales (e.g., Guzzetti et al., 2007; Guo et al., 2016). Based on Caine's achievement, Guzzetti et al. (2008) normalized the rainfall dataset to deal with the impacts on slope failures from the variations of rainfall characteristics in different climatic zones. After the update, the threshold from the new relationship is lower obviously, and whose applicable duration was extended to 35 days (Guzzetti et al., 2008).

$$I = 14.82 * D^{-0.39} \; (0.167 < D < 500) \qquad 2.1$$

In some areas, debris flows are initiated not only by intense rainfall but also by long-duration and low-intensity rain. In this case, antecedent rainfall plays a vital role in debris flow occurrence (Guo, Cui, & Li, 2013). Effective antecedent rainfall mainly triggers debris flows in the place where the hydraulic conductivity of soil is low (Pan et al., 2018). The I-D relationship neglects the influences of antecedent rainfall. It is hard to quantify the impacts of antecedent rainfall on debris flow as it mainly works on the soil heterogeneity (Guo et al., 2013). For critical thresholds estimation considering antecedent rainfall, what usually is done is to calculate the daily antecedent rainfall by a weighted sum equation (Glade, Crozier, & Smith, 2000). The rainfall factors affecting debris flows can be grouped with three elements, (1) indirect antecedent precipitation, which rise water content in the soil; (2) triggering rainfall, it is the factor that triggered the debris flow; (3) direct antecedent rainfall, which reduces the critical conditions through saturating soil (Guo et al., 2013). The basic idea of threshold analysis considering antecedent rainfall is to integrate the three factors with I-D relationships relying on historical debris flow events and rainfall events (e.g., Glade et al., 2000; Guo et al., 2013; Mathew et al., 2014). Based on the relationship, the critical threshold is built statistically for early warning.

The reliability of empirically derived rainfall thresholds is limited by the insufficient understanding of physical process. The hydro-meteorological threshold that is based on soil water calculations is better than the empirical rainfall thresholds. The estimation of the I-D threshold links with soil hydraulic properties, different conditions of initial moisture, and catchment water balance (Bogaard & Greco, 2018). However, this kind of rainfall thresholds functions counterintuitively in the long timescale of rainfall. The I-D curves tend to be flat, which indicates the sensitivity of initiation thresholds to rainfall intensity becomes lower in the cases of long-duration rainfall (Bogaard & Greco, 2018).

Rainfall thresholds are or have been implemented for warning systems globally (e.g., Keeefr et al., 1987; Aleotti, 2004; Godt, Baum, & Chleborad, 2006). The advantages of the methods of rainfall threshold are that they can be simply defined by rainfall, soil moisture, and hydrological conditions, and it can be applied to various scales according to the geographic extent of the dataset (Guzzetti et al., 2008). The rainfall thresholds curves can be established correctly with a 0- to 3- hour lead time (Hsu et al., 2018). Nevertheless, the application of some rainfall thresholds is limited by false alarms and data requirements. The rainfall thresholds need to work with other measures to ensure the occurrence of debris flow further. Hence, the conclusions obtained from the comparison only indicate the possibility of occurrence of debris flows rather than lead to an evacuation. Segoni, Piciullo, and Gariano (2018) recommended that a standardized procedure should be established, and rapid and periodic updating of critical thresholds should be carried out to assure the method is objective and repeatable if rainfall thresholds are employed for early warning widely.

2.3. Methods based on physically-based modeling

Classification of methods

Essentially, physically-based models follow two fundamental laws, conservation of mass and conservation of momentum. Physically-based models can be applied for simulation of hydrology, entrainment, and debris flow initiation. Some models are designed for a particular process of debris flow like final deposits simulation and runout distance simulation. The integrated type can simulate the multiple processes of debris flow contains hydrological process, slope failure, erosion process, and runout and must implement interactions between these processes. The r.avaflow and TopFlowDF are GIS-based tools for runout simulation (Mergili et al., 2017; Han et al., 2016). RAMMS is a model developed for runout distance simulation based on depth-averaged equations of motion (Christen et al., 2012). FLO-2D is a two-dimensional finite model for runout distance simulation (O'Brien, Julien, & Fullerton, 1993). Comparing with FLO-2D, Debris-2D is better for simulation of granular debris flows (Wu, Liu, & Chen, 2013). MassMov2D is also a 2-dimensional model to simulate debris flow deposits based on depth-averaged motion equations in complex terrain (Beguería et al., 2009). Similarly, FLATModel is an adaptable two-dimensional approximate shallow-water code using the finite volume method (FVM) for simulation. This model can be applied for basal entrainment simulation, final volume estimation, movement process for aims to analyze flow dynamics, and accumulation mechanisms (Medina, Hürlimann, & Bateman, 2008). EDDA1.0 and EDDA2.0 are two versions of the software. Differently, EDDA1.0 is a quasi-three-dimensional integrated model that includes simulation of erosion, deposition like volume, runout distance, and inundate area, as well as changes of material characteristics (Chen & Zhang, 2015). What is different from EDDA1.0 is that the second version considers two initiation mechanisms dynamically (Shen et al., 2018). OpenLISEM Hazard is an integrated multi-hazard simulation physically-based model (Bout et al., 2018a). Three main components are contained in this model, hydrological cycle, slope stability, and failure, and sediment processes, this model has been run different countries and regions and obtained excellent results.

Table 2-2. Methods used for debris flow analysis

Type	Examples of available regional models	Application
2-D Dynamic model	r.avaflow (Mergili et al, 2017), RAMMS (Christen et al, 2010), Flo-2D (O'Brien et al., 1993), Debris-2D (Wu et al., 2013), TopFlowDF (Han et al, 2016)	Runout
	FLATModel (Medina et al., 2008), MassMov2D (Beguería et al, 2009),	Final deposit
	OpenLISEM Hazard (Bout et al., 2018a)	Integrated
quasi 3-D	EDDA 1.0 (Chen & Zhang, 2015)	Integrated

Parameterization

Parameterization is vital to represent the soil properties and underground situation in the use of physically-based models. The parameters for debris flow models can be grouped into main categories as follows, (1) topographic factors (such as slope and catchment area, local drain direction, roughness, outlet point), (2) soil properties (such as friction angle, soil cohesion, root cohesion), (3) hydrological parameters (water content, porosity, hydraulic conductivity), (3) surface factors (vegetation cover, surface roughness), soil depth and rainfall (Guimarães et al., 2003; Arnone et al., 2016). The topographic parameters are generally required in physically-based models, and their reliability relies on the quality and resolution of elevation data (Guimarães et al., 2003).

Soil properties are important for the slope stability module in debris flow models, and they either can be applied following exact spatial distribution when data is available or as averaged values obtained in field surveys generalize across the entire study area (Guimarães et al., 2003). The hydrological processes drive the debris flow processes through rainfall duration, rainfall intensity, and antecedent rainfall, in interaction with the hydrological soil properties (infiltration, saturated hydraulic conductivity) and land cover (evapotranspiration, surface roughness) (Guimarães et al., 2003). Soil thickness has a large impact on the accuracy of modeling results, and the spatial information of soil thickness is often limited and hard to measure (Melchiorre & Frattini, 2012; Bout et al., 2018a). Thus, spatial soil thickness is often estimated through statistical correlation (Kuriakose, Beek, & Westen, 2009) or using a physical model (Saulnier, Beven, & Obled, 1997).

Table 2-3. General parameters for physically-based model running

	Parameters	Method to obtain
Topography related	Gradient	Elevation data
	Drain direction	
	Outlet	
	Output locations	
Rainfall related	Hourly rainfall	Rain gauges, rainfall products
Surface related	Surface roughness	Field measurement, Literature value
	Manning'S N	Field measurement, Literature value
	Landuse	Satellite imagery
	Vegetation cover	NDVI
	Vegetation height	Field measurement, literature value
	LAI	NDVI
Erosion related	Soil cohesion	Field measurement
	Root cohesion	Field measurement, derived from vegetation cover
	Median grain diameter	Field measurement
Slope stability related	Soil density	Field measurement
	Internal friction angle	Field measurement, experiment
	Grain size for debris flow material	Field measurement
Infiltration related	Saturated conductivity	Field measurement Derived from open-source soil maps in hydrological software
	Wetting point	
	Porosity	
	Initial moisture content	
	Soil depth	Elevation data National database of soil depth

Note: Green: general required; blue: hydrology process required; tan: sediment process required

Parameter sensitivity

Parameter sensitivity analysis is a necessary process to determine the rate of changes in model outputs that affected by the changes in model inputs (Huang et al., 2020). The purpose of parameter sensitivity analysis is to indicate the key parameters and parameter precisions to speed the calibration process (Ma & Li, 2017). Evaluating parameter sensitivity is useful for systematic parameter optimization strategies. The sensitivity is variable for the different model parameters in different models. For example, some model is most sensitive to the thickness of soil layer (e.g., Huang et al., 2020), some model is very sensitive to friction angle and soil cohesion (e.g., Guimarães et al., 2003; Kuriakose et al., 2009). Besides, some parameters may affect the modeled results mutually. For example, saturated hydraulic conductivity, Mannings'N, and root cohesion increase with the rise of vegetation cover (Sankar et al., 2006; Shen et al., 2017). So, when the values of vegetation cover change during parameter sensitivity analysis, the values of the mentioned factors should change as well. There are a lot of methods can be used for parameter sensitivity analysis, such as one-parameter-at-a-time method is adopted for parameter sensitivity analysis based on discrete values (Zieher et al., 2017), State-Dependent parameter method (SDP) (Young, McCabe, & Chotai, 2002), and perturbation analysis method (Chen, Liang, & Chen, 2011).

Model calibration

Calibration is a common task in modeling to fine-tune the parameters systematically to optimize the modeled results. The calibration is performed for specific purposes, which is supported by certain information that is collected and measured in the field, such as time of debris flow occurrence, the discharge, variation in groundwater level, soil water fluctuations, volume, etc. In case of debris flows. The collection of certain observed conditions is a difficult issue. Discharge data is unavailable for debris flow (Franzi & Bianco, 2001). The time of occurrence is often not accurate without video evidence. And there were also no piezometers or tensiometers that would provide soil water data. The calibration of volume and runout was based on the final sediments at the outlet area (Bout et al., n.d.). The actual volume can be estimated to make a calibration, while the runout distance and the amount of material deposited in the channels only can be calibrated visually with imageries. It is because there are no measurements done for these two aspects, and the human activity would eliminate the actual runout distance immediately after the hazards. By contrast, the calibration of occurrence time is based on the eyewitness. Normally, multiple runs are required for this work, and some tools can be used for automatic calibration, such as PEST calibration. Besides, the calibration process based on actual events would likely result in equifinality that the similar modeled outputs can be obtained from multiple compositions of parameters (He et al., 2017). In this case, it is difficult to analyze which combinations most fit with the reality, and not to take combinations of parameters where the values out of the normally measured range. And the different combination of parameters would likely result in different outputs either in other watershed or other events, equifinality may affect the accuracy of validation of the calibrated model.

Model validation

The purpose of validation is to test the reliability of models, by comparing the model prediction with an actual occurring event, preferably different than the one used in the model calibration (Schilirò et al., 2016). The validation can be performed with a back analysis of happened events either in one catchment or in different watersheds. In the case of debris flows, giving correct warning of occurrence is important and even more so to give the exact debris flows arrival time in the outlet of the watershed. Underprediction might result in casualties because of untimely emergency actions. Overprediction may result in less reliability and ultimately that the threatened communities do not take the warning seriously. The purpose of validation with actual events is to test whether models are good enough to give warnings, and how accurate the tested models can predict the time of arrival of the debris flow. By contrast, the validation with rainfall events that did not result in debris flows is to check whether the models do not overpredict. These strategies can be applied for the analysis of temporal applicability. Model validation in different catchments can be implemented with rainfall time series that either resulted in debris flows or not. It is important to not only test the spatial applicability of models but also examine whether the spatial applicability interacts with temporal applicability.

Figure 2-1 presents a conceptual diagram of the methods used for validation. Besides, it is critical to consider the reliability of data on the observed events and the limitations of models when validation is based on the comparison between model predictions and independent response events (Mroczkowski, Raper, & Kuczera, 1997).

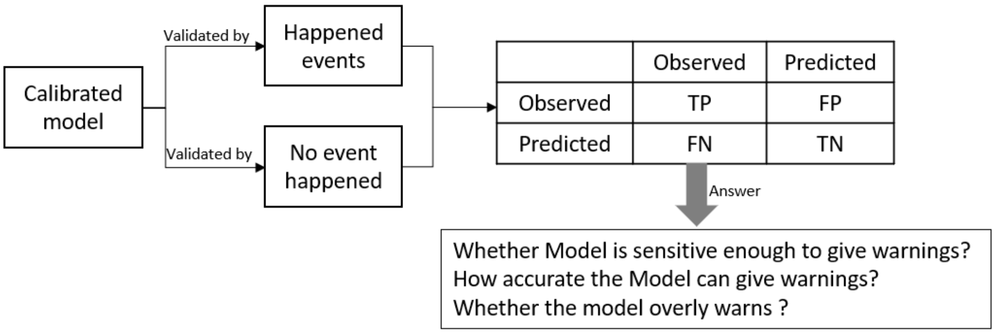

Figure 2-1.Conceptual diagram of validation methods

Model transferability

Model transferability is the capacity of a model that is calibrated for one time period and study area to generate acceptable results at other times and study areas (MacDougall & Flowers, 2011). The methods used for transferability analysis are flexible according to available data and purposes. For example, Shrestha et al. (2007) calibrated and validated a hydrological model in six nearby catchments for spatial transferability analysis. They adopted two different scenarios, in which every dataset was derived from different years, for assessing temporal transferability. In the first scenario: one dataset was used for calibration, and another dataset used for validation, and a third dataset was used for evaluation considering changes in some factors. In the second scenario: the third dataset was used for calibration, the fourth one for validation, and the first dataset was used for elevation. NSE and HMLE were measures used for final analysis. Heckmcacnn and Becht (2009) investigated model spatial transferability by extensive cross-validation in different study areas. MacDougall and Flowers (2011) examined the parameter transferability in space, in time, and both in space and time combined. In their research, the parameter values extracted for one study area or one time were employed for other studies and times. Parameters associated with one study area were transferred to others for the same year for joint-transferability analysis. In their study, MPE and RMSE were used for final transferability analysis. Benjamin et al. (2018) analyzed the spatial transferability of the model by applying the calibration to nineteen further events across varyingly complex terrain. Table 2-4 illustrates the useful measures for transferability analysis.

Table 2-4. Summary of measures

Measures	Explanation
Nash-Sutcliffe efficiency (NSE)	A normalized statistic that determines the relative magnitude of the residual variance compared to the measured data variance
Heteroscedastic maximum likelihood estimator (HMLE)	A method of estimating the parameters of a probability distribution by maximizing a likelihood function
Mean percentage error (MPE)	Average of percentage errors by which forecasts of a model differ from actual values of the quantity being forecast
Root mean square error (RMSE)	A statistic to illustrate how concentrated the results are around the line of best fit
Cohen's kappa	A statistic to measure the inter-rater reliability (also intra-rater reliability) for qualitative items

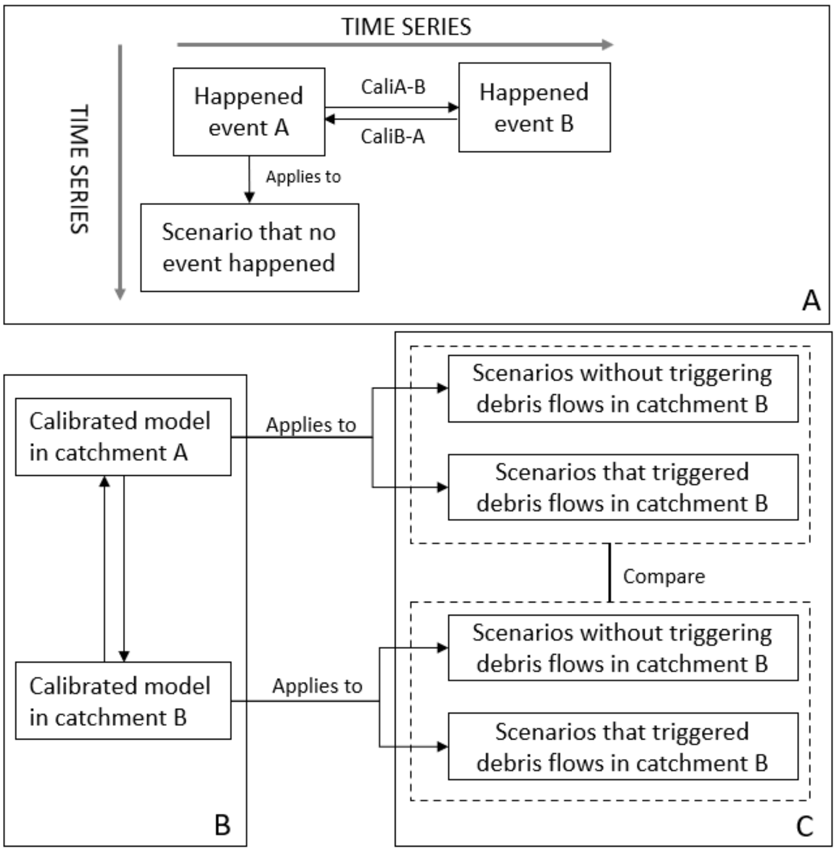

Figure 2-2. Methods for transferability analysis

A: temporal transferability analysis; B: spatial transferability analysis; C: to analyze whether spatial transferability integrates with temporal transferability

3. STUDY AREA

This chapter introduces the secondary hazards produced by the 2008 Wenchuan earthquake. Based on the hazard inventory in the Wenchuan area, more focus was given to the catchments around the earthquake epicenter to select several suitable watersheds for model running. After that, the information on geology, climate, and soil in the selected watersheds are introduced.

3.1. Wenchuan earthquake-affected area

Sichuan province, China, is an earthquake-prone area, where post-seismic debris flows are common second hazards after the 2008 earthquake in this region. The 8 Mw Wenchuan earthquake that happened in 2008 triggered a large amount of co-seismic landslides, estimated around 200000 over an area of 35,000 km^2 (Xu et al., 2014). Tang et al. (2016) and Fan et al. (2018) summarized the post-seismic landslide activity in watersheds near the epicenter by multi-temporal satellite image interpretation and field data (Table 3-1). A total of 2,408 debris flow events were recorded after the 2008 shock until 2017 (Huang & Fan, 2013; Fan et al., 2019). These frequent secondary mass movements resulted in large numbers of casualties, destroyed buildings, and roads almost, which occurred almost every year. The ten years following the earthquake witnessed various changes in the mountainous earthquake-stricken area. The rainfall thresholds for landslide and debris flows sharply dropped just after the earthquake then increased gradually during the ten following years (e.g., Zhou et al., 2014; Pan et al., 2018; Zhang & Zhang, 2017). According to the research done by Zhang and Zhang (2017), the debris flow materials in the same catchment became coarser over time. Besides, Tang et al. (2019) indicated that the loose material amount had reduced to the same level as before the earthquake, although a distinct increase existed during the few years after the earthquake. Moreover, vegetation on the whole regenerated in most of the areas during the ten years (Lu et al., 2012; Li et al., 2014).

Table 3-1. Landslide inventories near the epicenter of Wenchuan earthquake, 0-3 means level of activity, "/" means no information, "-"implies none (data of 2009 from (Tang et al., 2016); data of 2008,2011,2013,2015 form (Fan, Domènech, et al., 2018))

Year	Channel deposit	Co-seismic/Post-seismic		Level of activity				New landslides
		Active slides	Active debris flow	Dormant co-seismic deposits	Remobilized co-seismic deposits			
				0	1	2	3	
2008	98	8825	364	-	-	-	-	-
2009	/	/	/	4855	452	250	182	83
2011	109	3544	1273	4013	1166	1069	1801	781
2013	59	1041	439	7611	442	299	379	360
2015	72	108	105	8976	131	33	41	8

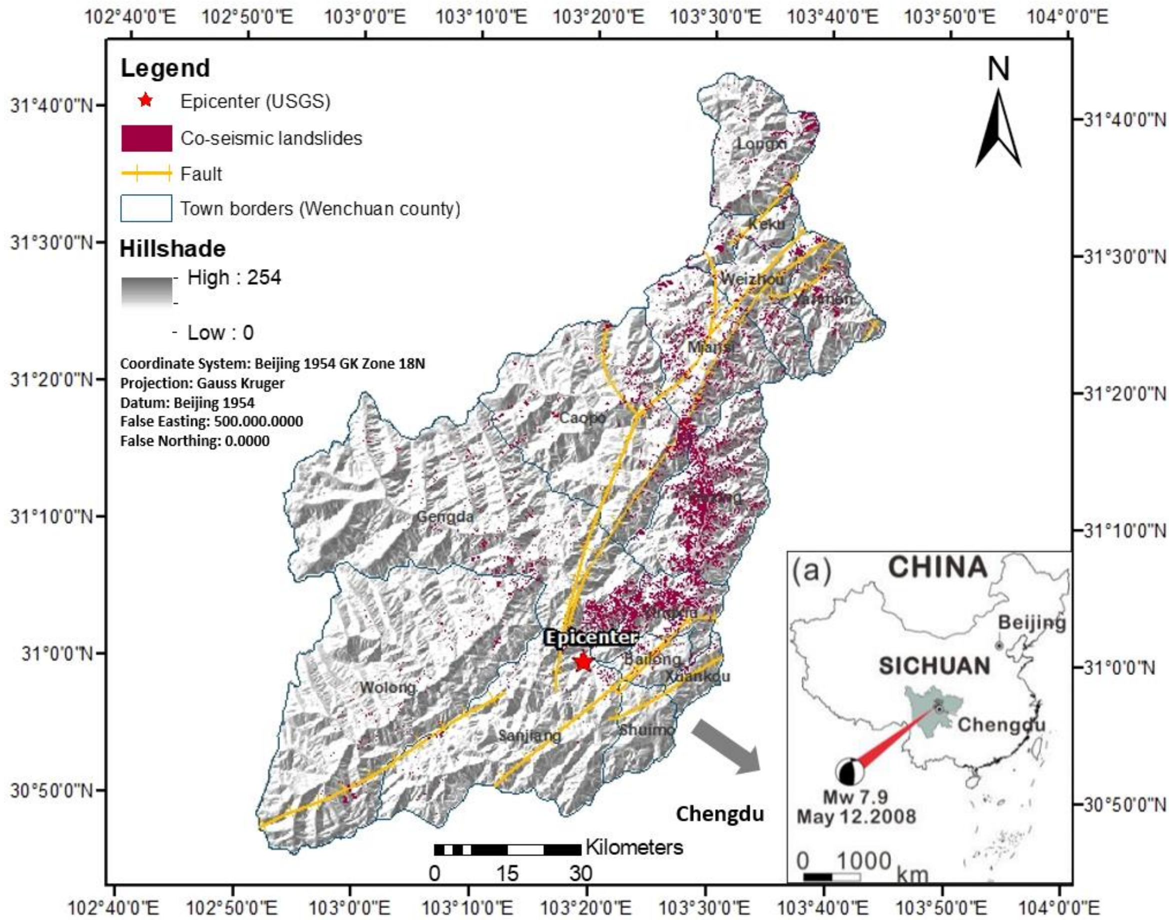

Figure 3-1. Location of Wenchuan county and co-seismic landslides

3.2. Selection of watersheds

The selection of potential watersheds for this study was based on a number of criteria. First, the watershed should be close to the epicenter of the earthquake, near Yingxiu town, and specifically close to the Hongchun catchment. The Hongchun catchment is one of the catchments that has been studied most frequently by various researchers, and also *OpenLISEM Hazard* was applied in this catchment with excellent results (Bout et al., n.d.). In this watershed, many debris flows happened within five years after the earthquake. The second condition is that these catchments should have been impacted severely by co-seismic landslides, which changed the geo-environment significantly. The third criteria was that these catchments should have witnessed massive debris flows after the earthquake, which should have been recorded. Running the model over a longer period can be more representative to illustrate the influence of the rebalancing of the geo-environment on the temporal transferability. Hence, if the watershed experienced debris flows recently, it could be considered a priority. That massive debris flows happened in the catchments is a basic condition to carry out temporal transferability analysis. Besides, the candidate catchment should be close to the Hongchun catchment so that their soil properties are relatively similar, which can partly eliminate errors in spatial transferability caused by the differences of soil properties. Besides, what is best is that the simulated debris flows in the candidate catchments were triggered by the same rainfall event. Otherwise, the performance of spatial transferability may be affected by rainfall properties. Naturally, data availability and sufficient related previous research are critical to ensure the feasibility of this research.

As a result, Lianhuaxin (sub-catchment of Niujuan gulley) and Bayi watersheds were selected because they fulfilled the criteria mentioned above. These catchments experienced rainfall-induced debris flows within the same period in 2010, 2011, and 2013. Model simulations of post-seismic debris flow have been done by others for events that happened in 2010 in these catchments, which provide a reliable foundation for model running and calibration in this research.

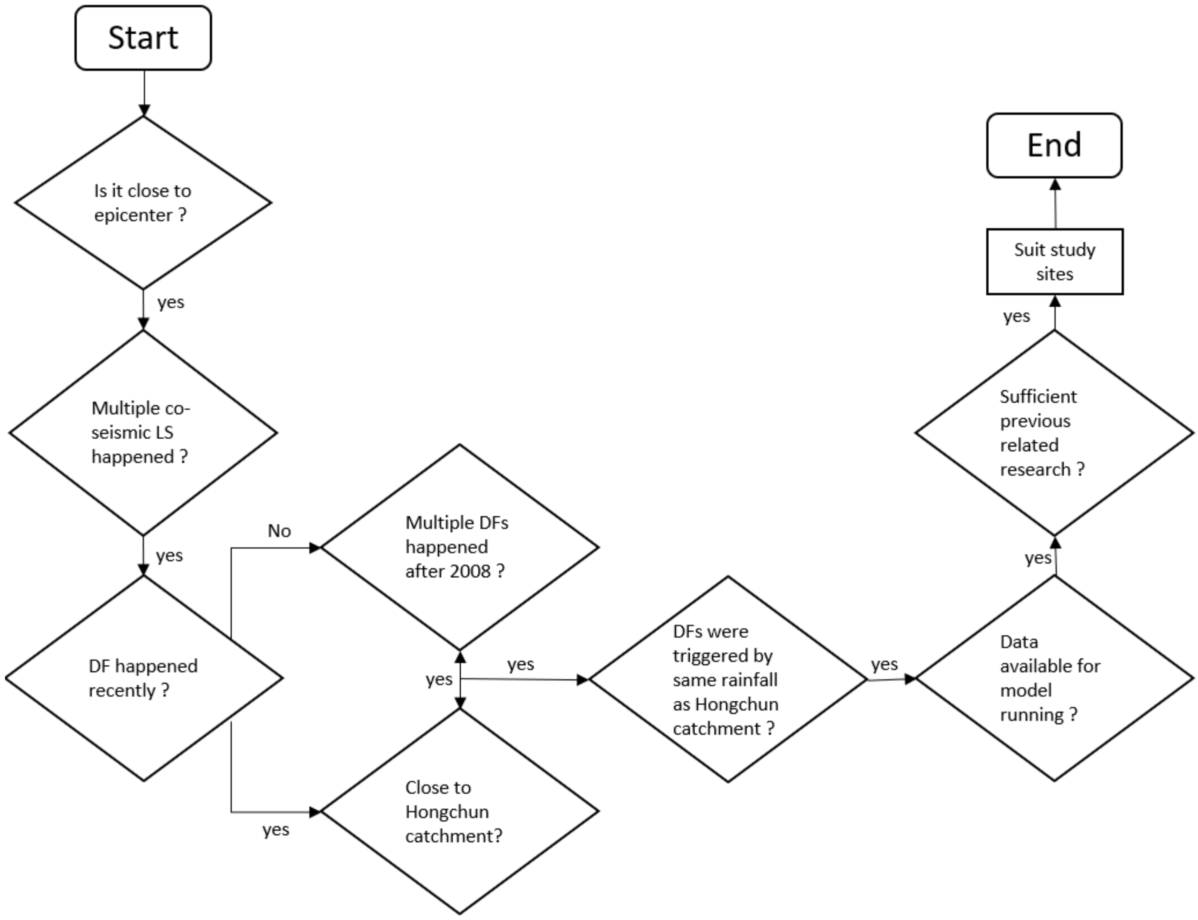

Figure 3-2. Flow chart of catchments selection

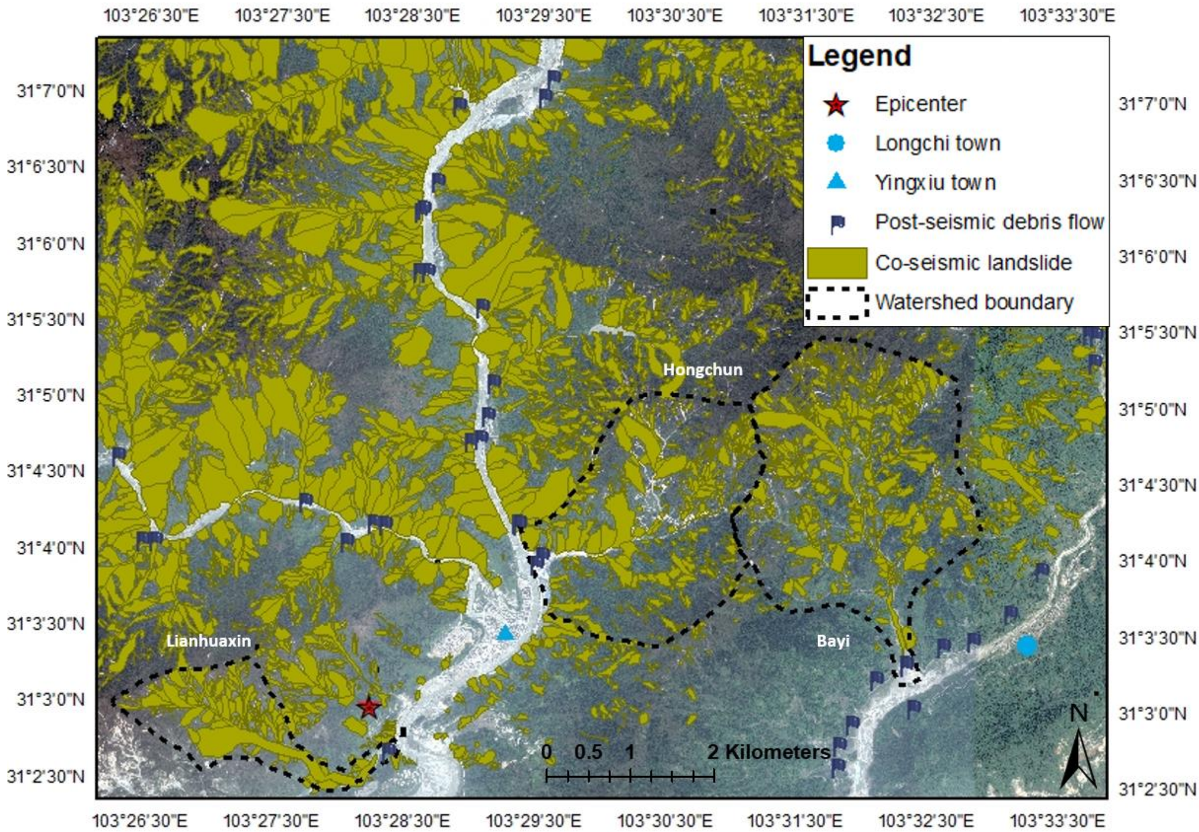

Figure 3-3. Location of the study sites and distribution of post-seismic debris flows

3.3. Study sites

Geology & Soils

The Hongchun gully is characterized by the steep slopes, sharp incision, and deep-cut V-shaped channels, ending in flatter alluvial fans downstream. The tributary gullies in these watersheds are distributed like branches. After the earthquake, the terrain of Hongchun gulley has changed significantly so that part of the slopes shifted from convex to concave. Consequently, channel accumulation and blockage became severer, and the source area was expanded (Xu et al., 2012). The regional geological structures of Niujuan catchment are complex as the Yingxiu-Beichuan fault passes through this gully. And the neotectonics movement is characterized by a sharp rise of the slopes of up to 10 meters caused by fault activity. A large co-seismic rock avalanche occurred in this watershed, which filled up the valley almost to the outlet point. Consequently, the width of the gully expanded from 35 ~ 40 meters before the earthquake to 80 ~ 120 meters after the quake. Oppositely, the width of the upstream part gradually narrowed to 6 ~15 meters, based on a field investigation report from a local engineering company. Bayi gully belongs to low to intermediate mountainous terrain, although the upper part is very steep. Given the effects of geological structures, the valleys were incised shallower in the Longchi area. The channels in the Bayi watershed have a V shape. Three river terraces are developed on both banks of the Longxi river, among which the first terrace is 7 meters higher than the riverbed. The second terrace has a relative height of 25 meters, and the third terrace has a height of around 70 m. Overall, the high, steep slopes and large gradient make it easier to trigger the loose materials to move and transport in the channels (Ming, 2014； Ma & Li, 2017).

The strong tectonic uplift of the mountain characterizes the Hongchun gully and Lianhuaxin gully. The main exposed strata in the gullies are the Sinan system (Z), Proterozoic system (Pt), and Quaternary alluvial deposits (Q^{3al+pl}). The lithology mainly consists of granitic rocks, with some pyroclastic rocks, limestone and sandstone. The surface soil is the loose quaterbary sediments (Tang et al., 2011). Owing to the impacts of the Wenchuan earthquake, the surface soil is loose with many joints and fissures. The Bayi gully is covered by silty clay, marls, sandstones, and mudstone. These rocks contain a large amount of clay material and more prone to debris flow.

The Hongchun gulley covers an area around 5.35 km^2, and has a length of 3.6 km. The highest source area is at 2168.4m, and the elevation of this gulley is from 880 to 2168 m. The average slope is around 35.8° (Xu et al., 2012). The terrain of Niujuan gully is undulating and ranges between 20° and 75° degrees, with an average of 27°. The length of Lianhuaxin gully is around 2.12 km, and the area is about 3.0 km^2. For Bayi catchment, the elevation ranges from 870 to 2503 m. The average slope is around 37.6°, and the length of this gully is 4.23 km, with a catchment area of 8.30 km^2 (Zhou et al., 2014).

Table 3-2. Characteristics of study catchments

Catchment	Area (km2)	Main length (km)	slope	Elevation (m)
Hongchun	5.35	3.6	36	880-2168
Lianhuaxin	3.0	2.12	27	859-2700
Bayi	8.3	4.23	37.6	870-2503

Climate

The study area belongs to the mid-subtropical monsoon climate zone in the Sichuan Basin. Precipitation properties are inhomogeneous because of the influences of topography. The average annual rainfall in Yingxiu town is 1253 mm. The maximum yearly rainfall that occurred in 1964 was 1688 mm while the minimum precipitation occurred in 1974 was 863 mm, see graph Figure 3-4. In the nearby Longchi region, the maximum yearly rainfall was 1605 mm (1978), and the minimum annual rainfall 713 mm (1974), so slightly less than in Yingxiu (Ming, 2014). The rain is concentrated in the monsoon (especially in July and August), intensities of hourly rainfall, daily rainfall, as well as frequency are high, but the duration is short. See Figure 3-4.

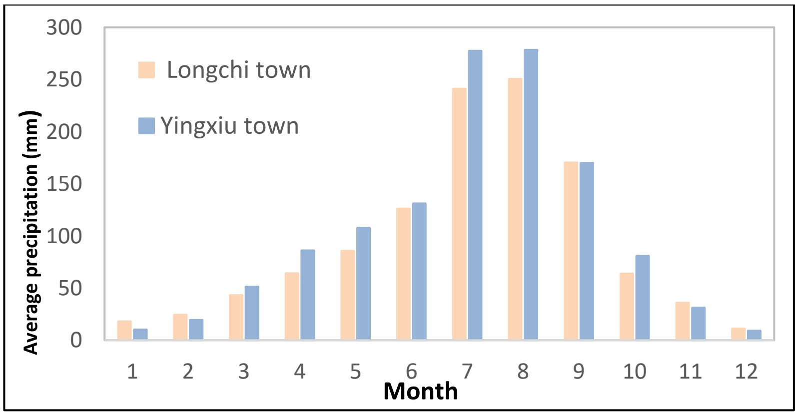

Figure 3-4. Average monthly rainfall in Yingxiu town and Longchi town

3.3.1. Hongchun catchment

This catchment had not experienced debris flows for around forty-six years until the earthquake activated a large number of co-seismic landslides. After the earthquake, the total amount of loose material is 35.8×10^5 m^3, among which approximate 15×10^5 m^3 new loose material was induced by the earthquake (Xu et al., 2012). After the Wenchuan earthquake, debris flows frequently happened in this catchment for five years after the earthquake. In the 08.14.2010 event, the debris flow material was around 7.11×10^5 m^3 in total. About 4.0×10^5 m^3 material moved into the powerful Min river, and a temporary dam was formed that blocked the river. As a result, the river diverted and floodwaters poured into the newly reconstructed Yingxiu town from the right bank, which caused critical property loss (Tang et al., 2011). Table 3-3 summarized the post-seismic debris flows happened within five years.

Table 3-3. The debris flows happened in the three catchments

	Hongchun		Niujuan		Bayi	
Year	**Occurrence**	**Damage**	**Occurrence**	**Damage**	**Occurrence**	**Damage**
2009	-	-	○	The Min river was blocked	○	The tea-horse road, 400-meter Du-Wen highway, numerous farmland, and temporary houses were destroyed
2010	○	The newly reconstructed Yingxiu was flooded	○	The earthquake ruins were destroyed, and the old Baihua bridge was buried	○	Around 136 houses were destroyed, 280-meter Du-Wen road was buried, direct economic loss: 150,00000 (RMB)
2011	○○	The highway, the nearby houses were destroyed	○○	The national highway 213 was destroyed	○○	The road in the outlet area was blocked
2012	○	?	-	-	-	-
2013	○	?	○	Two access roads to this village were destroyed	-	-

Note: ○: "debris flow"; ○: "mitigation measure"; "-": no debris flow happened; "?": no detailed information

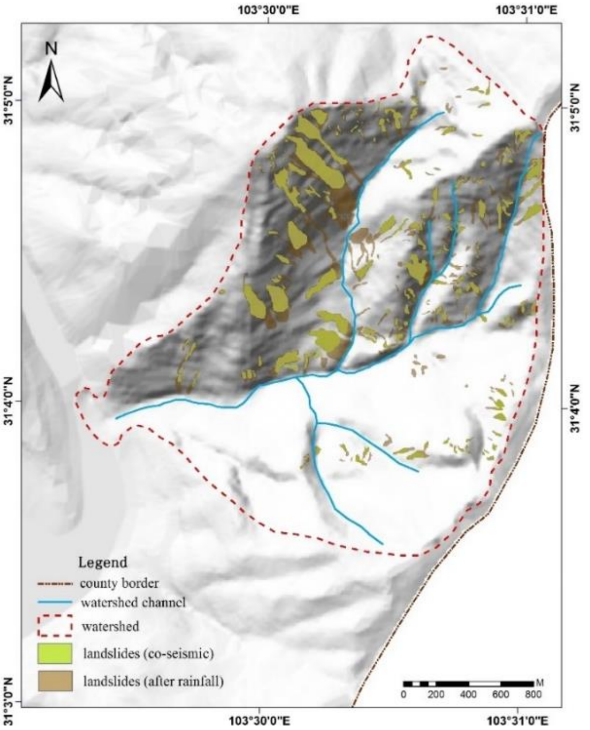

Figure 3-5. Distribution of historical landslides in Hongchun catchment

3.3.2. Niujuan catchment

Before the Wenchuan earthquake, no mass movement events were recorded in this catchment, and there was no prominent debris flow deposition. The earthquake generated around 69.5×10^5 m^3 of new material in total, which dominated the material in this catchment. During the Wenchuan earthquake, a large rock avalanche occurred in the upper sub-watershed of Njuguna catchment, called the Lianhuaxin watershed. This rock avalanche filled the downstream valley parts to form a dam lake after they hit the right bank of the main channel (Figure 3-6). The initiation volume of the debris flow event that occurred on 14th Aug in 2010 was $1.49\times10^5m^3$. According to the field investigations, and engineering dam at the dammed lake blocked part of the initial solid material. The rest of the material deposited in the channel, while around 0.83×10^5 m^3 of loose material moved into Min River, blocking about one-third of the river width. And the old Baihua bridge was buried by the debris flow material. The debris flows happened in this catchment are illustrated in Table 3-3.

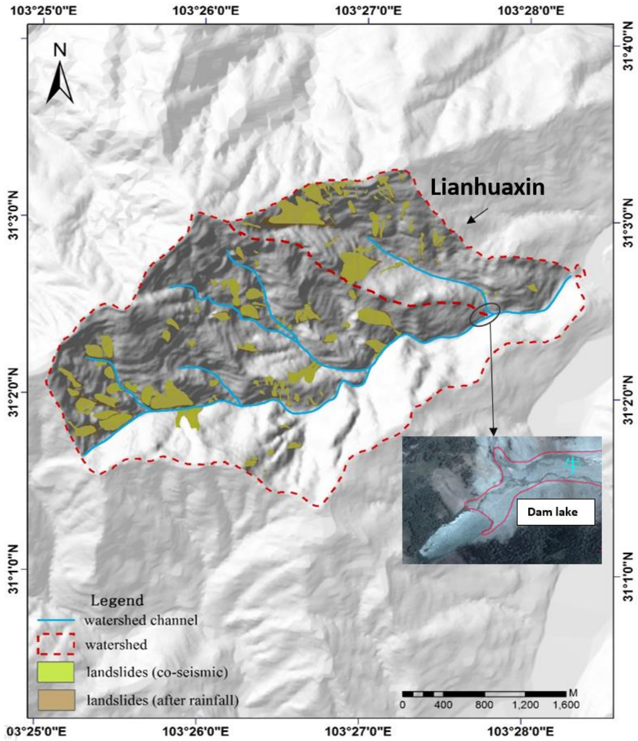

Figure 3-6. Distribution of historical landslides in Niujuan catchment

3.3.3. Bayi catchment

Bayi catchment was a multi-stage old debris flow gully before the Wenchuan earthquake with three huge-scale debris flows that were recoded before 2008, namely in I stage, II stage, and III stage. The I stage and III stage formed huge deposition fans at the outlet, and the scale of II stage was smaller that most materials stopped in the channels (Ma et al., 2011). The strong shaking of the Wenchuan earthquake triggered numerous co-seismic landslides, especially in the middle section of this catchment. According to field measurement, abundant loose material, around 75.7×10^5 m^3 was formed by the co-seismic landslides, among which the unstable reserves were about 43.8×10^5 m^3 (Zhang, Zhang & Zhang, 2010). Three debris flows happened in 2008 and 2009, with a volume of 11.4×10^5 m^3. The events in 2009 resulted in severe damage to the more than one hundred temporary houses and the Du-Wen highway. A new access road and tunnel had to be constructed. According to field surveys, on 14th August 2010, debris flows had broken out in three sub-gullies at the same time while the main gully did not participate in the debris flow processes or provide loose material, but received a lot of deposits (Ma et al., 2011). In total, approximately 1.37×10^5 m^3 solid materials moved during this debris flow event, and most of the material was deposited in the channels and outlet areas (Ming, 2014). The debris flows happened in this watershed are illustrated in Table 3-3.

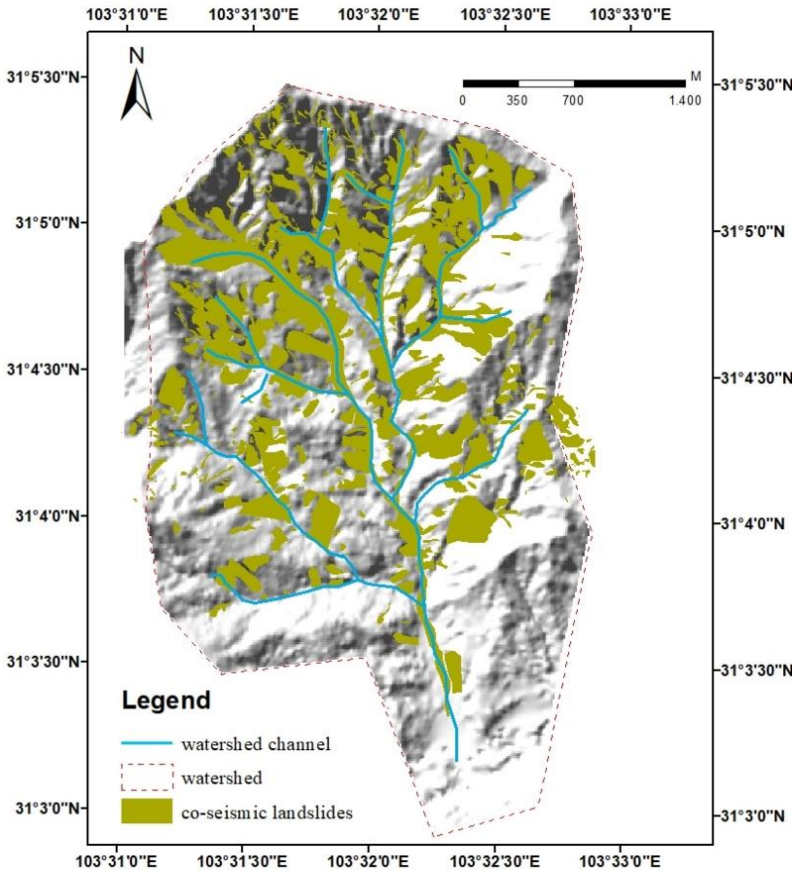

Figure 3-7. Distribution of historical landslides in Bayi catchment

Many measuring instruments and monitoring devices were installed in the earthquake-stricken area (Qingping, Yingxiu, Longchi) for debris flow monitoring and early warning, such as automatic telemetry rain stations, video cameras, radar mud gauges, infrasound alarms, and pressure sensors, etc. However, most of them did not function anymore after some years due to bad maintenance, destruction of the debris flow in 2010, and stealing of solar panels and batteries so that no warning was issued for the recent events.

4. METHODOLOGY

This chapter introduces the *OpenLISEM_Hazard*, and described the input data, scenarios, and methods. It first introduces the theoretical background and governing equations of *OpenLISEM_Hazard*. The second section illustrates the sources of the input data and how they were preprocessed. Also, the modeling scenarios are briefly introduced. Finally, the methods used for sensitivity analysis, calibration, and transferability analysis are presented.

4.1. Introduction of OpenLISEM hazard

OpenLISEM Hazard is a physically-based model developed to simulate runoff, sediment dynamics, flooding, and mass movement processes. The first version of *OpenLISEM* was published and improved by De Roo (1996) and Jetten & de Roo (2001) as a distributed erosion and hydrology model. Then the model was further developed and enhanced to include also flood simulations. In the past years, the model was extended to become a multi-hazard modeling tool for single rainfall events and tested in several studies on debris flow simulation (Bout et al., 2018a; Bout et al., n.d.; Augusto, 2019). This multi-hazard version contains three main processes: water processes, sediment processes, slope processes. The main components of *OpenLISEM_Hazard* are:

Surface Storage
Runoff
Erosion
Slope stability and failure
Debris flow initiation and runout
Flooding
Mass movement runout

OpenLISEM Hazard is an event-based simulation tool, and long-term processes such as groundwater flow and evapotranspiration are not directly implemented. Changes in related properties must be set through the initial conditions of the model. This model is meant to simulate the effects of changes in source material, land use type, and mitigation works on the development of dynamic activities. The model can be divided into three main classes: the hydrological processes, the sediment processes, and the slope processes. The model simulates the processes using a deterministic approach, and no probabilistic components, e.g., related to the uncertainty of the input parameters, have yet been implemented.

4.1.1. Hydrology

The hydrological part of *OpenLISEM Hazard* includes

Precipitation
Interception
Storage
Infiltration

Runoff flow

Precipitation

OpenLISEM Hazard simulates rainfall from rainfall intensity data (mm/h) for a given rainfall event with a duration of hours, subdivided in timesteps, which can also be given spatially or a single set of values for the entire area. In order to correct the fact that less rain remains on the steeper slopes, the cell width and length that receive rainfall changes following the slope of the local topography. The surface area of the cells with a steeper slope is enlarged.

Interception

Interception is calculated for vegetation, buildings. *OpenLISEM Hazard* ignores evaporation since the short nature of the rainfall event make this less relevant, and the evapotranspiration is playing a minimal role during the intensive rainfall events. Hence interception is set as fixed storage. The canopy interception is calculated with (Aston, 1979), while rainfall that is not intercepted reaches the soil with the same rainfall intensity as rainfall.

$$I_c = S_{max}\left(1 - e^{-k\frac{P_{cum}}{S_{max}}}\right) \quad 4.1$$

$$\mathrm{k} = 1 - \mathrm{e}^{-(\mathrm{co}*\mathrm{LAI})} \quad 4.2$$

Where *Ic* is the total intercepted storage at a given time (mm), *Smax* is the maximum canopy storage, *Pcum* is the total precipitation (mm), *co* is the canopy openness (-), and *LAI* is the leaf area index (-). *Smax* is calculated from LAI with an empirical equation within *OpenLISEM Hazard*, is changing for different vegetation situations.

Storage

Rainfall generally is stored in micro depressions in the soil surface. The runoff flow starts gradually with the increase of the water level in micro depressions. *OpenLISEM Hazard* uses the surface roughness to estimate the fraction of water that is stored in micro depressions (MDS) and the water that is released as runoff. The equation was taken from (Kamphorst et al., 2000).

$$\mathrm{MDS} = 0.243\mathrm{RR} + 0.010\mathrm{RR}^2 + 0.012\mathrm{RR} * \mathrm{S} \quad 4.3$$

Where MDS is the micro depression storage (mm), RR is the standard deviation of the surface heights (mm), and S is the slope (mm^{-1}).

Infiltration

Water starts to transport from surface to subsurface when water in the micro depressions is over the limiting conditions (the pore space in the soil and infiltration capacity. The Green & Ampt model was widely used for *OpenLISEM Hazard* applications in the Wenchuan area. And the model for one layer simulation is enough for this study. Hence, the 1st layer Green & Ampt model was chosen for the infiltration process.

The model uses the empirical Darcy equation to illustrate the soil-water balance at the vertical level.

$$\frac{\partial \theta}{\partial \tau} = -\mathrm{K_s} \frac{\partial_\mathrm{h}}{\partial_\mathrm{z}} \qquad 4.4$$

In this equation, θ is the soil moisture content (m^3 m^{-3}), h is the hydraulic head(m), z is the vertical elevation (m), Ks is the saturated conductivity (ms^{-1}).

Green & Ampt model (1911) assumed that the wetting front moves down to the parallel layer to the soil surface during infiltration. Hydraulic conductivity, porosity, initial soil moisture content, and matric stress are used to dictate the infiltration rate. This model not only simplified the data requirements but also reduces the dimensions to be modeled only to simulate infiltration in the vertical direction. This model is sensitive to the Ksat and initial soil moisture. An assumption in this model is that the downwards speed of the wetting front changes with the saturated conductivity changes.

$$\mathrm{f} = \mathrm{K_s}\left(\varphi \frac{\mathrm{F}}{\theta_\mathrm{s} - \theta_\mathrm{i}} + 1\right) \qquad 4.5$$

Where *f* is the potential infiltration rate (ms^{-1}), *Ks* is the saturated hydraulic conductivity, *F* is the cumulative infiltrated water (m), θs is the porosity (m^3 m^{-3}), θi is the initial soil moisture content (m^3 m^{-3}).

4.1.2. Slope stability and failure

Slope failure in *OpenLISEM Hazard* is based on the Iterative Failure Method (Bout et al., 2018a). This method defines the failure from toe to top. There are several assumptions used in the process. Firstly, the failure surface is simply considered to be parallel to the surface gradient at any point. The second one is that the altered elevation results in changing forces in the neighboring cells. The third assumption is that the slope failure is calculated by the maximum of the slopes on both sides. This method reverses the Factor of Safety (FOS) to address the remaining depth of the soil layer at which the local stability is achieved.

$$\mathrm{FOS} = 1 = \frac{\mathrm{c_1} + \mathrm{c_2} * \mathrm{coscos}(\tan^{-1}(\frac{\mathrm{h}-\mathrm{h_0}}{\mathrm{d_x}}))^2 * \tan(\varphi)}{\mathrm{c_3} * \sin(\tan^{-1}(\frac{\mathrm{h}-\mathrm{h_0}}{\mathrm{d_x}})) * \cos(\tan^{-1}(\frac{\mathrm{h}-\mathrm{h_0}}{\mathrm{d_x}}))} \qquad 4.6$$

Where C_1 is apparent soil cohesion (kPa), $C_2 = ((\gamma - m\gamma_w)h_s + m\gamma_w h_s)$, $C_3 = ((\gamma - m\gamma_w)h_s$, with γ.is the density of the slope material (kg m^{-3}), γ_w is the water density (kg m^{-3}), and m is the fraction of the saturated soil depth from the basal boundary (-), and h_S is the depth of the failure plane (m). φ is the soil internal friction angle (-), h is the elevation above the failure surface (m), and h_0 is the lowest neighboring elevation (m).

4.1.3. Flow dynamics

In *OpenLISEM Hazard*, the dynamics of mass and momentum are calculated with a discretization of the continuity equation for solids and fluids (Bout et al., 2018a). The two-phase debris flow equation proposed by Pudasaini (2012) is used for flow dynamics simulation.

$$\frac{\partial \mathrm{h}}{\partial \mathrm{t}} + \frac{\partial(\mathrm{hu_x})}{\partial \mathrm{x}} + \frac{\partial(\mathrm{hu_y})}{\partial \mathrm{y}} = \mathrm{R} - \mathrm{I} \tag{4.7}$$

$$\frac{\partial \mathrm{hu_x}}{\partial \mathrm{t}} + \frac{\partial(\mathrm{hu_x^2})}{\partial \mathrm{x}} + \frac{\partial(\mathrm{hu_x u_y})}{\partial \mathrm{y}} = \mathrm{gh}\left(\mathrm{S_x} - \mathrm{S_{f,x}}\right) \tag{4.8}$$

$$\frac{\partial hu_y}{\partial t} + \frac{\partial(hu_y^2)}{\partial y} + \frac{\partial(hu_x u_y)}{\partial x} = gh\left(S_y - S_{f,y}\right) \tag{4.9}$$

Where h is the flow height (m), u is the flow velocity (m/s), R is the rainfall (mm), I is the infiltration (m), g is the gravitational acceleration (m s^{-2}), S is the friction term (m s^{-2}), $\mathrm{S_f}$ is the momentum source term (m s^{-2}).

For adapting the two-phase debris flow equations to the catchment-based model, water flow friction is calculated with the Darcy-Weisbach equation instead of frictional force. In order to complete these equations, several flow properties are estimated based on the volumetric sediment content. Viscosity is given by an empirical relationship (Brien, Julien, & Fullerton, 1993).

4.1.4. Deposition

In this model, the generalized deposition equations developed by Takahashi et al. (1992) are selected to simulate various specific deposition-based processes (Bout et al., 2018a).

$$\mathrm{D} = \left(1 - \frac{|\vec{\mathrm{u}}|}{\mathrm{p}|\vec{\mathrm{u}}|_{\mathrm{cr}}}\right)\frac{\alpha_{\mathrm{eq}} - \alpha}{\alpha^{\mathrm{b}}}\mathrm{V} \tag{4.10}$$

$$|\vec{u}|_{cr} = \frac{\frac{2}{5d_{50}}\sqrt{\frac{g\sin(\theta_c)\rho}{0.02\rho_s}}1h^{1.5}}{\left(\frac{a^b}{a}\right)^{-\frac{1}{3}} - 1} \tag{4.11}$$

$$\tan(\theta_c) = \frac{\alpha(\rho_s - \rho_w)\tan(\phi^b)}{a(\rho_s - \rho_w) + \rho_w} \tag{4.12}$$

$$\alpha_{\mathrm{eq}} = \frac{\rho_{\mathrm{w}}\tan(\theta)}{(\rho_{\mathrm{s}} - \rho_{\mathrm{w}})(\tan(\phi^{\mathrm{b}}) - \tan(\theta))} \tag{4.13}$$

With D the deposition rate ($m\ s^{-1}$), $|\vec{u}|_{cr}$ the critical velocity for deposition ($m\ s^{-1}$), p the calibration factor for the critical velocity for deposition (-), α_{eq} the equilibrium volumetric solid concentration (-), α^b the solid volumetric concentration of the bed material (-), and $d50$ is the median grain size (m).

4.1.5. Entrainment equations

For entrainment estimation, the equations by Takahashi et al. (1992) is implemented in this model (Bout et al., n.d.).

$$\mathrm{E} = \mathrm{K}(\tau - \tau_{\mathrm{c}}) \tag{4.14}$$

$$\tau = \rho_{\mathrm{flow}}\mathrm{ghS_f} \tag{4.15}$$

$$\mathrm{S_f} = \frac{\tau_{\mathrm{y}}}{\rho_{\mathrm{flow}}\mathrm{gh}} + \frac{\mathrm{K}}{8\rho_{\mathrm{flow}}\mathrm{gh}^2} + \frac{\mathrm{n_{td}^2}|\vec{u}|^2}{\mathrm{h}^{\frac{4}{3}}} \tag{4.16}$$

$$\tau_{\mathrm{c}} = c^b + (1 - C_s)\alpha(\rho_s - \rho_w)gh\cos^2(\theta)\tan(\phi^b) \tag{4.17}$$

Where τ is the shear stress (Pa), τc is the critical shear stress (Pa), Sf is the surface friction term (-), τy is the yield stress (pa), K is the resistance parameter for laminar flow (-), ntd is the turbulent dispersive coefficient ($m^{1/2}s-1$), c^b is the bed material cohesion (Pa), and Cs is the coefficient of suspension (-).

4.2. Input data

OpenLISEM Hazard requires a large number of input parameters. Nevertheless, we can use four basic types (material properties, vegetation, topography, and rainfall) to make an OpenLISEM simulation dataset in PCRaster see Figure 4-1.

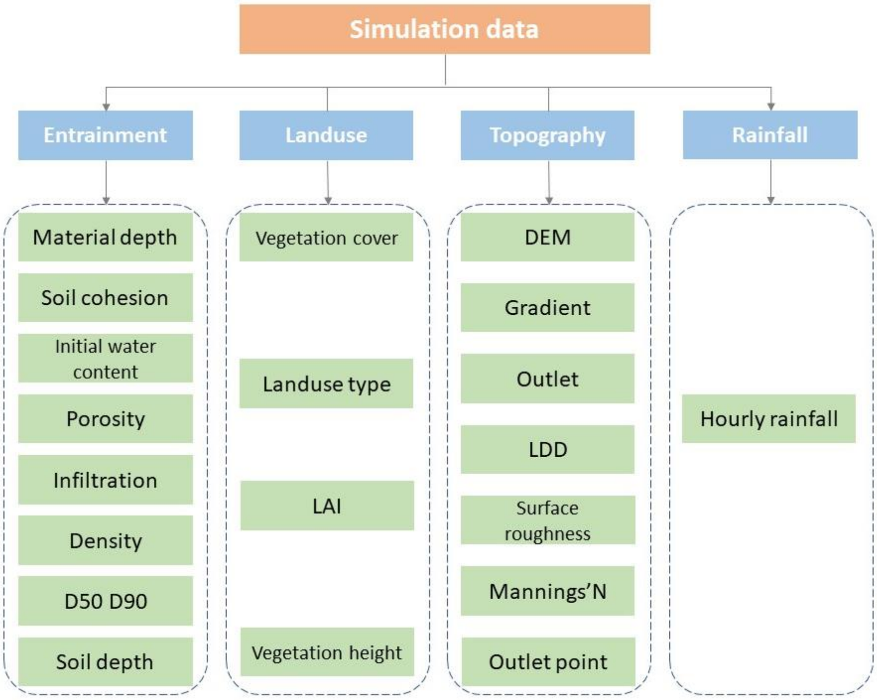

Figure 4-1. Input data for OpenLISEM Hazard

Meteorological data

OpenLISEM Hazard needs rainfall intensity (mm/h) data as input. The rainfall intensity data used for model running are from published data by Fan et al. (2019). The published dataset provides records of many rain gauges for four rainfall events in 2010, 2011, 2013. The rain gauges that are too far from the study sites were excluded. The available rain gauge records with the highest resolution were selected for model running. These records were compared with the descriptions of rainfall events in previous research. For the available rainfall record in 2010 for Bayi gulley, the data from Fan et al. (2019) was very different from that in other papers (Ming, 2014; Ma & Li, 2017). Because the data used in Ma & Li (2017) and Ming (2014) is similar to the most descriptions, we decided to use this rainfall data as input. These rain gauges are installed in the nearby towns (Yingxiu and Longchi), but the debris flow initiated from the upper and steep areas in the catchment. Therefore, due to the high spatial variability of the rainfall, as also evidenced by the differences between the nearby stations of Yingxiu and Longchi, the measured rainfall might deviate considerably from the rainfall that actually triggered the debris flow. Naturally, it increases the systematic bias for debris flow simulation since the spatio-temporal patterns of rainfall events in the mountainous region can be significant inhomogeneous on account of the elevation and topographic relief. It means the rainfall that was recorded in the rain gauges deviates considerably from that which triggered the debris flows.

Morphology data

The DEM data used in the Bayi catchments for model running are a pre-earthquake DEM with a spatial resolution of 25m, derived from stereo satellite image and ground survey, and reported by Tang et al. (2019), and the DEM used for Lianhuaxin catchment was obtained from stereo satellite image and ground survey in 2014, and reported by Tang et al. (2019), and the DEM used for Hongchun catchment was derived in 2017 by drone photogrammetry with a spatial resolution of 1m by the Chinese research institution (SKLGP), and data were reprocessed in their computer into a lower resolution. The DEMs were resampled to the pixel size used for the model running, which was 10 by 10m. In PCRaster, a gradient map, Local Drain Direction (LDD) map, outlet map, and watershed map were produced as input maps. All these maps, except the gradient map, were calculated from the LDD map.

The LDD map indicates the drainage direction for each cell. Another critical LDD function is to remove artificial pits by setting the pit size threshold as artificial pits are often much smaller than real pits. Artificially pits may be included in the DEM errors and have to be eliminated, which are defined as cells that are surrounded by neighboring higher cells. After removal of pits, the remaining pits are assigned as outlet points while the outlet of the largest catchment of the watershed map is assigned as the main outlet point.

Landuse data

The land-use map used in Hongchun catchment was based on the Sentinel-2 classification at 10m resolution. No detailed classification was made in Lianhuaxin and Bayi catchments as limited land-use types were present in these catchments. Except for a land-use map, the required land-use data includes vegetation-related maps. The vegetation cover and LAI were calculated based on NDVI. Vegetation cover (0-1) which can be calculated by a linear relation to NDVI (Keisuke & Susumu, 2001). LAI can be derived from both NDVI and vegetation cover. In this research, for excluding the system error (NDVI also was used to estimate vegetation cover), LAI was calculated by NDVI directly. Vegetation height maps were generalized as average values based on related fieldwork in previous research (Bout et al., n.d.). In terms of vegetation height, the average height was assigned to the entire map for model running. The other land-use maps were set to a value of zero.

$$Vegetation\ cover = NDVI/max(NDVI) \qquad 4.18$$

$$LAI = 0.57 * exp(2.33 * NDVI) \qquad 4.19$$

Root cohesion is also a significant factor for debris flow simulation. Bout et al., (n.d.) did fieldwork for root cohesion measurement in the Hongchun catchment. Hence, based on previous work, root cohesion can be calculated by vegetation cover.

$$root\ cohesion = vegetation\ cover * max\ (root\ cohesion) \tag{4.20}$$

Surface data

The surface data consists of surface roughness, Manning's N, stoniness, crustiness, compactness, and hard surfaces. However, the later four components were ignored with setting values as zero. Manning's N was considered as an average value to be generalized across the whole catchment, as was done in previous simulations (Bout et al., n.d.). The surface roughness was processed in the same way as Mannings'N.

Slope stability data

The model requires the following parameters for slope stability analysis: soil density, soil cohesion, internal friction angle, rock fraction, rock size, soil depth, and depth of loose material. Fieldwork and related experiments had been done in these three catchments by other researchers (Bout et al., n.d.), from the results were used in this study. As it was impossible to obtain the exact debris material depth, co-seismic landslide deposits were used to calculate the material depth based on the empirical relationship between volume and area (Tang et al., 2019).

$$V = 0.0156 * A^{1.533} \tag{4.21}$$

Since the Green and Ampt method was selected for the infiltration phase, this method needed the saturated hydraulic conductivity (Ksat), average suction at the wetting front (ψ), the initial moisture content, the porosity and the depth of the soil layer as input. Besides soil depth, values of other infiltration properties were derived from previous work.

Soil depth plays a significant role in modeling results, but it is hard to be measured. Soil depth was calculated by both the empirical method and physical relationship. The physical relationship is suitable to calculate the material depth at the upper area of the catchment and more reliable for the landslide area (Saulnier, Beven, & Obled, 1997). The soil depth obtained from the empirical relationship is better to be used for estimating the soil depth in the channel (Kuriakose, van Beek, & van Westen, 2009). In this research, we used the average of the two soil depth models as input for model running. Table 4-1 summarizes the input parameters for the three watersheds.

Table 4-1. Input data for 2010 scenario

		Sources of data in watershed		
Base map	**Parameter**	**Hongchun**	**Lianhuaxin**	**Bayi**
Rainfall	Max hourly rainfall-30mm	Fan et al. (2019)		(Ma et al., 2011)
Elevation	DEM	DEM in 2017	DEM in 2014	Pre-earthquake DEM
Land surface	Land cover classes	Sentinel-2 classification at 10m resolution	Average value from Hongchun catchment	
	Manning's N (n)	Literature comparison with field photos (Bout et al., n.d.)		
	NDVI	Landsat5 images at 30m resolution (2010)		
	Vegetation cover	Estimated from NDVI using the empirical method		

	Root cohesion	Measured from field samples (Bout et al., n.d.)	Calculate based on vegetation cover	
Soil material	D50	Measured from field samples (Bout et al., n.d.)		Measured from samples (unpublished modeling work in OpenLISEM hazard, SKLGP)
	ksat	Measured from field samples (Bout et al., n.d.)	(Bout et al., n.d.) and unpublished field investigation report	
	Internal friction angle	Measured from field samples (Bout et al., n.d.)	(Bout et al., n.d.) Literature values	
	Cohesion	Measured from field samples (Bout et al., n.d.)	Unpublished field investigation report	
	Porosity	Literature Values	Literature values	
	Density	Measured from field samples (Bout et al., n.d.)	Average value from Hongchun catchment	
	Soil depth	Physical and empirical relationships	Physical and empirical relationships	

4.3. Debris flow scenarios

According to the debris flow inventory (Fan et al., 2019a), In 2010, debris flows happened in Bayi, Lianhuaxin, and Hongchun on 13th and 14th August. Hence, the 2010 scenario was selected as the triggering rainfall event. In 2011, a debris flow happened in Bayi catchment on 3rd July. One month later, a debris flow occurred in Hongchun catchment on 20th August and Niujuan watershed on 21st. In 2012, no debris flow was recorded in these three gullies. In 2013, Hongchun and Liahuaxin experienced debris flows on the same day when nothing happened in Bayi gully.

Five changing variables were considered in this research for model running in different years: rainfall, elevation, vegetation cover, root cohesion, and depth of loose material. The DEM used for model running was the DEM after model running under the previous scenario, which therefore includes the erosion and accumulation areas. The changes of vegetation cover were calculated from satellite images from subsequent years, using NDVI, and root cohesion changes were correlated with the changes of vegetation cover. The depth of loose material was represented by the difference between the depth of loose material in 2010 and the erosion depth after the 2010 event. The deposition depth was not considered since debris flow material was moved by bulldozers and trucks immediately after the debris flow. Because no debris flow happened in 2012, the data used for the 2012 scenario are the same as the data used for the 2013 scenario. In Table 4-2, "N" is the year for simulation, "N-1" is the year of the most recent event

Table 4-2. How varying parameters over time were considered

Temporally variable factor	Strategy
Elevation (DEM)	DEM in year N = final DEM after year N-1
Vegetation cover	NDVI in year N (landsat5 in 2011, landsat7 in 2013)
Root cohesion	Vegetation cover in year N × original maximum root cohesion
Depth of loose material	Depth of loose material in year N – entrainment depth in year N

4.4. Methods of sensitivity analysis and calibration

Sensitivity analysis is to analyze changes in which parameter will result in large changes in model outputs. Only when the modeled processes and environment are similar, the parameter sensitivity is the same in different watersheds. The "*one-parameter-one-time*" method was applied for parameter sensitivity analysis. An important principle in calibration is to alter the parameters with the strongest influence on model outcomes. By doing so, the best performing simulation can be acquired. However, because of the large number of simulations required with many calibration parameters, it is efficient to select only the most influential parameters for the calibration process. There are several alternative parameters for model calibration. The entrainment coefficient affects the solid volume significantly. The flow internal friction angle can affect shearing resistance that determines the amount of moving material that can stop in the channel. Consequently, it can leave more material in channels to shorten the runout distance and delay the arrival time of sediments to the outlet area. Except for these two parameters, initial water content, soil internal friction angle, and Manning's N were tested for the influences on volume, runout distance, especially arrival time. Before determining sensitivity analysis to be done for which factors, the model had run with the default settings. Around six to eight testing runs with larger variations (around 0.2) were made in each catchment to select parameters for sensitivity analysis. After we found a relative optimum combination of parameters, the parameters were refined manually. Totally, the model run around fifteen times in each watershed for parameter sensitivity analysis.

The models were calibrated after the sensitivity analysis using a trial and error method. This method is to run the model repeatedly with the fine-tuned parameters based on previous errors until success. In general, at least five-time more model runs were applied in each watershed based on outcomes of sensitivity analysis, and every model run took 8 to 13 hours (depending on the scale of the modeled area, rainfall scenario, and computer performance). The calibration can start with calibrating simulated volume as it can be simply calibrated by tuning the entrainment coefficient, and it will not be affected by other parameters significantly. The next step is to calibrate the arrival time and runout distance. The calibration of both indicators can be operated at the same time as they are affected by similar factors.

The indicators used for calibration are volume, runout distance, and arrival time. The extent of the deposition could not be used for calibration as those were unavailable. In this research, it was assumed that the threshold for determining the predicted arrival time in the model is once the percentage of solid phase reached 15%. This threshold for debris flow definition is arbitrary however can have influences on the efficiency on early warning and taking appropriate responses for risk reduction. Since the recorded time of a debris flow is mostly the time when debris flow material arrived in the outlet area, a point around the junction of the watersheds and the Min river was selected to estimate the arrival time in the model. However, the recording of the exact arrival time based on eyewitness accounts and press information can be less accurate than the recording using video cameras, which were not available. The model calibrations were done with actual events. The accuracy of the runout distance is hard to be quantified, especially because most of the debris flows ended in the main river. Hence, visual interpretation was applied to evaluate the modeled runout distance. Table 4-3 shows the debris flow information used for model calibration.

There was no detailed information for the events that happened in 2011 and 2013. Hence, the model runs for the two years could not be calibrated.

Table 4-3. Available information on debris flows

Event	Time	Volume ($\times 10^5$ m^3)	The ending point of runout
		Hongchun	
08.14.2010	16:00	7.11	One-third of the width of Min river
08.20.2011	02:00	?	The road at the outlet was destroyed
2012	?	?	?
07.10.2013	?	?	?
		Lianhuaxin	
08.14.2010	16:00	1.49	One-third of the width of Min river
08.20.2011	?	?	The road at the outlet was destroyed
2012	-	-	-
07.10.2013	9:00	?	The access road at the outlet was destroyed
		Bayi	
08.13.2010	02:00	1.37	Longxi river
07.03.2011	?	?	Outlet
2013	-	-	-

-: no event happened; ?: happened without detailed information

4.5. Methods of transferability analysis

Cross-validation was employed for spatial transferability analysis. Owing to the limited information on debris flows that happened in 2011, 2012, and 2013, cross-validation was not possible for the temporal transferability. Hence, the calibrated model in 2010 was run under 2011, 2012, and 2013 scenarios to test how applicable the model is with the time to predict the occurrence of debris flow. Cohen's kappa was used to assess the spatial transferability in terms of accuracy of volume and time, see below.

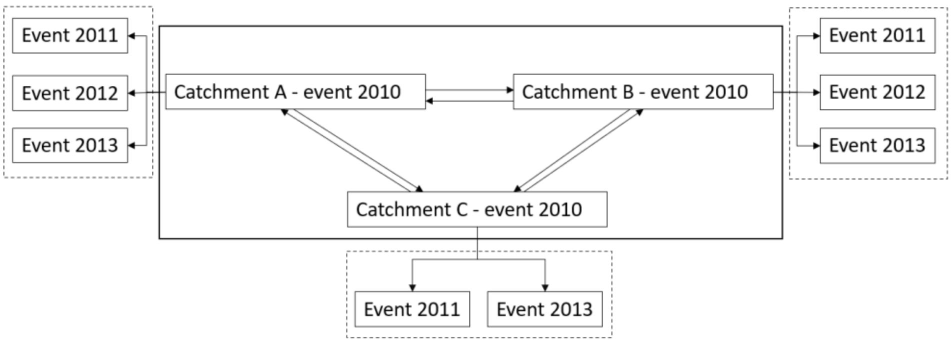

Figure 4-2. Diagram of transferability experiments.

The procedures in the solid-line square are for spatial transferability analysis. The procedures in the dash-line square are for temporal transferability.

Modelled for watershed	Calibrated _catchment 1	Calibrated _catchment 2	Calibrated _catchment 3	SUM
Catchment1	A	A1	A2	E
Catchment2	B	B1	B2	E1
Catchment3	C	C1	C2	E2
SUM	D	D1	D2	F

Note: (The Ai, Bi, Ci are the volume accuracy, time accuracy. D= A+B+C, E= A+A1+A2, F= D+D1+D2

$$\mathrm{p}_0 = \frac{\mathrm{A} + \mathrm{B1} + \mathrm{C2}}{\mathrm{F}}$$

$$P_e = \frac{(D*E)+(D1*E1)+(D2*E2)}{F*F}$$

$$k = \frac{p_0 - p_e}{1 - p_e}$$

p_0 is the relative observed agreement among raters (identical to accuracy), p_e is the hypothetical probability of chance agreement. K=0 implies that there is no effective agreement between two raters, K=1 if the raters are in complete agreement.

5. RESULTS

The results of sensitivity analysis, calibration, and transferability analysis are presented and discussed in this chapter.

5.1. Sensitivity analysis

In this section, the selected parameters, the value ranges, and the results of the sensitivity analysis of different parameters concerning different indicators are explained. The rainfall scenario used for sensitivity analysis is the 2010 rainfall event (Figure 5-1; Table 4-3).

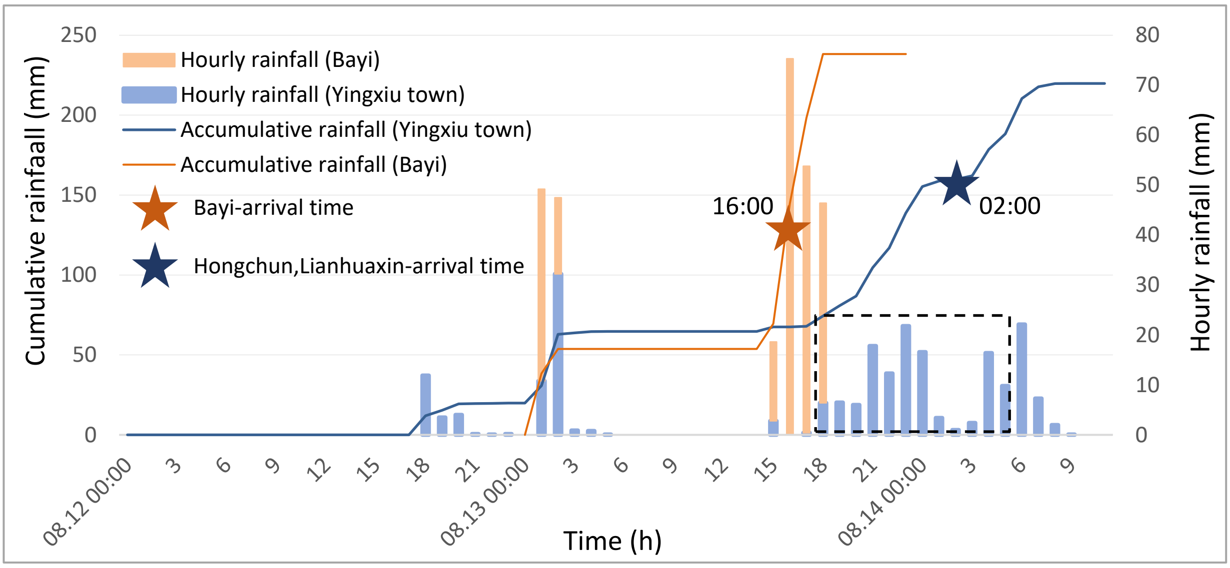

Figure 5-1. 2010-Triggering rainfall in Hongchun, Lianhuaxin, Bayi catchments. (The period in the black dashed-line square is the rainfall scenario used in Hongchun and Lianhuaxin catchment)

Hongchun catchment

In this watershed, soil internal friction angle and Manning's N are insensitive. The initial moisture is extremely sensitive that a slight decrease can lead to no debris flow is reproduced in the model. Finally, the parameter sensitivity analysis was carried out with three groups of parameters (Table 5-1). The results were presented as the percentage change from the volume (green line = 100%) and the difference in minutes with the time of arrival (pink line = 0 mins), as shown in Table 4-3. The negative time error means the simulated arrival time is earlier than the actual time, and the positive values mean delay. The changes of solid-phase percentage with modeling time is shown in figures b (Purple dashed line indicates the threshold used for debris flow: the percentage of solid phase equals 15%; the red dashed line is the real arrival time). According to the results of testing running with different EC, the simulated volume is close to the measured volume when the EC is around 0.35. Hence, the sensitivity analysis was made with little changing interval. The results of analysis A illustrate several facts (Figure 5-2). The model results with respect to the debris flow volume are best when EC is 0.25, and the accuracy of volume estimation decreases sharply with an increase of the EC within the tested range. It is also found that the volume accuracy would show a dropping trend with the decline of EC when the EC is lower than 0.25. The accuracy of arrival time prediction changed similarly with that of volume with increases of EC. Both the arrival time and the changing trend solid-phase percentages were affected by EC insignificantly (Figure 5-2b). The solid-phase percentage remains high, also after the peak rainfall, and hardly drops until the end of the simulation. However, completely different behavior is seen for the Flow Internal Friction Angle (FIFA): a slight change of the FIFA parameters affects the behavior of the EC parameter to the model, and the same changes in EC now have different model outcomes. Figure 5-3a shows that the accuracy of the modeled volume decreased a lot compared to scenario A. Figure 5-3b shows that the influence of a different FIFA values affects the shapes of solid-phase-percent lines very much. Especially when EC equals to 0.25 and FIFA equals to 0.6, the percentage of solids decreases again after the peak rainfall (Figure 5-3b). The accuracy of the volume shows a fluctuation with the increase of EC rather than a simple decrease (Figure 5-3a). The time errors also show a non-linear behavior with an increase of EC first increasing and then reducing again. In analysis C (Figure 5-4), the shapes of solid-phase-percent lines with increasing FIFA are similar, and the decrease after the peak value becomes more evident with increasing FIFA values (Figure 5-4b). Overall, the analysis for Hongchun showed that the time error is the lowest when EC is 0.35 in analysis B (200 minutes earlier than observed) while it is the highest in analysis A (330 minutes), with a change of FIFA from 0.5 (A) to 0.6 (B). So, it is clear that both EC and FIFA are highly interdependent. The analysis also shows that changes in these important parameters overall do not scientifically improve the modeling of the correct arrival time. Overall, the modeled arrival time in this catchment is always earlier than the real arrival time. Adversely, the accuracy of the modeled volume reduces directly with the increase of FIFA. Besides, EC and FIFA are ineffective to shorten the runout distance in this catchment.

Table 5-1. Parameter compositions of sensitivity analysis

Code	**Parameter compositions**	
	Entrainment coefficient (EC)	Flow internal friction angle (FIFA)
Analysis A	0.25-0.35 (interval:0.05)	0.5
Analysis B	0.25-0.35 (interval:0.05)	0.6
Analysis C	0.3	0.5-1.0 (interval:0.1)

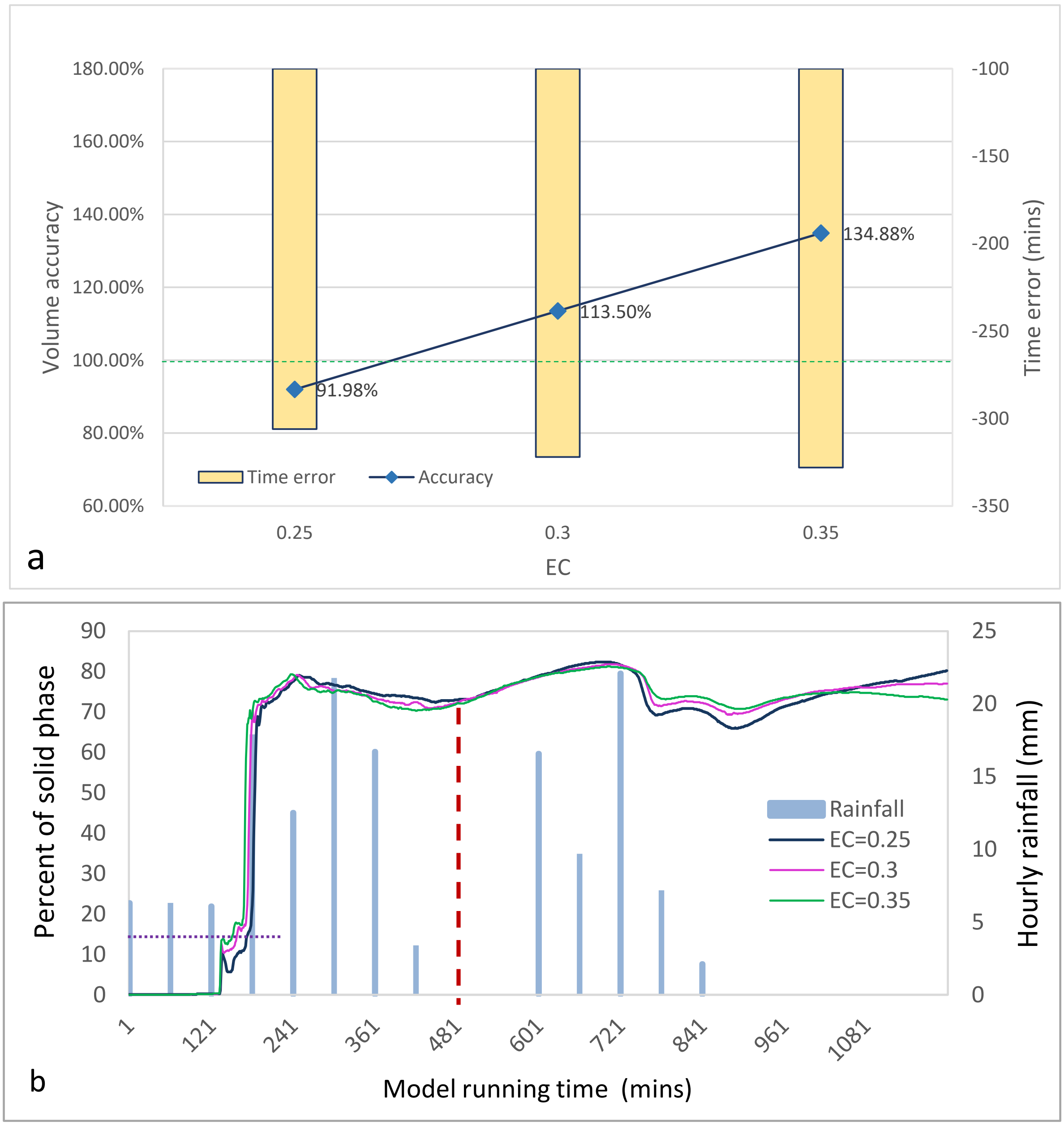

Figure 5-2. Hongchun-Analysis A

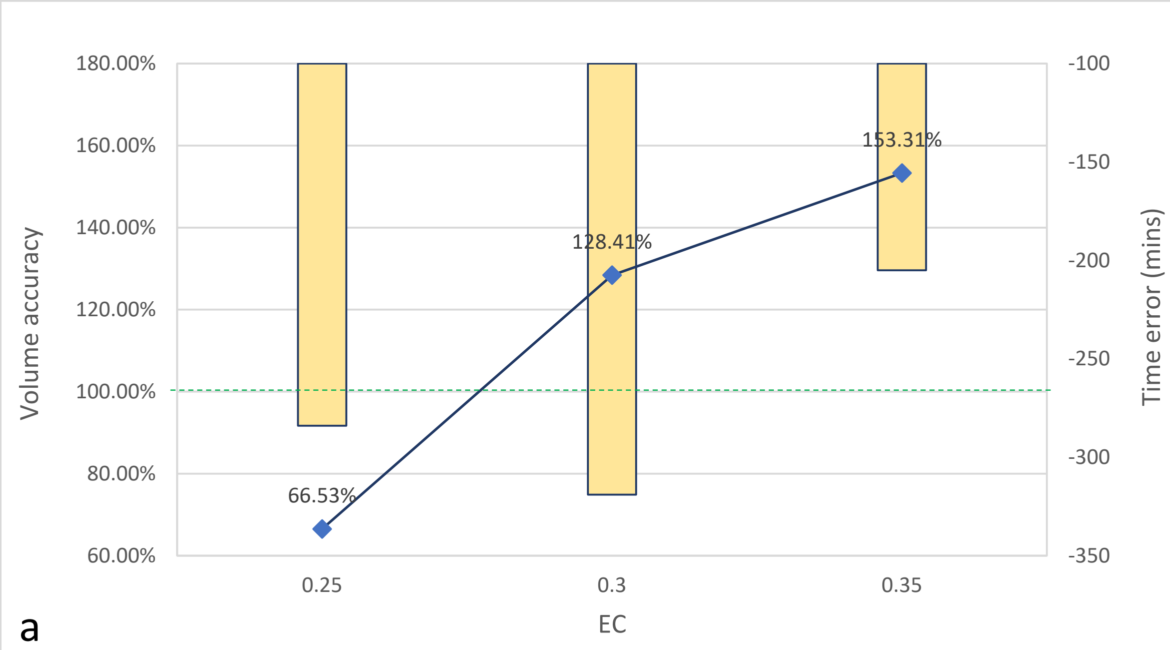

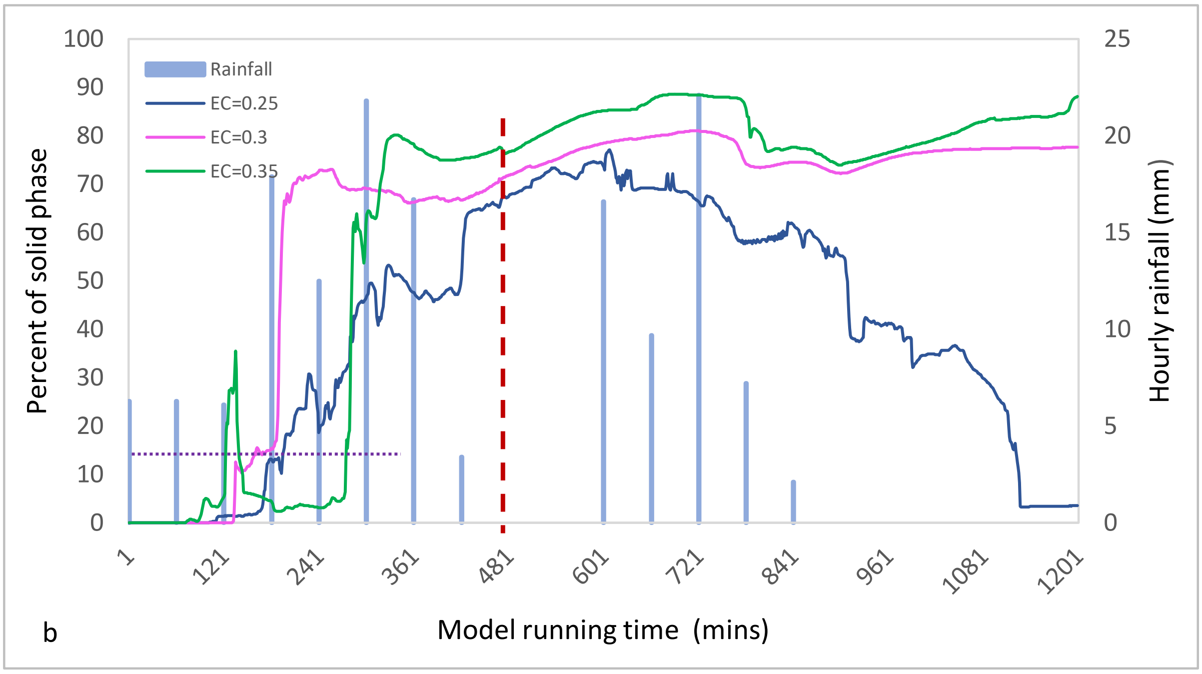

Figure 5-3. Hongchun-Analysis B.

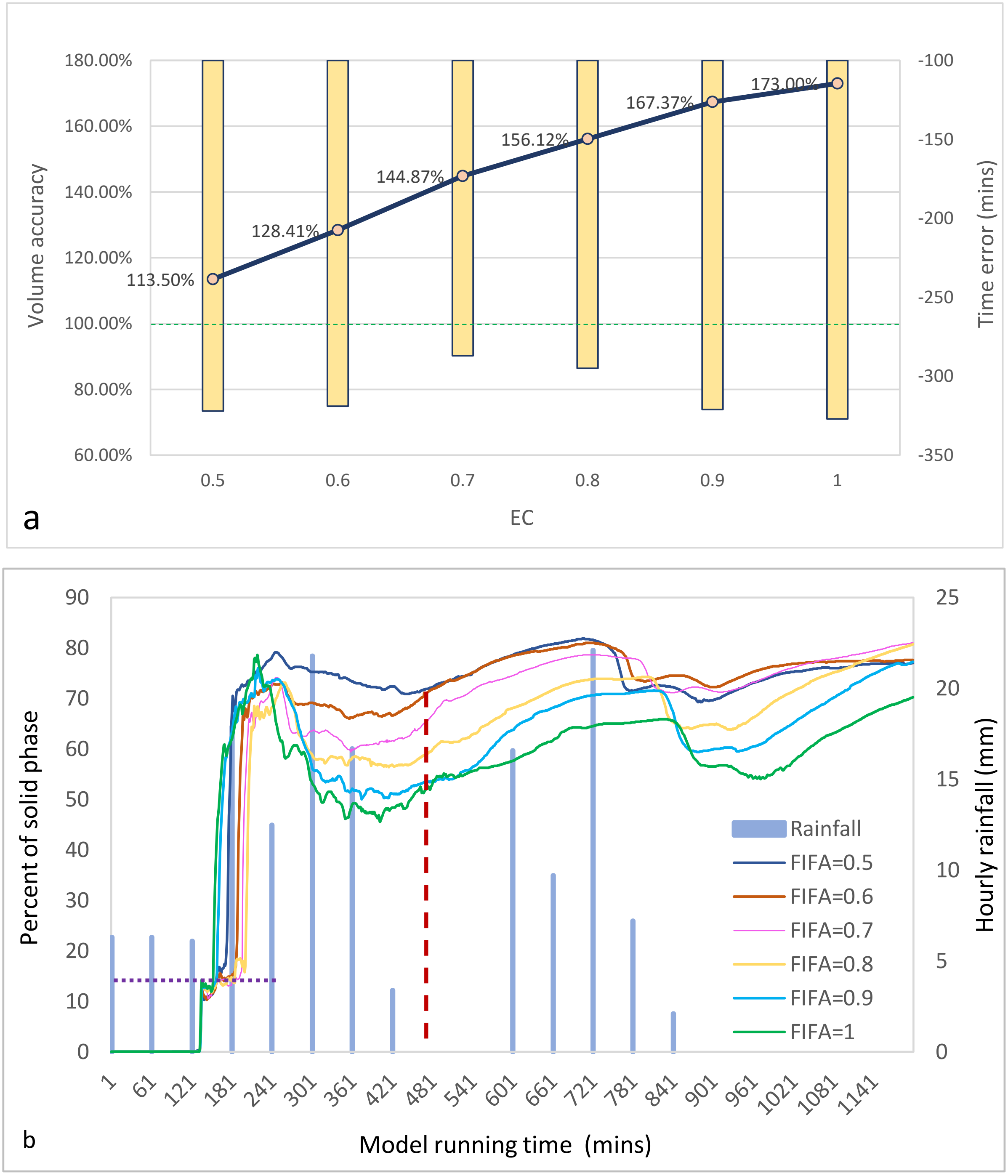

Figure 5-4. Hongchun-Analysis C.

Lianhuaxin catchment

On the basis of parameter sensitivity analysis in the Hongchun catchment, the EC and FIFA parameters were also used for the sensitivity analysis in the Lianhuaxin watershed. At first, the model was run in this gully with parameters set in Hongchun gully. The results show that the model setting underestimated the volume a lot. Hence, the values of EC had to be increased during in order to obtain an optimally performing set of input parameters. Besides, test runs were done for other parameters. As a result, the soil internal friction angle was considered as well as it is a relatively critical factor to affect the arrival time and runout distance in this gully. The same rainfall scenario was used for sensitivity analysis as in the Hongchun catchment.

The values of input parameters are given in Table 5-2. As shown in Figure 5-5, the volume is modeled with 95% accuracy when EC equals 0.4, and decrease with increasing EC values. Thus, for this watershed, an EC value of 0.4 can be considered as an optimal value. Increases of EC affect the accuracy of the arrival time only slightly in this watershed (Figure 5-5a). The graphs of solid phase percentage (Figure 5-5b) show the tendency to rise first and then drop, with different behavior for EC of 0.8 as compared to lower values (Figure 5-5b). The changes of FIFA affect the arrival time considerably (Figure 5-6a). The modeled arrival time increases directly with the rise of FIFA within the tested range of values. There is a critical value (1), at which the modeled starting time is almost as same as the real arrival time (Figure 5-6a). The changes of FIFA affected the shapes of graphs of solid phase percentage also considerably. The line for the FIFA value of 1 (and EC 0.4) reaches the threshold of 15% after several-hours of intense rainfall with timing close to the observations. During this, the solids increase first to a high solid percentage (60%) before decreasing again (Figure 5-6b). It can be concluded that increasing FIFA is more effective for shortening the arrival time than EC, but it is not as sensitive as EC to volume. The effects of SIFA with respect to the arrival time and debris flow volume were less than those covered by EC and FIFA (Figure 5-5). Except for the excellent simulated arrival time, the model, in general, gives the arrival time earlier when the predicted volume is excellent.

Table 5-2. Parameter compositions of sensitivity analysis

Code	**Parameter compositions**		
	Entrainment coefficient (EC)	Flow internal friction angle (FIFA)	Soil internal friction angle (SIFA)
Analysis A	0.4-0.8 (interval:0.2)	0.5	2
Analysis B	0.4	0.5-1.5 (interval: 0.5)	2
Analysis C	0.4	1	2-8 (interval:3)

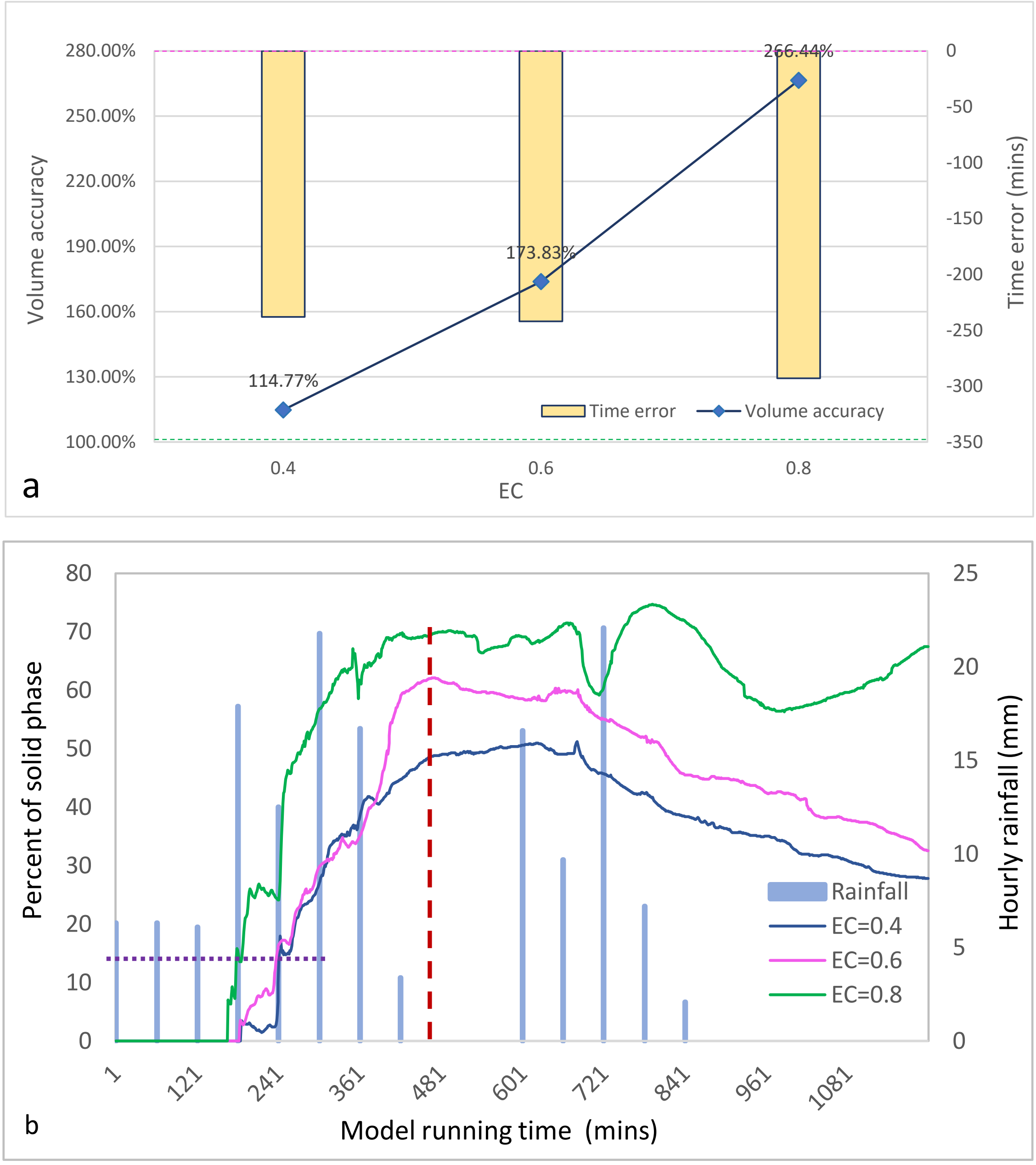

Figure 5-5. Lianhuaxin-Analysis A

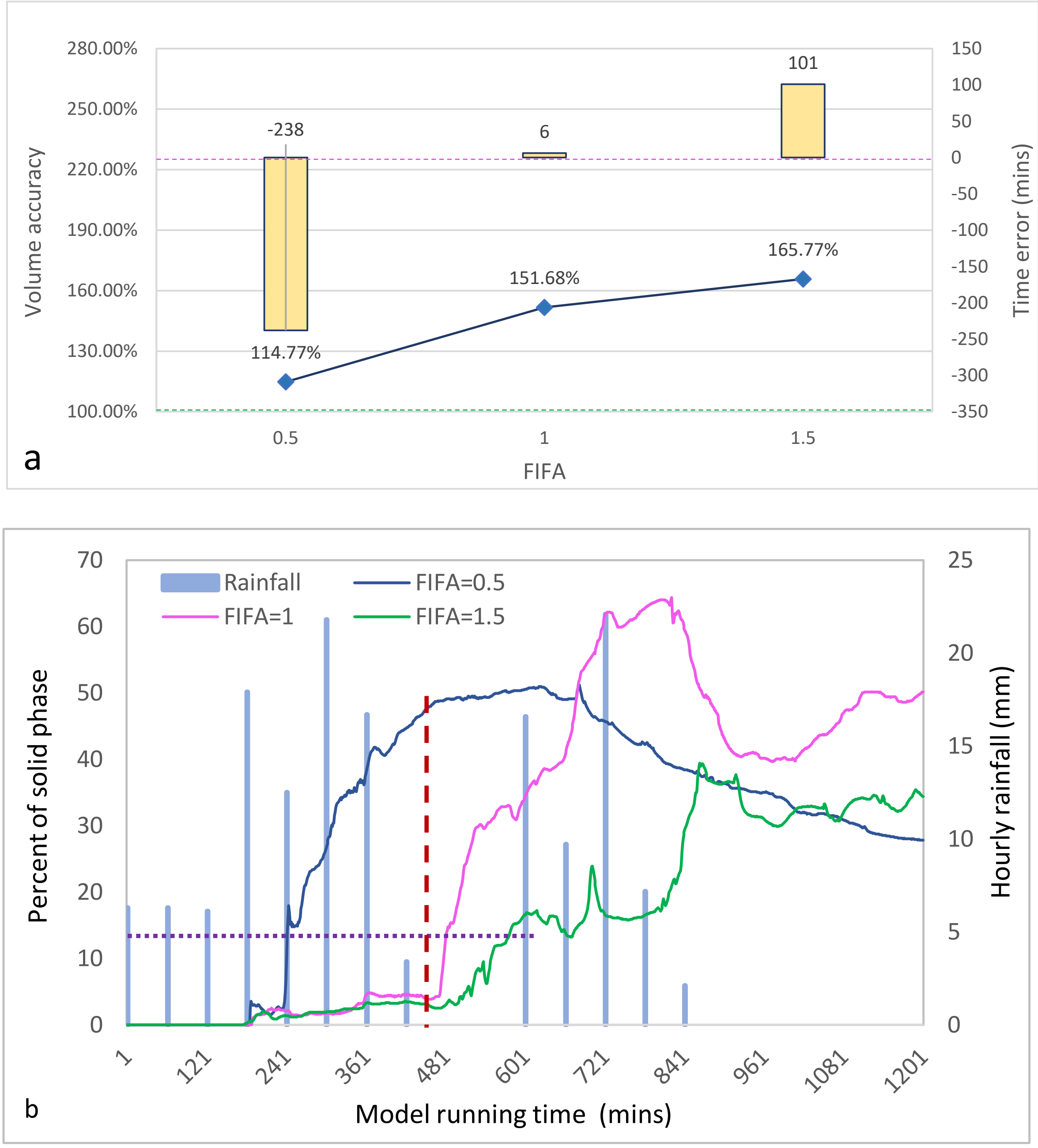

Figure 5-6. Lianhuaxin-Analysis B

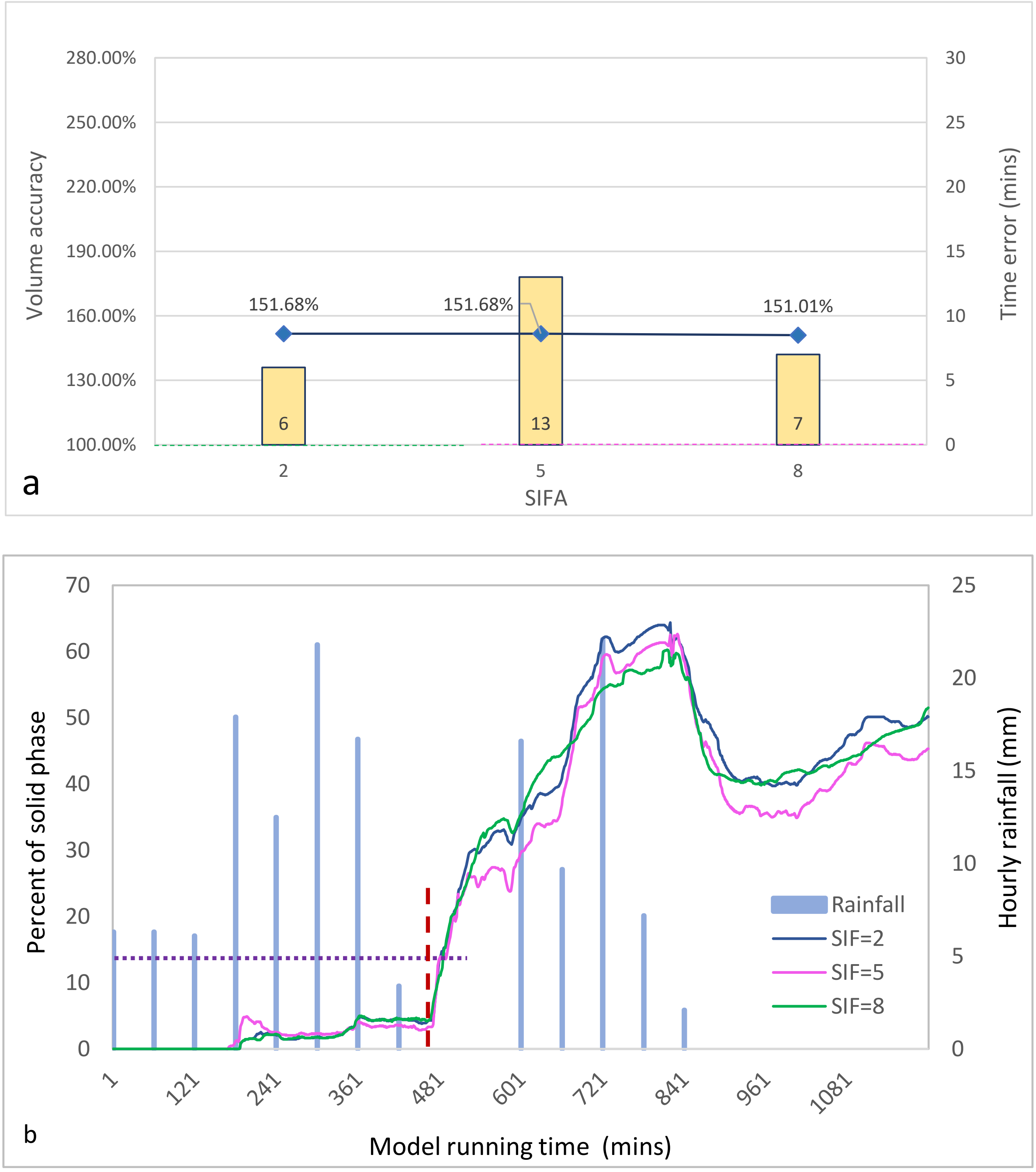

Figure 5-7. Lianhuaxin-Analysis C

Bayi catchment

Based on the sensitivity analysis in the former two catchments, parameters used for sensitivity analysis were decided. Since the soil internal friction angle did not show many varieties in the Lianhuaxin watershed (Figure 5-7), it was not selected. Also, Manning's N and Ksat were tested, but both did not show any major change in model output. Initial water content was chosen instead since the antecedent rainfall of this rainfall event (2010 rainfall event) might affect the model performance significantly. After running the model with the parameter settings in Hongchun catchments, the value ranges employed for the sensitivity analysis were defined (Table 5-3).

The parameter sensitivity analysis was done with the combinations in Table 5-3. As shown in Figure 5-8, the results were similar to the other two catchments, with higher EC lower volume accuracy was modeled. It is possible to obtain excellent volume results by only tuning EC and keeping the other values constant. The EC variations are insensitive to the modeled arrival time, as was the same in the other two catchments. However, in Bayi watershed, the modeled arrival times always occur around one hour after the intense rainfall and two hours after the reported arrival time. Because of the typical temporal distribution of rainfall, the soil-phase-percent lines are characterized by sudden jumps from zero (Figure 5-8b). Compared with EC, FIFA affects the modeled arrival times more than EC, while it affects volume accuracy less. On the whole, FIFA reshaped these lines, although the arrival times did not change a lot (Figure 5-8b). And the steepness of the line decreases with higher FIFA values. The effect of these two parameters (EC and FIFA) on declining runout distance is insignificant in this catchment. The impacts of changing the initial water content values (Theta) are minimal on both volume accuracy and time error (Figure 5-10). Generally speaking, the tested parameters have limited effects on the solid-phase percentages and modeled arrival time. The latter is always later than the actual reported arrival time.

Table 5-3. Parameter compositions of sensitivity analysis

Code	Parameter compositions		
	Entrainment coefficient (EC)	Flow internal friction angle (FIFA)	Initial moisture (Theta)
Analysis A	0.2-0.4 (interval:0.1)	0.5	1.2
Analysis B	0.2	0.5-1.5 (interval: 0.5)	1.2
Analysis C	0.2	0.5	1.2-1.8 (interval:0.3)

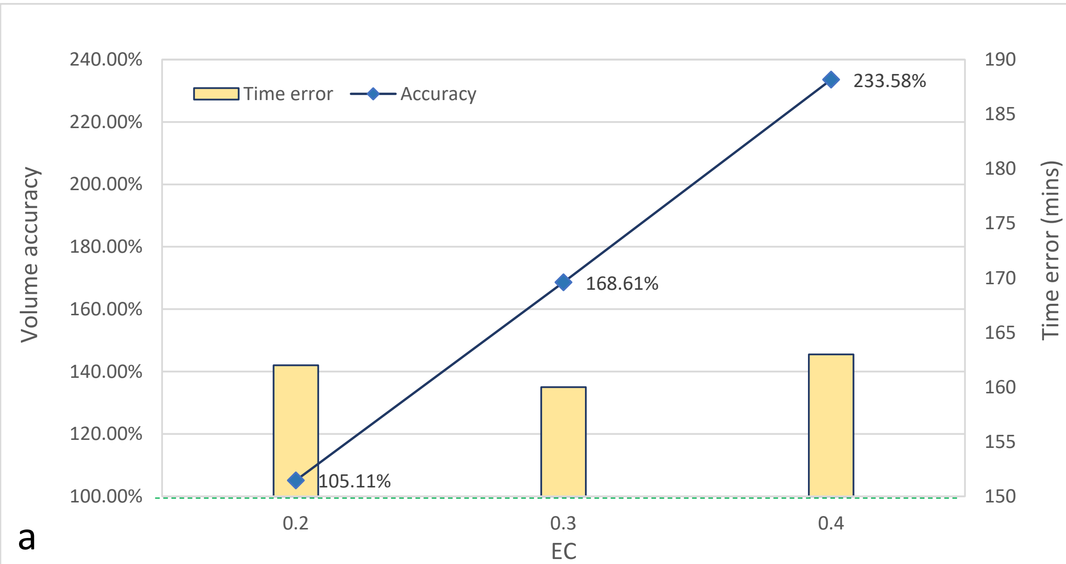

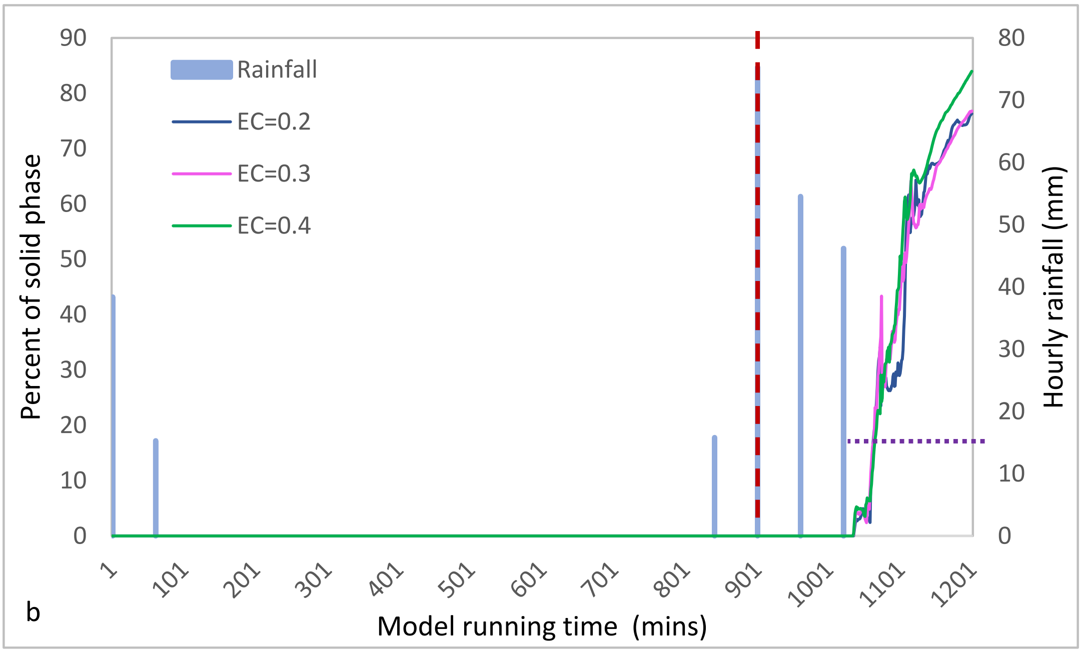

Figure 5-8. Bayi-Analysis A

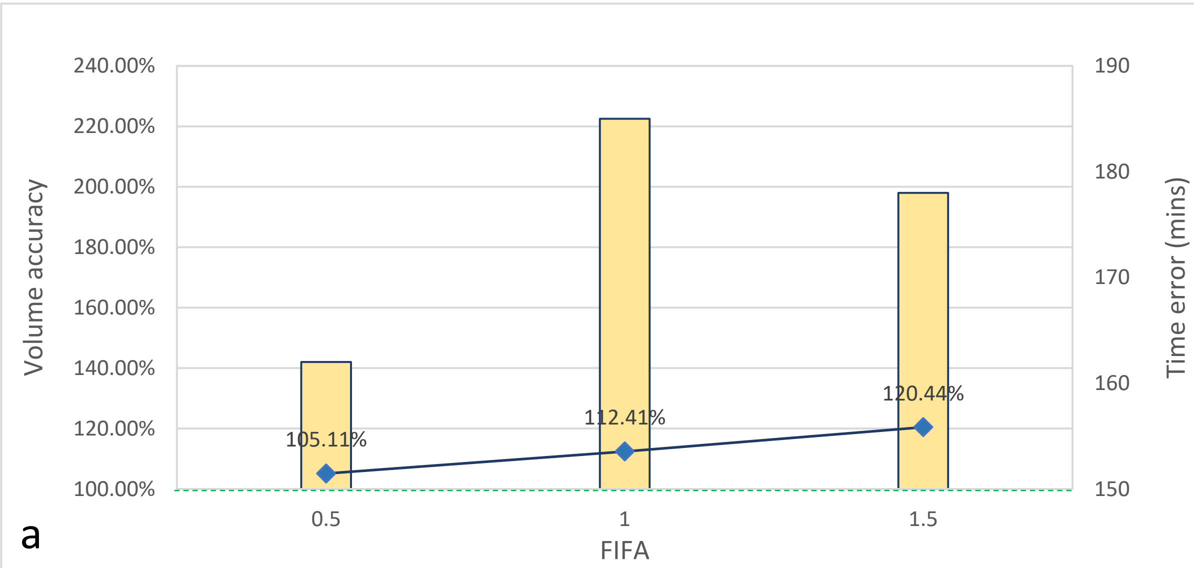

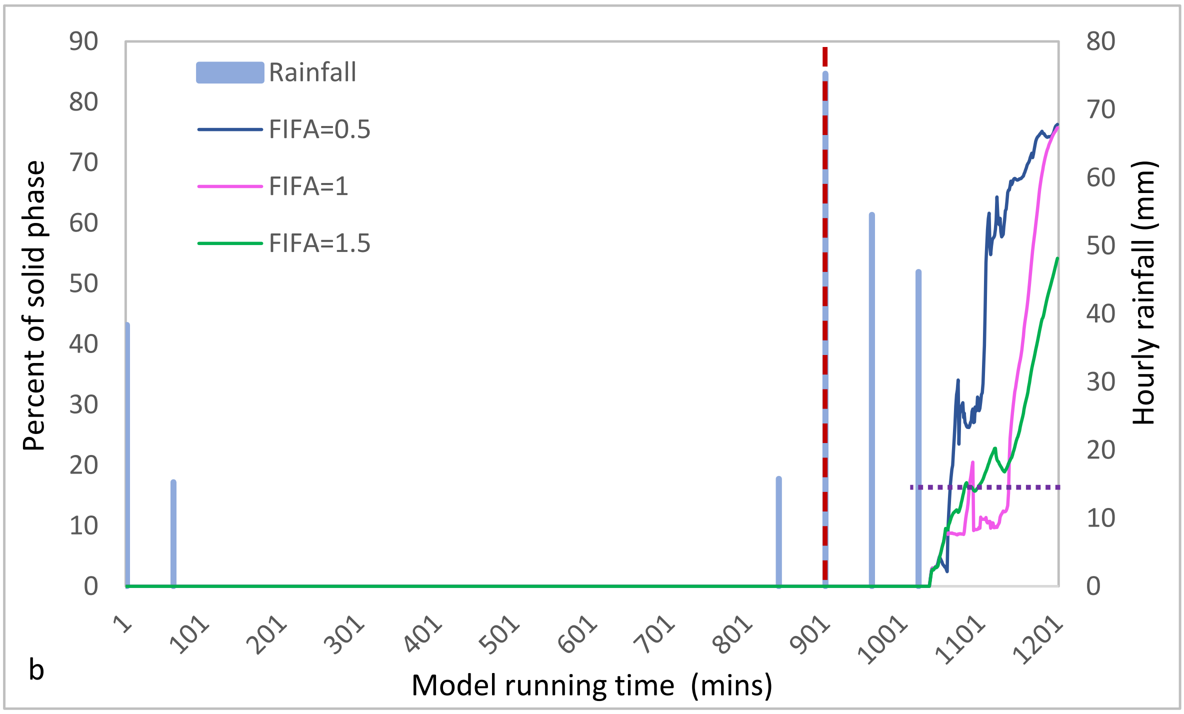

Figure 5-9. Bayi-Analysis B

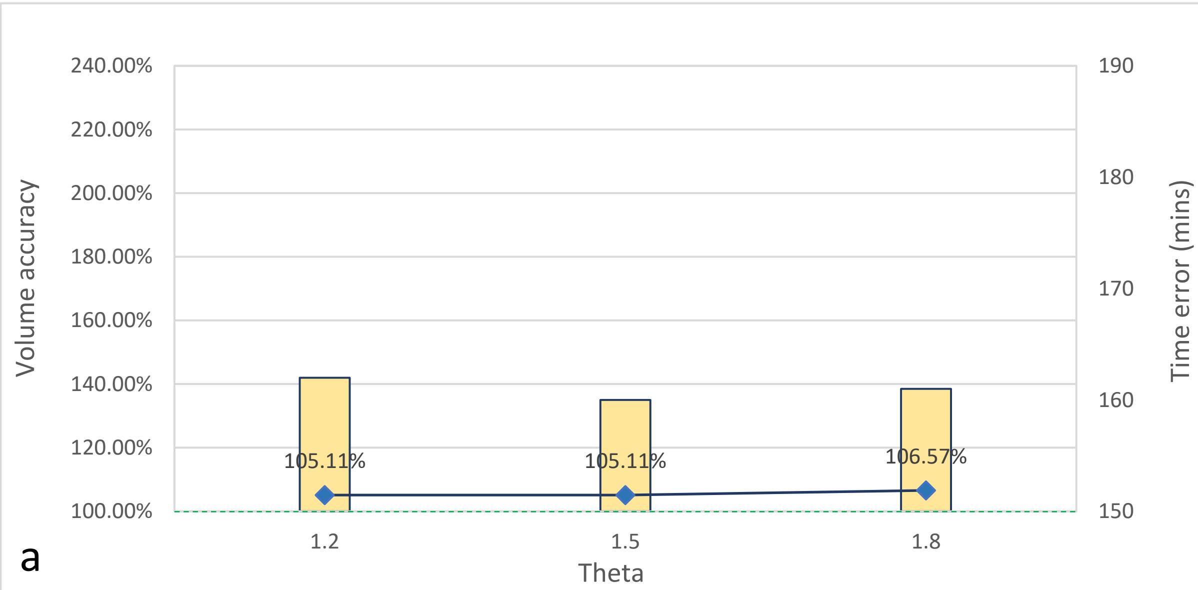

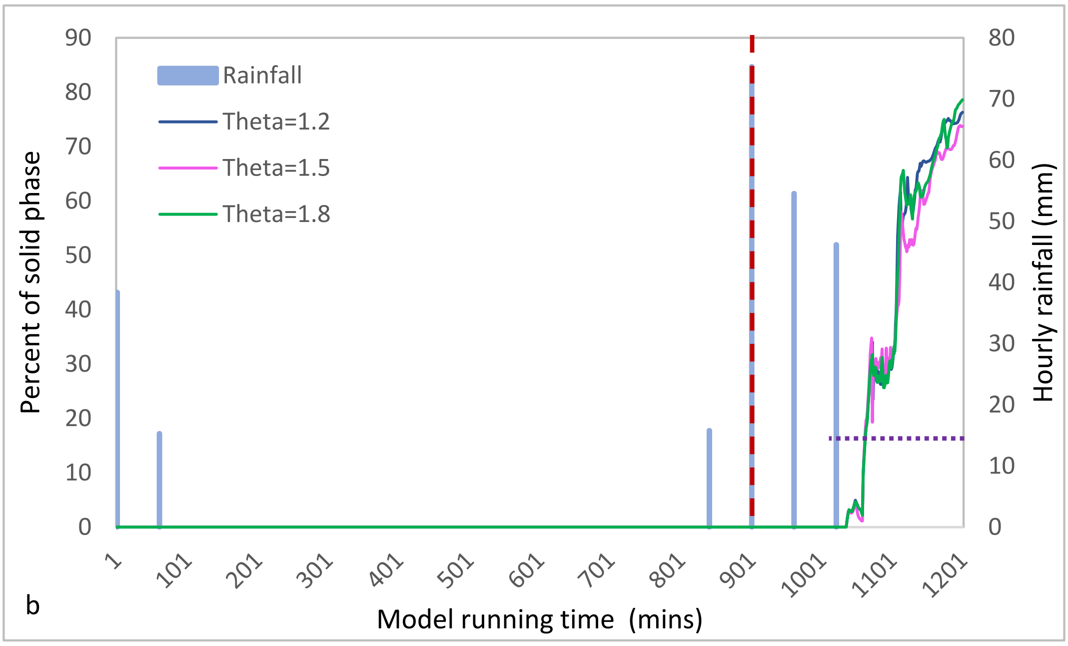

Figure 5-10. Bayi-Analysis C

Based on the results of the sensitivity analysis in the three watersheds, the following can be concluded:

- Out of the investigated parameters, only the entrainment coefficient (EC), Flow Internal Friction Angle (FIFA) have a significant influence on three modeled indicators: the arrival time of the debris flow, the total volume, and the solid fraction.
- The EC variations do not produce significant changes to the modeled arrival time, as was the same in the other two catchments.
- The EC variations are sensitive to the total volume in the three catchments in general. The entrainment process is critical to determine the final volume during the debris flow event.
- The best-defined value of EC is different in these three catchments. Entrainment processes are directly related to a change in basal topography. Entrainment at the steep slope is more significant. Also, the loose material stop in the channel can affect the entrainment. Comparing with Hongchun gully and Bayi gully, the Lianhuaxin gully is relatively flat. Thus, the calibrated EC is relatively higher than the other two catchments.
- The variations of FIFA also have influences on volume but not as sensitive as EC, which can be explained with the interaction between entrainment deposition and flow properties, and the effects of FIFA on volume is not as direct as EC.
- The effects of FIFA angle with respect to the modeled arrival time is varying in the different catchments. This case may be affected by the steepness of the gully. The flow internal friction angle is more influential at relatively flat slope than the steep slope, as the high kinetic energy of material may counteract the effects of flow internal friction angle at the steep slope

5.2. Calibration

This section introduced the processes of calibration for the three catchments, calibrated parameters, and outcomes. The calibration started in Hongchun catchment as only two parameters are influential for the calibrated results. This is followed by calibration in Lianhuaxin gully since the calibrated FIFA was fixed, and only EC required further fine tuning. Bayi gully is the last to be calibrated as the specificity of the rainfall lead to more trials were required in this gully. In *OpenLISEM Hazard* the calibration of parameters is operated by multiplying these input maps with a scalar value.

Table 5-4. Overview of the default multiplier of parameters (source: previous calibration in Hongchun)

	Parameters	**Value of multiplier**
Hydrology	Ksat slope	0.500
	Manning's N slopes	1.000
	Theta slopes	1.200
	Ksat channel	1.000
	Manning's N channel	1.000
Sediment	Erosive power	1.00
	Transport capacity	1.00
	Settling velocity	1.00
	Soil cohesion	0.50
	Grain size	1.00
Solid phase flow properties	Internal friction angle	0.30
	Dynamic viscosity	1.00
	Drag force	99.99
	Solid phase friction	1.00
	Release volume	1.00
Slope stability	Soil cohesion	20.00
	Internal friction angle	2.00
	Soil depth	0.90

Hongchun catchment

Due to the limitations of information (See Table 4-3), only the simulation of 2010 events were calibrated. According to the outcomes of the sensitivity analysis in this catchment, the model gave the relative highest volume when EC is 0.25 and FIFA is 0.5 (See previous section Sensitivity analysis and Figure 5-2), the combination of these two values is called calibration1. However, the relatively lowest time error was given when EC equals 0.35 and FIFA was 0.6 (see Figure 5-3), the combination of these two values is called calibration2. The most influential variables, EC and FIFA were changed as little as possible based on the results of sensitivity analysis. The outcomes of trials show that the changed parameters decreased the volume accuracy a lot but affected the arrival time slightly. Comparing the results of calibration1 (EC=0.25, FIFA=0.5) and calibration2 (EC=0.3, FIFA=0.6), the two calibrated results of arrival time are close (six minutes difference). Hence, the decision was made to minimize the volume error as excellent as possible. The results of the final calibration are shown in Figure 5-11 (a: maximum debris flow height; b: volume of deposited sediment). The calibrated parameters are shown in Table 5-5. Compared with the actual reported event, the calibrated model underestimated the total volume (7.11×10^5 m^3) with 6.54×10^5 m^3. The predicted arrival time in the model is around 5 hours earlier than the actual arrival time. Through visual interpretation (Figure 5-11), it was found that the simulated runout distance is close to the actual runout distance: both end up in the Min River. However, the modeled debris flow material was more widely distributed in the Min river than the actual event, including in the upstream part, as the model did not incorporate the powerful effect of the river.

Table 5-5. Calibrated multipliers in Hongchun catchment

Parameter	Hongchun	Lianhuaxin	Bayi
EC	0.25	0.4	0.2
FIFA	0.5	1	0.5
SIFA	2	5	2
Theta	1.2	1.2	1.2
Manning's N	1	1	1

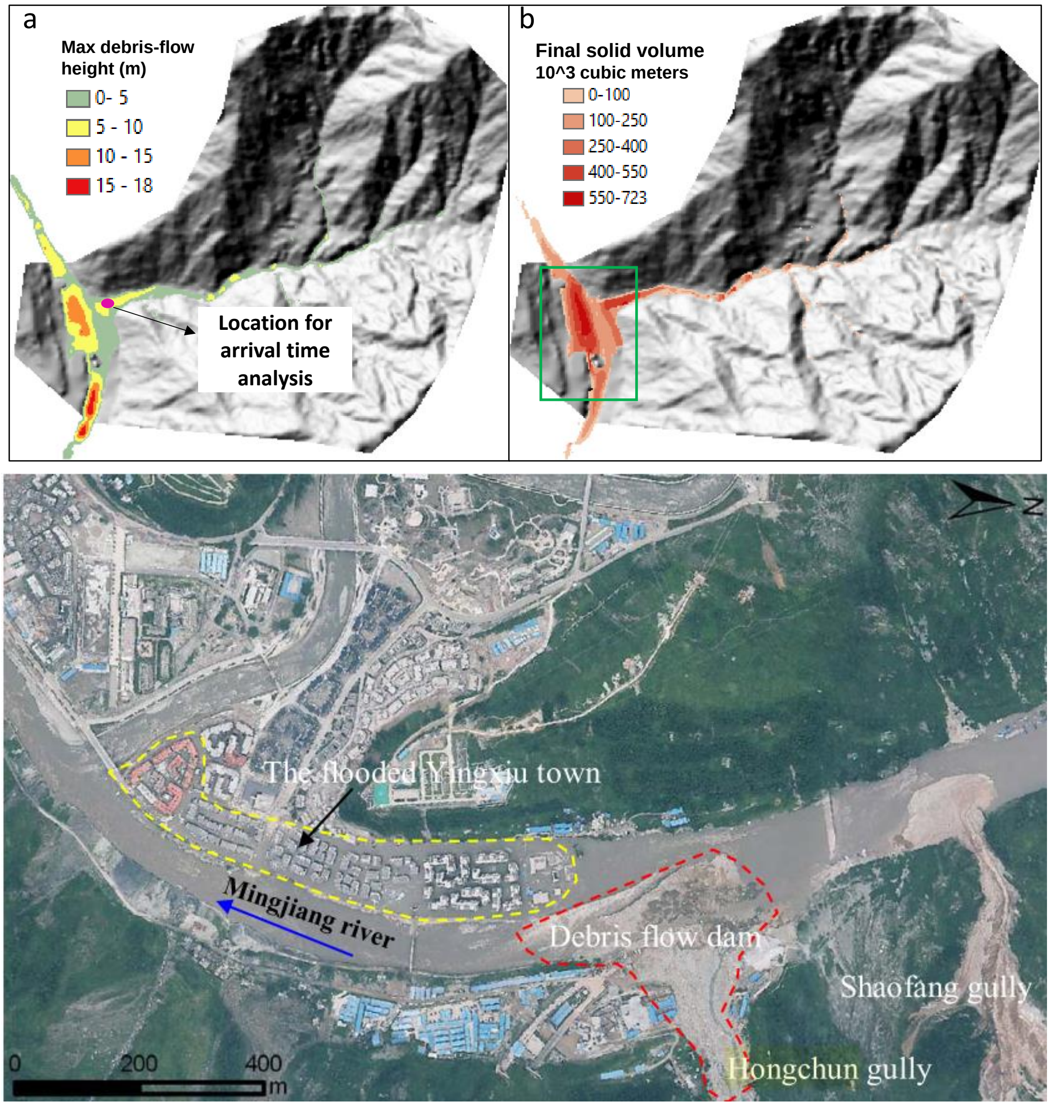

Figure 5-11. Hongchun-Results after calibration. The aerial photo was supplied by Sichuan geological environmental monitoring station (Xu et al., 2012)

Lianhuaxin catchment

Opposed to the results for Hongchun catchment, the model gave a good simulated arrival time in this catchment (calibration values were EC=0.4, FIFA=1, SIFA=2). Using EC 0.4 was also the best in terms of volume accuracy. Based on the results of the initial calibration, to further test if the modeling accuracy on volume could be improved, the EC was reduced a little (to 0.35). As a result, the volume accuracy was only improved a little (from 79.6% to 88.2%), whereas the time error sharply increased. The time error did not decrease while the model started to underestimate the volume and volume accuracy fell when the EC continued to be reduced. For debris flow early warning, explicit prediction of arrival time is much more important than the exact volume. Hence, the best results were from the initial calibration, as shown in Figure 5-12. The calibrated parameters are given in Table 5-5. The model overestimates the total volume (1.77×10^5 m^3), in contrast to the simulations for Hongchun, where volume was underestimated. The volume accuracy declines with 26.5% compared with the Hongchun catchment. By contrast, the error in arrival time is only 6 minutes in this catchment, which is considered very good. The boundary of the sediments in the Min River can be seen observed very poorly in the satellite image, also due to the fact that the Min River end in a reservoir and the materials are dispersed. The modeled debris flow heights in the river are quite low, as shown in the simulated debris-flow-height map. Besides, the simulated runout distance is close to the actual runout distance by visual interpretation. And the spread of debris flow material in the Min river is similar to the actual event.

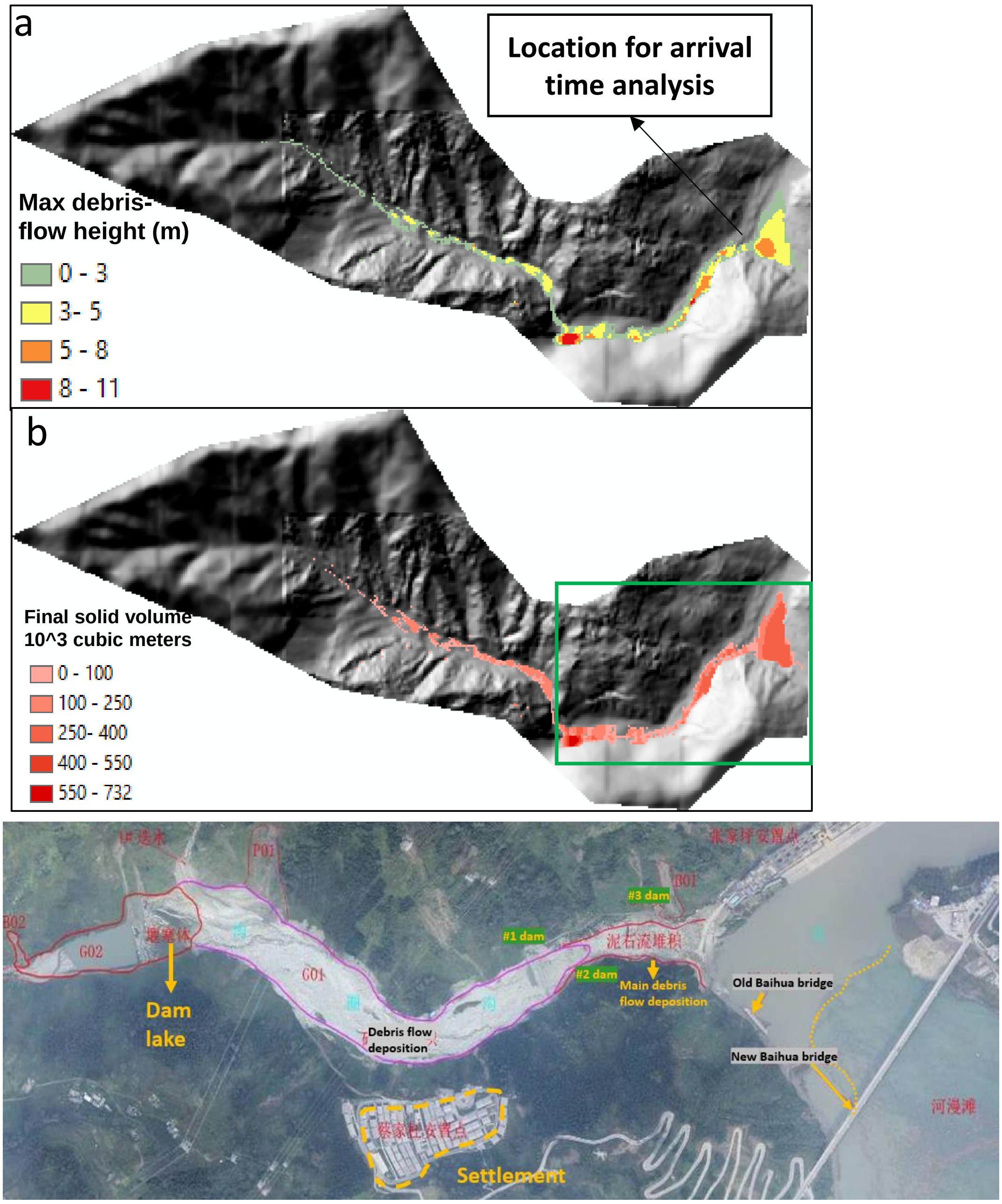

Figure 5-12. Lianhuaxin-Results after calibration. The 08-14 satellite image from unpublished investigation report represents the area in the green square

Bayi catchment

According to the results of the sensitivity analysis, an EC value of 0.2 is the best for volume accuracy, after which the model overestimated the volume a little bit. However, the effect of higher EC value on arrival time was insignificant. To further calibrate the model, the EC was reduced as little as possible. The volume accuracy is sensitive to the changes of EC. When EC dropped from 0.2 to 0.15, the accuracy decreased by about 34% (underestimation), but the difference of time error was only one minute. The rainfall lasted throughout the whole day on 12th August, so antecedent rainfall may affect the debris flow a lot. Hence, the initial water content was increased from 0.048 to 0.092 and 1.13 separately for calibration by changing initial input data rather than increase the calibration multiplier. However, the increase of initial moisture did not improve the simulated arrival time in this watershed. For Bayi it was easy to obtain a correct debris flow volume, while the calibration of the arrival time was difficult. The calibration results were given in Figure 5-13. The degree of overestimation of the volume is much lower than Lianhuaxin gully with only 0.07×10^5 m^3 (95.14%). By contrast, the predicted arrival time in this catchment is around one and a half hours later than the actual arrival time. The modeled runout length is shorter than the actual one, as the sediments stopped at the outlet area, whereas they moved further in the Dujiangyan reservoir in the real event.

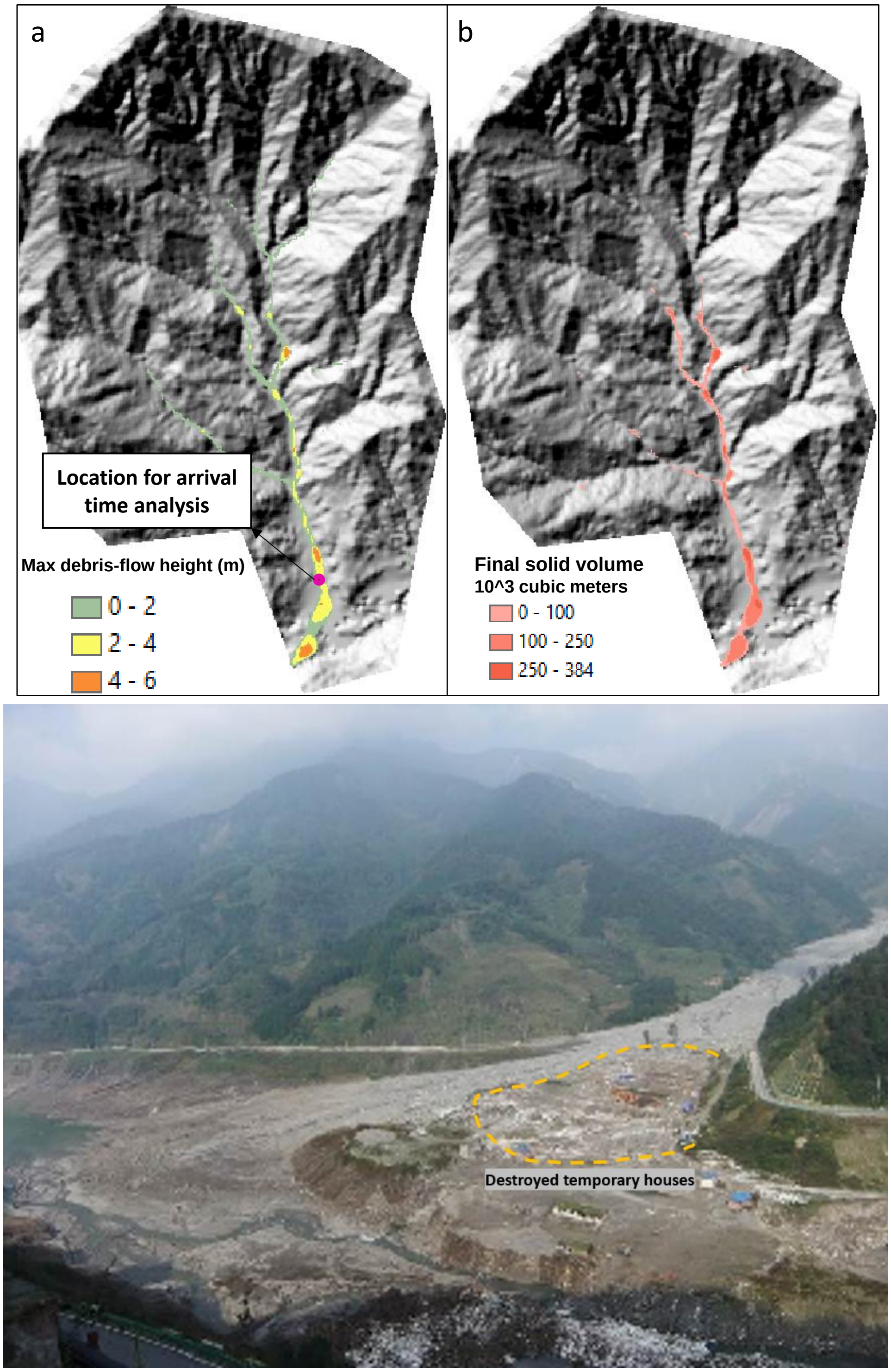

Figure 5-13. Bayi-Results after calibration. The photo after 0813 is from (Ma & Li, 2017)

5.3. Spatial transferability analysis

The parameter values used for spatial transferability analysis are given in Table 5-6 (codes were given to these three catchments, Hongchun: H, Lianhuaxin: L, Bayi: B). The results are shown in Table 5-7, and the resulting maps in Figure 5-14, Figure 5-15, and Figure 5-16. In terms of the modeled results in H, the calibrated parameters in L are higher than that in H, the model with calibrated parameters in L thus overestimated the volume while the influence on time error is small as the parameters are not sensitive to modeled time, and more sediment stopped in the channel with the increase of FIFA. Conversely, the calibrated parameters in B are as same as that in H except for EC, the calibrated model with calibrated parameters in B hence underestimated the volume due to the decline of EC, the changes of time error and runout distance are small. The calibrated parameters in H and B are lower than that in L. Hence, the calibrated models underestimate the volume significantly in L, and the decreasing EC and FIFA resulted in larger time error and less material stopped in the channel. Oppositely, the calibrated parameters in H and L are higher than that in B. Hence, the calibrated models overestimated the volume with the rise of EC, the effects of calibrated parameters in H are smaller than that of L. The modeled runout distance and time error did not change a lot as the parameters are not sensitive much in Bayi gully respecting these aspects. As the calibrated parameters in H and B are almost similar, the validation outcomes changed less between them compared with the outcomes with Calibrated parameters in L. In general, the results of cross-validation can indicate the affected scale and magnitude were impacted less by the transferred parameters. The volume accuracy decreased with calibrated parameters in other catchments. A low Cohens Kappa (0.02) was obtained in terms of volume accuracy. The effects of parameters on arrival time are not significant with a relative better Cohens Kappa (0.38), although the predicted arrival times in the model are generally unacceptable.

The results of spatial transferability analysis are rather expected. Based on the results of the cross-validation in the three watersheds, the following can be concluded:

- When the calibrated values are applied for the same watershed (yellow boxes in Table 5-7), the volume accuracies are always higher than when applying calibrated values from other watersheds.
- When using the calibrated values from other watersheds, the volume accuracy sometimes changes very drastically from overprediction to underprediction.
- EC is the most influential parameter to volume accuracy in space. The changes of volume accuracy with different calibrated parameters mainly depend on the variations of EC.
- The time error obtained when applying the original calibrated parameters is not definite the lowest.
- The smaller the differences between the calibrated parameters from the same catchments and that from other catchments, the smaller the changes of modeled results are.
- The changes between results obtained from original calibrated parameters and that from cross-validation are closely correlated with the values of parameters and the specific parameter sensitivity.

Table 5-6. parameters set up for cross-validation

Watershed	Calibrated parameters		
	EC	FIFA	SIFA
H: Hongchun	0.25	0.5	2
L: Lianhuaxin	0.4	1	5
B: Bayi	0.2	0.5	2

Table 5-7. Results of cross-validation

Modeled for watershed	Indicators					
	Volume Accuracy			Time error		
	Calibrated H	Calibrated L	Calibrated B	Calibrated H	Calibrated L	Calibrated B
H	91.98%	206.19%	71%	-306	-345	-293
L	66%	151.68%	42%	-170	+6	-143
B	135.04%	248.91	105.11%	+162	+161	+163

Note: "+" means delay; "-" means earlier; volume accuracy= (modelled volume/actual volume)×100%

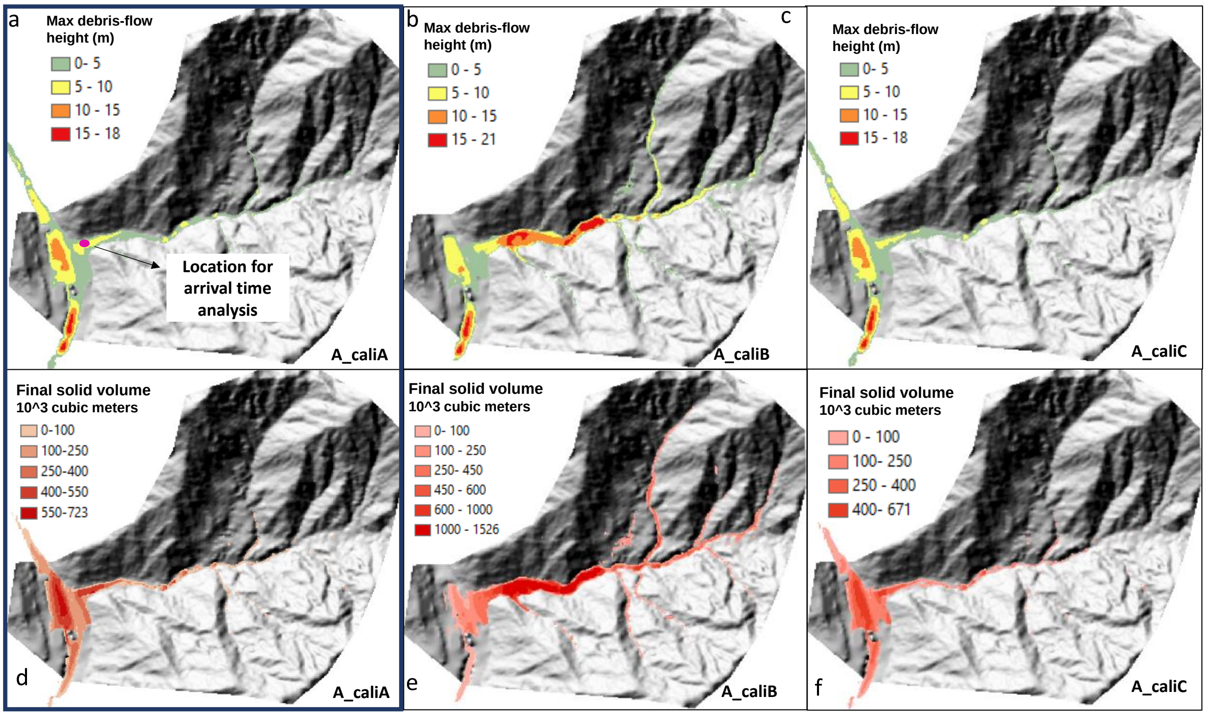

Figure 5-14. Results of cross-validation in Hongchun catchment. a,b,c: the max debris-flow height produced with Cali_H, Cali_L, Cali_B; d,e,f: the final sediment volume produced with Cali_H, Cali_L, Cali_B

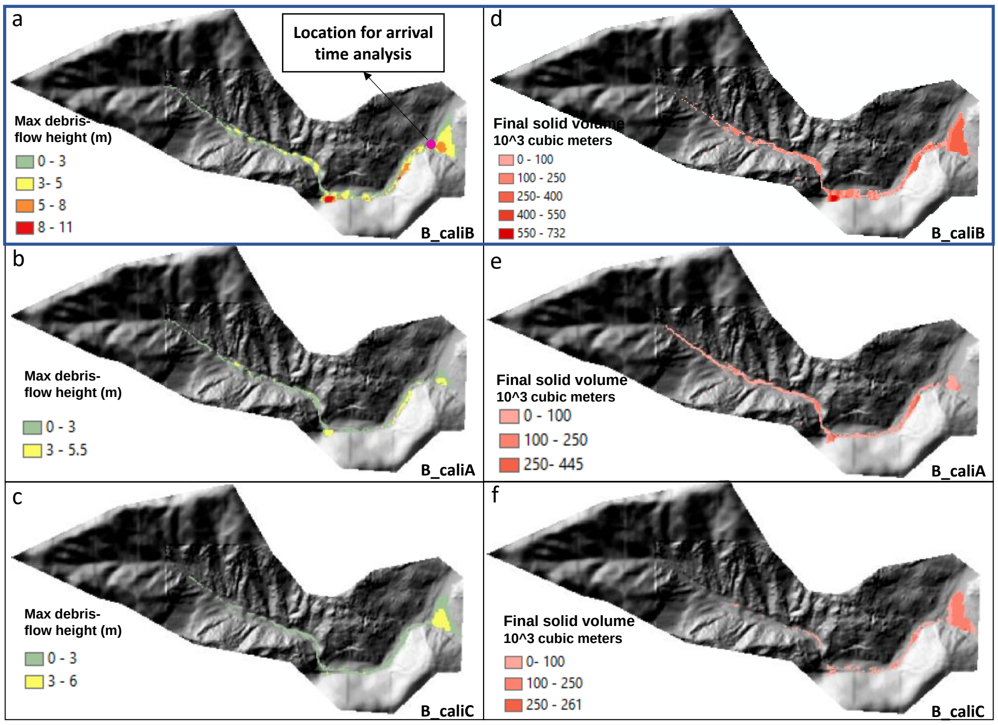

Figure 5-15. Results of cross-validation in Lianhuaxin catchment. catchment. a,b,c: the max debris-flow height produced with Cali_H, Cali_L, Cali_B; d,e,f: the final sediment volume produced with Cali_H, Cali_L, Cali_B

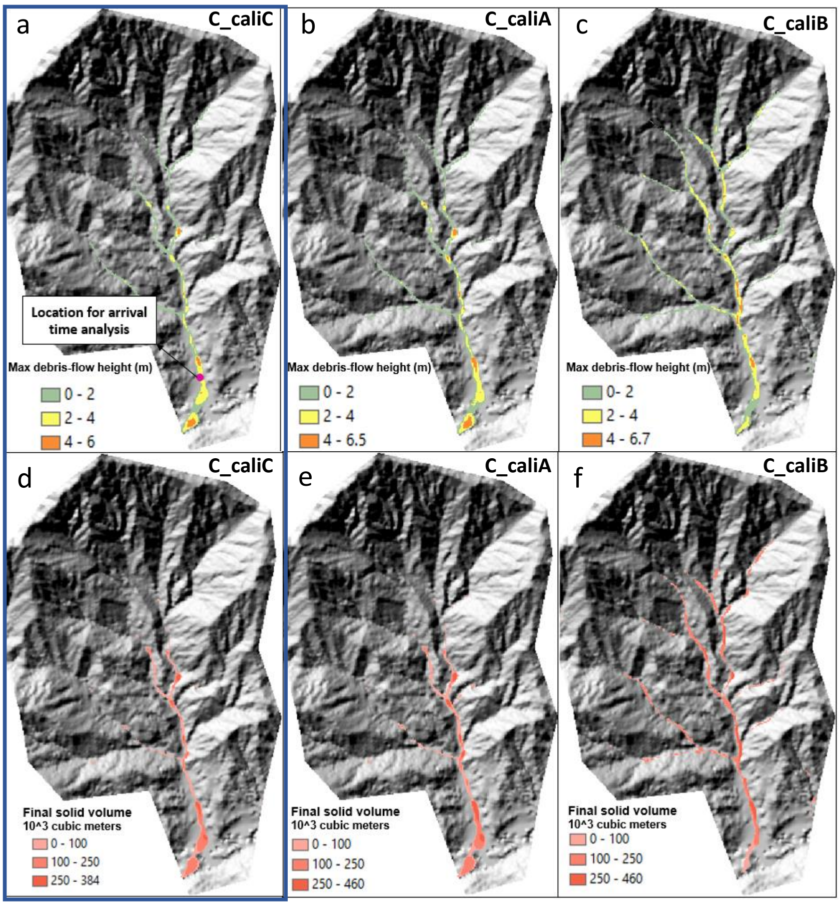

Figure 5-16. Results of cross-validation in Bayi catchment. a,b,c: the max debris-flow height produced with Cali_H, Cali_L, Cali_B; d,e,f: the final sediment volume produced with Cali_H, Cali_L, Cali_B Cali_C, Cali_A, Cali_B

5.4. Temporal transferability analysis

Hongchun catchment

The calibrated parameters for one watershed in 2010 were subsequently applied for other rainfall scenarios in different years. The related outcomes about temporal transferability are shown in Table 5-8, and in Figure 5-17. Generally speaking, this model can predict the occurrences of debris flows over time in this watershed. The calibrated parameters made the model give a five-hour earlier warning in the 2010 scenario while they allowed the model to produce an excellent arrival time in the 2011 scenario. The earlier warning means there is enough time to take action in advance. If the model predicts the debris flows exactly on time, there is at most one hour for evacuation as debris flow material takes around one hour to transport to outlet area from the initiation area in this region (Guo et al., 2016). In this case, predicted rainfall should be used for model running rather than measured rainfall to leave more time for evacuation. The model can predict debris flows triggered by two-types of rainfall (Figure 5-17), namely short and intense rainfall (rainfall events in 2010,2011,2012), and long stable duration rainfall events (rainfall event in 2013). Besides, the arrival times of debris flows under any scenario in the model are close (2010: 174th minutes; 2011: 130th minutes; 2012: 127th minutes; 2013: 129th minutes) and the shapes of the lines are similar (Figure 5-18). Normally, the percentage of debris flow material can witness an increase then a decrease to indicate the occurrence of debris flows. However, the percentage of solids did not go down within the modeled timescale in this study. The location for time analysis can account for this question that most debris flow material stopped at the outlet area at the end, so the percentage of solids at the outlet area kept a high value within a long time.

Table 5-8. Hongchun-Outcomes under different rainfall scenarios

Year	Prediction of occurrence	Volume accuracy	Time error	Modeled time (mins)	Modeled volume (10^5 m^3)
2010	TP	91.98%	-306	174	6.54
2011	TP	?	+10	130	1.72
2012	FP	?	?	127	2.54
2013	TP	?	?	129	3.95

Note: “TP”: True Positive: the model predicted the actual debris flow; “FP”: False Positive: the model predicted a debris flow but no event was reported; “?”: debris flow happened but no detailed information available to check; “-”: earlier; “+”: delay

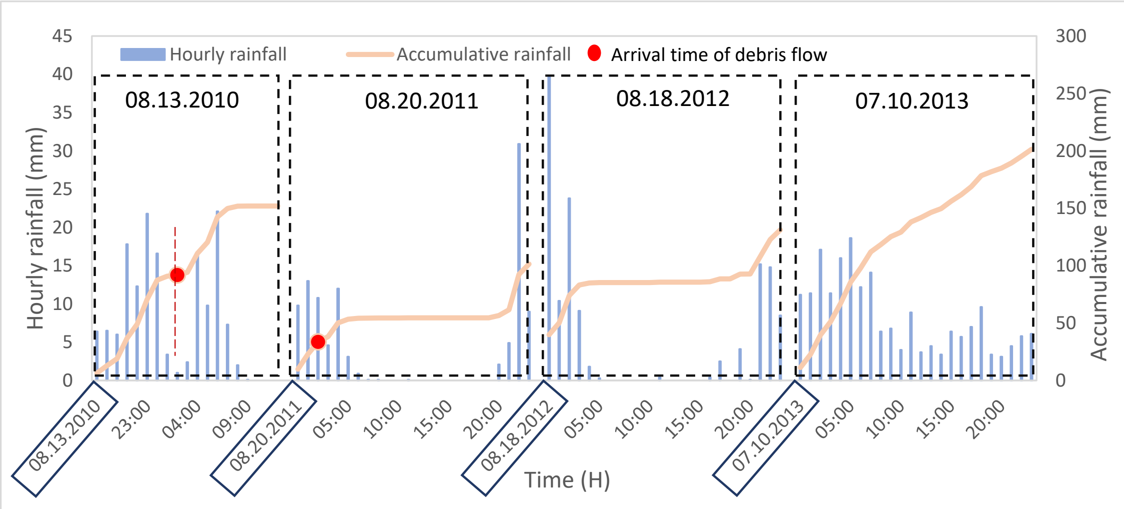

Figure 5-17. Hongchun-Rainfall scenarios in different year

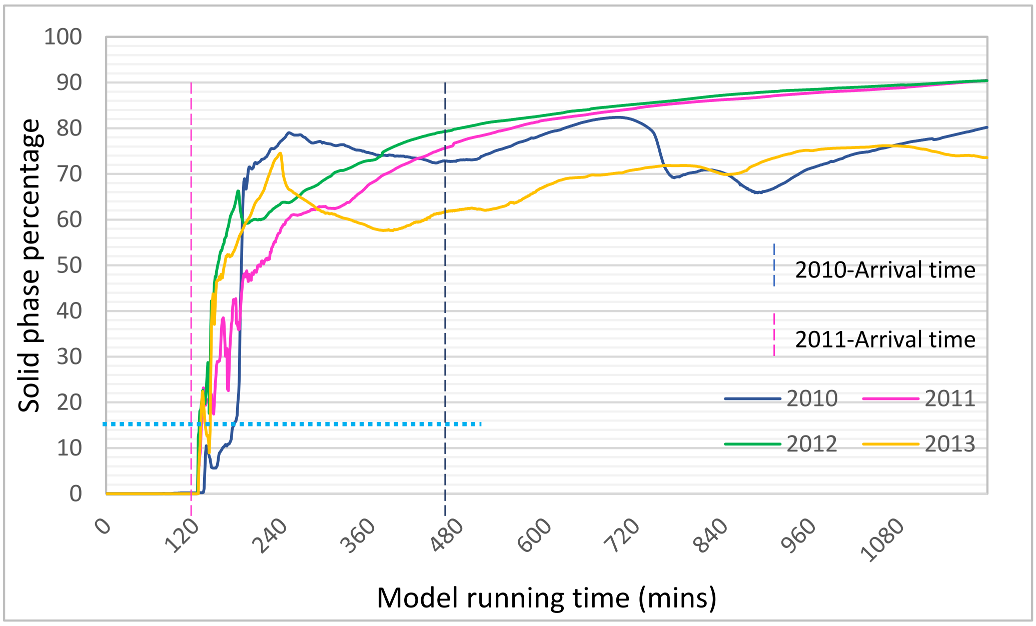

Figure 5-18. Hongchun-Changes of solid phase over time under different scenarios

Lianhuaxin catchment

The outcomes with the calibrated parameters for the 2010 event for the different rainfall scenarios in the following years are presented in Table 5-9. The model predicted the debris flows in 2010, 2011, and 2013. The modeled results in 2011 and 2013 show that some sediments deposited in the Min river. The results agree with the reality that the roads in the outlet area were destroyed (Table 3-3). Although the model produced material movement in the 2012 scenario, only little material (0.42×10^5 m^3) was moved during the simulation in the channel. Limited sediments stopped at the outlet area (as the percentage of solid material is around 11%, it cannot be defined as debris flow) Figure 5-20. When the solid-phase-percentage lines were put together, it is similar to the Hongchun catchment that the simulated arrival times are close to each other (2010: 486 minutes; 2011: 498 minutes; 2013: 454 minutes). And the lines are shaped similarly, especially the section before the percentage of solid sediments over 15% (Figure 5-20). Figure 5-19 illustrates the triggering rainfall events in different years. The rainfall in 2011 looks like that in 2012, and the duration of the triggering rainfall in 2013 is longer. The type of rainfall shows no effects on the shape of the solid-phase-percentage line as the line of 2010 is analogous to that of 2011, while the line of 2012 is absolutely different from that of 2011.

Table 5-9. Lianhuaxin-Outcomes under different rainfall scenarios

Year	Prediction of occurrence	Volume accuracy	Time error	Modeled time (mins)	Modeled volume (10^5 m^3)
2010	TP	151.68%	+6	486	2.26
2011	TP	?	?	498	0.42
2012	TN	-	-	-	0.54
2013	TP	?	+4	454	1.03

Note: “TP”: True Positive: the model predicted the actual debris flow; “TN”: False Positive: the model predicted a debris flow but no event was reported; “?”: debris flow happened but no detailed information available to check; “-”: debris flow did not happen; “+”: delay

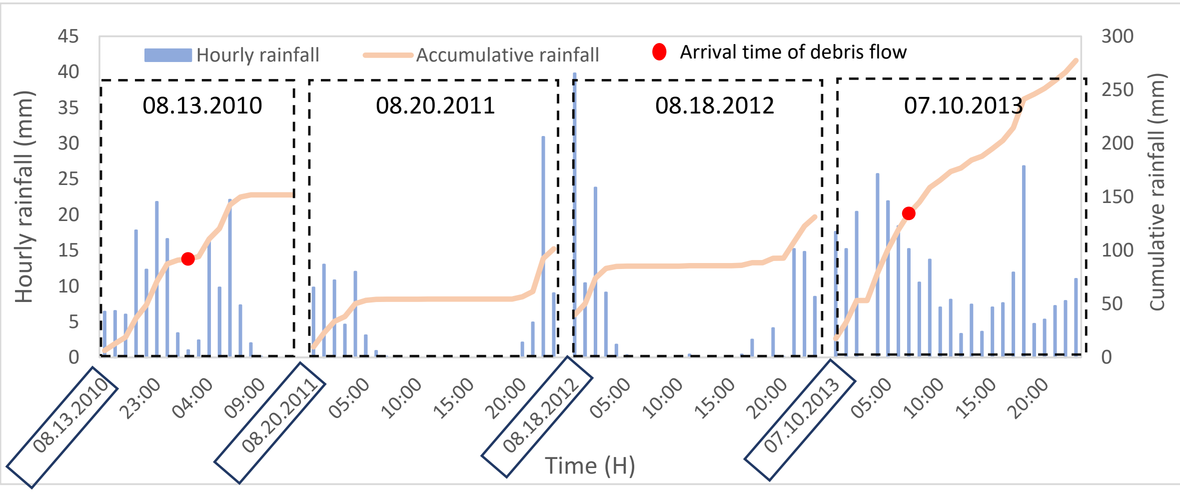

Figure 5-19. Lianhuaxin-Changes of solid phase over time under different scenarios

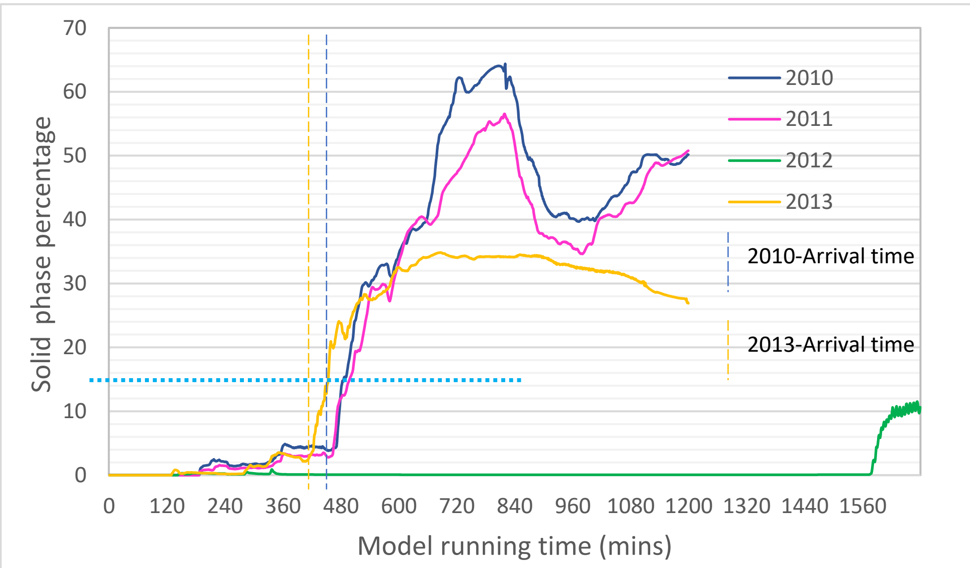

Figure 5-20. Lianhuaxin-Changes of solid phase over time under different scenarios

Bayi catchment

The results of the modeling in the Bayi watershed for different years are listed in Table 5-10. The different rainfall scenarios are shown in Figure 5-21. The patterns of the three rainfalls are all quite different. The triggering rainfall in 2010 experienced over ten-hour blank rainfall periods between the intense hourly rainfall. The intensity of triggering rainfall in 2011 was lower, and the interval of rainfall was not as long as that in 2010. Adversely, the rainfall in 2013 was more stable and low-intense on the whole. The rainfall pattern affected the shapes of solid-phase-percentage lines visibly in this catchment (Figure 5-22). According to the debris flow inventory, there were no debris flows happened in 2011 and 2013. The model predicted a debris flow under the 2011 scenario. However, the total volume of this event was low with only 0.44×10^5 m^3. Most sediments just moved and stopped in the channel, and limited material was sedimented close to the outlet area. In reality, the debris flow materials blocked the road at the outlet area. The model did not produce debris flows in 2013 when there was no debris flow happen.

Table 5-10. Outcomes under different rainfall scenarios

Year	Prediction of occurrence	Volume accuracy	Time error	Modeled time (mins)	Modeled volume (10^5 m^3)
2010	TP	105.11%	+162	1062	1.44
2011	TP	?	?	609	0.44
2013	TN	-	-	-	-

Note: “TP”: True Positive: the model predicted the actual debris flow; “TN”: T Negative: the model did not predict a debris flow and no event was reported; “?”: debris flow happened but no detailed information available to check; “-”: debris flow did not happen; “+”: delay

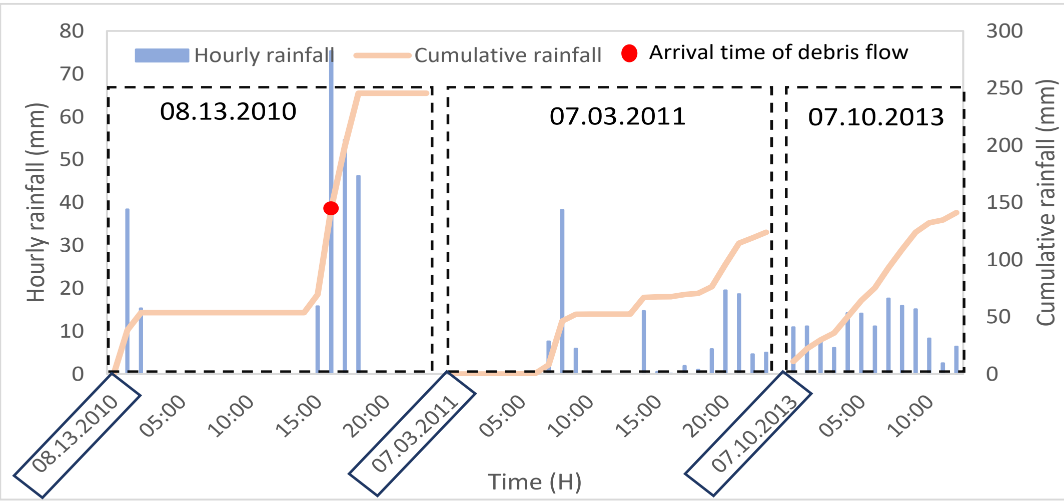

Figure 5-21. Rainfall scenarios in different year

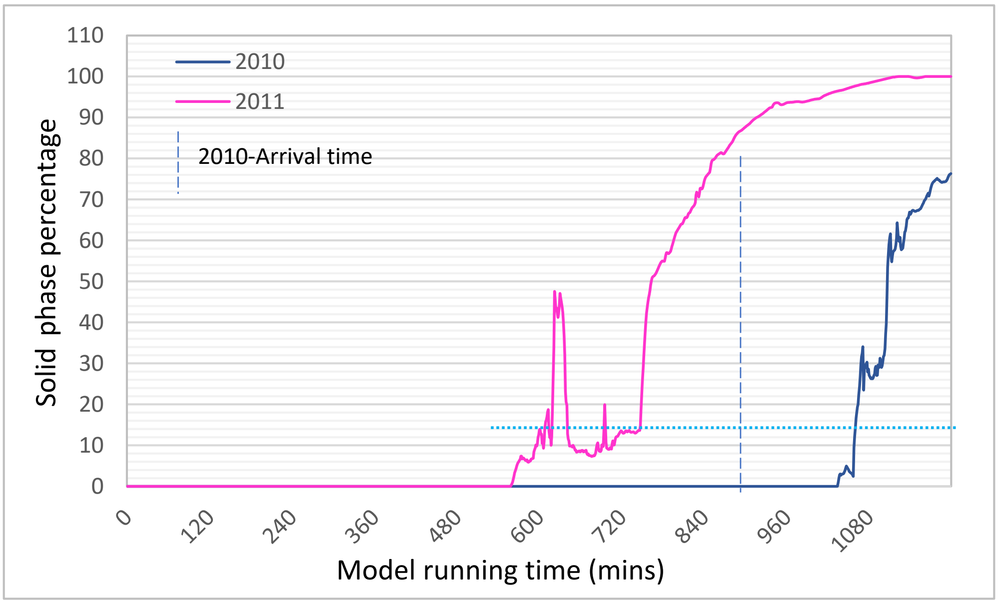

Figure 5-22. Changes of solid phase over time under different scenarios

6. DISCUSSION, CONCLUSIONS AND RECOMMENDATIONS

6.1. Discussion

This section discusses the key findings and the main limitations of this study. The following critical findings will be discussed:

1) The sensitivity of parameters is not only specific in different models but also specific in different watersheds;
2) The model is not transferable between catchments in space respecting prediction of debris-flow volume, runout distance, and arrival time;
3) The model is capable with the applicability over time to predict the occurrence of debris flows in one catchment;
4) The significance of the rainfall pattern to the arrival time is weakened in this model. But rainfall is still a critical aspect to predict the exact arrival time of debris flow;
5) Overall aspects related to the use of the physically-based model for debris flow early warning.

The outcomes of the parameter sensitivity analysis indicate that the sensitivity of parameters is specific not only for the specific model used (*OpenLISEM Hazard*) but also in the different watersheds. Contrarily, most previous research only evaluated the sensitivity of the parameter in terms of the model without considering the watershed-variability of parameters (Hessel et al., 2002, 2003; Mergili et al., 2012; Zieher et al., 2017). There is a variety of effects of these parameters on different watersheds. The entrainment coefficient and internal friction angle provide significant changes to the spatial transferability of parameter values. Even though it was initially thought that the study catchments have a good similarity, there are still some differences between them. One important difference is the slope that the average slope of Lianhuaxin is flatter than other two gullies. As shown in the section of Sensitivity analysis, the entrainment coefficient and flow internal friction angle are more sensitive in the Lianhuaxin gully than in the other two, and the calibrated entrainment coefficient is higher than the other two gullies. And the arrival time in the Lianhuaxin catchment is significantly affected by the flow internal friction angle. While these parameters have limit or no effect in the other two catchments. Another major difference between them is the vegetation that the quantity of vegetation in Hongchun is less than the other two gullies. Hence, theta is extreme sensitivity to the reproduction of debris flow processes in Hongchun while it is insignificant in the other two gullies.

The scores of Cohen's kappa respecting the volume (0.02) and time accuracy (0.38) (section of Spatial transferability) show that the spatial transferability of parameters between these simulations is not very high. This is caused predominantly by the entrainment coefficient, which is the most influential parameter to the modeled volume. Its effects can dominate the impacts of other parameters on volume accuracy. And the slight differences between calibrated EC in different catchments can result in a strong decrease in volume accuracy. In terms of the spatial transferability respecting arrival time, the calibrated parameters are insensitive to the modeled arrival time in the study sites except for Lianhuaxin gully. The Cohen's kappa with respect to time accuracy is better than that of volume accuracy. This result contradicts the claims of Shrestha et al. (2007) that the calibrated parameters are transferable between watersheds in a similar physiographic region. But only discharge was evaluated in Shrestha's research. Besides, the prediction of the debris-flow volume based on calibration is an achievable and most reliable goal that the model can achieve. At least the model can indicate the affected areas generally with calibrated parameters from other catchments. In fact, the exact prediction of the volume is not much critical for early warning as it will not affect the decision of evacuation. The spatial transferability regarding arrival time is acceptable as the parameters are insensitive to modeled arrival time besides Lianhuaxin. However, the performance of the model on the prediction of the exact arrival time is not very good, and the model results are specific in different watersheds. For the Hongchun catchment, the model always gave a warning earlier than the actual event. By contrast, the model always presented delayed warning time in the Bayi catchment. In the Lianhuaxin catchment, the calibrated models with calibrated parameters from other watersheds gave earlier warning time of actual event. Actually, It is better to predict earlier warning than the exact time for warning as the former one can leave more time to react and evacuate. Besides, the influences of the parameters on the arrival time are watershed-specific in space.

The temporal transferability of the model respecting arrival time and debris flow occurrence is different from what was expected. The application of the calibrated model for the 2010 event to later event resulted in correct predictions of the occurrence of debris flows. We didn't expect this since the conditions in the watershed had changed considerably in the years after the earthquake. In line with this result, although for a completely different process, Macdougall & Flowers (2011) found a model for glacier melt that could be applied over time without recalibration. The *OpenLISEM Hazard* model gave the accurate arrival time even with calibrated parameters in different years in the Hongchun and Lianhuaxin catchments. Although the problem of overestimation exists for the occurrence of debris flows. And the one over-predicted debris flows in Lianhuaxin cannot be defined as debris flows absolutely as the few materials just moved in the channel, the percentage of sediment that deposited close to the outlet is only 11%. This problem might be alleviated by decreasing the entrainment coefficient, which should be reduced due to two reasons. The first one is that the calibrated entrainment coefficient in 2010 overestimated the volume of the debris flow that happened in the same year. The second reason is that a lot of loose material transported to the outlet area during previous debris flow processes, less loose material either in the channel or on the slope can contribute to the entrainment process during later debris flow. Besides, it is remarkable that the arrival times were reported at the same model-running times in the Hongchun and Lianhuaxin catchment under different rainfall scenarios. Two possibilities might be able to answer why the arrival time occurred at a similar model-running time in different rainfall scenarios. The first one is that the effects of the rainfall patterns were weakened in this model. However, the influences of the rainfall pattern on time were presented in the Bayi gully. Another reason is that what this study analyzed was the arrival time, which not only relies on the rainfall pattern but also the soil properties and slope. Hence, the soil properties and slope may play a significant role in determining the arrival time. However, there is basically limited soil information available and large uncertainty in relation to the considered changing factors over time exist. And *OpenLISEM Hazard* is missing groundwater dynamics, also based on earlier rainfall is done very simply. More extensive and detailed analysis should be done on how influential the soil properties to the time prediction.

Comparing the rainfall scenarios 2011 and 2012 in Lianhuaxin, and 2012 and 2013 in Hongchun, we can find the similar rainfall events (2011 and 2012 in Lianhuaxin) performed differently in the model that rainfall in 2011 triggered a debris flow while that in 2012 did not. While the rainfall events with different patterns (2011 and 2012 in Hongchun) gave the arrival time of debris flows at a similar model-running time in the model. Hence, it seems that the integrated effects of the rainfall pattern were weakened in this model. Rainfall intensity is a very significant aspect to induce debris flows, and the model almost produced debris flow in any rainfall scenarios with relatively intensive rainfall, but the model did not produce debris flow in Bayi in 2013. Hence, more tests are required to check whether the model is built so that it may be easier to produce debris flows with lower precipitation threshold. Besides, the different patterns of triggering rainfalls show no effects on the transferability of the parameters of the model. The calibrated parameters in Bayi did not show significant effects on the other two watersheds, especially related to time. And the calibrated parameters from the other two watersheds did not affect the modeled arrival time in Bayi. Calibrated parameters seem to be applicable under different rainfall events over time. However, the influences of antecedent rainfall are difficult to really take into account in the model as *OpenLISEM Hazard* was designed to run with a short time scale.

When the physically-based models are applied for debris flow early warning, there are several aspects that need to be considered. The first one is to determine ROC curves (receiver operating characteristic curves) for the prediction of debris flows. The purposes of it are to figure out how often does the model predict debris flow correctly, how often does the model predict but there is no debris flow, and how often was there a debris flow that was not predicted. To obtain the curves, the model needs to run for many days to calculate the false positive rate and the false negative rate. However, it would be problematic as the model runs are time-consuming, and there is no sufficient information to support the calibrations. And uncertainties exist in the reported information for calibration, such as volume, time of occurrence, etc. The solution to this problem heavily relies on excellent debris flow inventory. Nevertheless, the model performed well on the prediction of debris flow over time in this study. Besides, rainfall is a significant but problematic issue for the prediction of debris flows in the model. The spatio-temporal variability of rainfall patterns in the mountainous area plays a critical role in affecting the prediction of debris flows in the model. To overcome this, the measures for collecting rainfall data should be improved to eliminate the variabilities. And with rainfall measurements, we can only do now casting rather than forecasting. Hence, the model needs to run with predicted rainfall that has even more spatial issues and uncertainties. The question of how the model performs with predicted rainfall only can be answered in practice. However, the results show that the transferred model in space and over time was functional to predict the occurrence of debris flows in different rainfall scenarios. The last aspect is how to use the outcomes from the model. If the model predicts the arrival time of debris flows correctly or too late, then there is too little time or no time to take action, and the early warning is not effective. Thus, only when the prediction is ahead of the actual debris flow, and always ahead, then the warnings given by the model can be used effectively. Besides, the warning should be delivered firstly to related institutions to further check the reliability of the warning by considering the antecedent rainfall, the rainfall threshold, and information delivered monitoring devices (if they are in function) synthetically. After that, the warning should be communicated to the people at risk to move to safer places temporally. It is possible that the model gives many false positives to make people relax their vigilance. In this case, the model should be recalibrated with recent debris flows and the input parameters should be updated with measured data in the field. Actually, regular updating should be carried out over time as the soil properties change significantly either in a long period or by human activities.

Some limitations hindered the spatio-temporal applicability of the model in debris flow simulation, respecting volume and time prediction, which will be explained further below:

1) The lack of adequate input data;
2) The lack of adequate validation data;
3) Errors and uncertainties related to the calibration data;
4) The uncertainties of rainfall data;
5) Uncertainties related to the assumption of variables over time;
6) The limitations of the model caused by the model assumptions.

The lack of adequate input data

The lack of input data was a major limitation in this study, which was not expected at the start, as this is one of the most studied areas in relation to post-earthquake debris flows in the last decade. However, limited field investigation for soil properties has been done in the gullies except for Hongchun, the soil properties used in most previous research are from the soil investigation in another gully (Shaofang gully) in the Wenchuan area after the earthquake. Even if there are some field measurements have been done in the other two catchments by local engineering companies, the reliability of the dataset is hard to ensure. And no field works have been done to update the soil properties over time. Besides, time-series elevation data is unavailable in the study area. To overcome this, the data from neighboring catchments were adopted to present the soil properties in these watersheds. The DEM used for modeling in Bayi is the previous elevation data, while the DEM used in Lianhuaxin and Hongchun were derived in 2014, 2017. The depth of the soil layer was estimated by physical and empirical relationships. And the depth of loose material was derived from depths of co-seismic landslides. The geotechnical and hydrological properties of soil are averages taken from literature values. The question is: can these mixed datasets extracted from different catchments, and different times approximately represent the real geo-environments? Of course, these data are imperfect but using imperfect data for debris flow research is reality. It is hard to answer how largely the input data affect the modeled result. However, it is the best estimation we can do for the input data.

Besides, the advantages of the *OpenLISEM hazard* model were not taken fully into consideration due to the scarcity of some input data. Various factors are integrated in this model for slope stability analysis, such as surface objects, root cohesion of different vegetation, and spatial variability of soil properties, etc. In this research, the influences of engineering objects such as check dams were excluded, the root cohesion and soil properties were treated as averages value across the whole watershed, and very limited samples for soil properties measurements were collected from deposited loose sediments or the channel in the different watersheds. These may influence the simulated volume and runout distance. Besides, the *OpenLISEM Hazard* software can also simulate the changes in the groundwater situation. This was not done for the watersheds before the debris flow simulation in order to simplify the work, as the model running time would be too large. Therefore, the influence of antecedent rainfall was ignored.

The lack of adequate validation data

The lack of calibration data and validation data also hindered the transferability analysis. Limited information on the actual debris flow occurrence times in time series, and the magnitude of the debris flows was recorded correctly, some of which only can be collected in the news. The reliability of this kind of data source is hard to check. And it is more difficult to collect the information for small debris flows. The cross-validation could not be carried out always to analyze the temporal transferability of parameters. And the most influential parameters regarding temporal transferability could not be evaluated due to a lack of accurate debris flow occurrence time and volumes. And after 2010, the government constructed large debris flow mitigation works in the watersheds. Hence, the model calibrated in 2010 should be recalibrated. However, there are no more recent debris flow events to calibrate them with. So, the debris flow prediction for post-construction time periods is difficult.

Errors and uncertainties related to the calibration data

Errors and uncertainties are involved in the reported data on debris flow volume and occurrence time. The actual volume was estimated roughly from either satellite images or changes of DEM by local engineering companies and previous research (e.g., Tang, 2019). The estimated volume does not precisely present the actual volume. For example, in the Lianhuaxin catchment, the debris flow material deposited in the dammed lake was not included in the final volume. However, the model did not consider the rupture of the dam lake. Hence, the model overestimated the final volume compared with the actual volume. The accuracy of volume prediction was affected. Also, the reporting times of debris flows were ambiguous. The source of time reporting is critical for the assessment of the accuracy of the time prediction using the model. For instance, the arrival time was defined as the time when local people heard the noise, or when local people saw the moved material around the outlet area, and then reported it to the local government. This time may have considerably errors. This may have led to either underestimation or overestimation of time in the model. Yang et al. (2019) suggested that the time recorded in the inventory refers to the arrival of the sediments in the outlet area. And in most catchments, the debris flows were able to reach the outlets from their initiation points within one hour (Guo et al., 2016b). Although video cameras had been installed in the gullies after the earthquake, most of them were destroyed in previous hazards or was not in function. Thus, there were no time records for debris flows in 2011 and 2013. The times used for these debris flows were derived from the news. The details of the information were unavailable.

Besides, the calibrations in this study were conducted manually, only using a limited number of model runs. Hence, parameters were only tested with limited values. However, equifinality that different compositions of parameters may result in similar results may lead to different results of the cross-validation. This is an inevitable limitation in the transferability analysis in this study.

The uncertainties of rainfall data

An important condition for the transferability of simulation parameters and accurate time prediction is the accuracy of rainfall data. The employed rainfall recordings were from rain gauges established within the catchment channel or near the catchment. Significant spatial and temporal variations may exist in one watershed, as patterns of rainfall in mountainous areas are extremely inhomogeneous (Marra et al., 2017). Yang et al. (2019) indicated that these rainfall recordings are not equal to the actual triggering rainfall events and cannot promise the runout distance. How much the errors in the rainfall scenarios can affect the final modeled results is hard to answer due to a lack of available high-resolution spatial rainfall patterns. It is believed that calibration is effective in decreasing the effects of rainfall data as much as possible.

Uncertainties related to the assumption of variables over time

The changes of elevation, depth of loose material, vegetation cover, and root cohesion over time were considered based on modeled results from last debris flows in the study. How exactly they can present the actual changes over time is unknown. And grain coarsening also plays an important role in the processes of debris flows (Domènech et al., 2019). However, this aspect was not considered in this study. Besides, the dynamics of the entrainment coefficient are more complex than the changes with the variables. Nevertheless, the assumptions were made as proper as possible in this study. And the model performed well in the prediction of debris flow occurrence over time.

The limitations of the model caused by the model assumptions

OpenLISEM hazard is an event-based model, thus neglects the long-term physical processes, such as lateral groundwater flow and evaporation. These processes are related to slope stability simulation in the model if considered over a long period. However, the occurrences of debris flows are not only controlled by the triggering rainfall as also other factors are relevant such as the influences of previous rainfall. Cornelis and Gabriels (2003) indicated that surface moisture affect the entrainment of soil by wind significantly, although it is hard to quantify. Iverson et al. (2011) proposed that the momentum grows pronounced during entrainment at wet bed sediment. It is worth to further study the relations between initial moisture patterns to entrainment prediction during debris flow processes.

6.2. Conclusions and recommendations

The purpose of this study is to analyze the spatio-temporal transferability of the physically-based model with respect to the volume, runout distance, and arrival time, which are useful criteria in debris flow early warning. To achieve this goal, the input geotechnical and hydrological parameters were collected from previous research reports. The cross-validations were made for event-based calibrated models between three similar watersheds, and calibrated models were validated in four years after the earthquake in one catchment.

The first critical conclusion is that the model is capable of predicting the occurrence of debris flow, magnitude and arrival time when the model parameters are spatially transferred. The internal model parameters can significantly affect the accuracy of the reproduced volume of debris flows. In general, the entrainment coefficient is the most effective parameter to affect the transferability of the model. Sometimes, these parameters can be more influential than the rainfall patterns. Besides, the performance of the model on the prediction of exact arrival time is problematic, which is closely related with the rainfall data. However, the calibrated model can predict the occurrence of debris flow correctly over time. In general, the model gives earlier warnings in the study sites when the modeled volume is the best. Earlier warnings are better than the exact prediction of arrival time so that more time is available for evacuation, and then the warning is effective. For the application of the physically-based model on early warning, the parameters should be carefully selected and calibrated when applying them to other catchments, and the calibrated arrival time should be earlier than the actual time. Furthermore, it can be considered that whether the actual arrival time of debris flow is earlier than the modeled time, especially when the antecedence rainfall may affect the occurrence of debris flow a lot, and predicted rainfall is used for early warning. Besides, regular updating of the input data should be made within a period (at least every four years). In contrast, the changes made by human activities should be considered for model simulation immediately.

For future research, it is recommended to focus first on the build-up of better debris flow inventories. The most problematic issue is that most areas will not have many debris flows, the data on past events might be incomplete to allow to test the performance of the model in the area. Currently, the inventory is not detailed enough to be employed as a validation tool to check how good the model can predict the debris flow events. And the transferability analysis might be affected by the scarcity of such an inventory. The creation of an inventory should rely on additional field observations and real-time monitoring, preferably using video cameras. The inventory should include as much information about the debris flows as possible, especially the information on the timing, discharge, and speed. After a better inventory has been created, firstly the calibrations for specific events and catchments should be done carefully, to analyze the spatial transferability of the model. Secondly, it is recommended to quantify the similarity of watersheds in the future to evaluate how relevant spatial transferability of parameters is for different watersheds that seem similar. Thirdly, it is advised to analyze which geo-factor is the most influential for spatial transferability. Fourthly, the calibrated model should be applied over time for a more extended period to check how the spatial transferability changes with time and how often the model can give warnings over time correctly. Additionally, the impacts of soil properties and rainfall patterns towards arrival time need to be further studied by more extensive modeling. These are helpful to improve the physically-based models on debris flow analysis and apply them to early warning widely.

This study also showed that the meteorological dataset in the Wenchuan area is not accurate enough to serve for debris flow early warning. It is therefore recommended to install some rain gauges close to the initiation area of the debris flows. Maintenance of these rain gauges is the main problem to ensure the reliable rainfall data is available for a long time. More equal the rainfall recordings to the true triggering rainfall, the more reliable the warning is. The available rainfall data may cause early or late warnings in the model. The accuracy of rainfall prediction and the use of these data as input for modeling are even more important for debris flow early warning. Hence, robust means of the meteorological forecast should be developed and applied for early warning. Besides, it is advised to apply automatic calibration instead of manual in future research to extract the best composition of calibrated parameters, which helps to decline the error to transferability analysis caused by the randomness of calibration.

If the model is planned to be used for early warning, it is suggested that extra soil samples and field measurements should be taken at least regionally. And a high-resolution DEM should be collected for this purpose. This data can be utilized to improve the model input, thus, to enhance the ability of the model on debris flow early warning. And it is necessary to make sensitivity analysis before applying any physically-based model to the early warning at any catchment as the sensitivity of parameters is model- and catchment-specific.

Overall, the physically-based model shows good applicability in space and over time in terms of occurrences and scales of debris flows in the earthquake-stricken area. However, the prediction of the exact volume is affected a lot by the calibrated parameters in space. And the effects of rainfall on the time simulation needs to be further studied, and such models should always be combined with observation-based early warning.

7. REFERENCE

Aleotti, P. (2004). A warning system for rainfall-induced shallow failures. *Engineering Geology*, *73*(3–4), 247–265. https://doi.org/10.1016/j.enggeo.2004.01.007

Alfieri, L., Salamon, P., Pappenberger, F., Wetterhall, F., & Thielen, J. (2012). Operational early warning systems for water-related hazards in Europe. *Environmental Science and Policy*, Vol. 21, pp. 35–49. https://doi.org/10.1016/j.envsci.2012.01.008

Arattano, M. (1999). On the use of seismic detectors as monitoring and warning systems for debris flows. *Natural Hazards*, *20*(2–3), 197–213. https://doi.org/10.1023/a:1008061916445

Arattano, Massimo, & Marchi, L. (2008). Systems and Sensors for Debris-flow Monitoring and Warning. *Sensors*, *8*(4), 2436–2452. https://doi.org/10.3390/s8042436

Arnone, E., Dialynas, Y. G., Noto, L. V., & Bras, R. L. (2016). Accounting for soil parameter uncertainty in a physically based and distributed approach for rainfall-triggered landslides. *Hydrological Processes*, *30*(6), 927–944. https://doi.org/10.1002/hyp.10609

Aston, A. R. (1979). Rainfall interception by eight small trees. *Journal of Hydrology*, *42*(3–4), 383–396. https://doi.org/10.1016/0022-1694(79)90057-X

Augusto, F. F. A. (2019). *Analysing Changing Multi- Hazard Risk To Flow-Like Phenomena for Urban Planning* (University Twente). Retrieved from https://library.itc.utwente.nl/papers_2019/msc/aes/FonsecaArevalo.pdf

Beguería, S., W. J. Van Asch, T., Malet, J. P., & Gröndahl, S. (2009). A GIS-based numerical model for simulating the kinematics of mud and debris flows over complex terrain. *Natural Hazards and Earth System Science*, *9*(6), 1897–1909. https://doi.org/10.5194/nhess-9-1897-2009

Benjamin, J., Rosser, N. J., Dunning, S. A., Hardy, R. J., Kelfoun, K., & Szczuciński, W. (2018). Transferability of a calibrated numerical model of rock avalanche run-out: Application to 20 rock avalanches on the Nuussuaq Peninsula, West Greenland. *Earth Surface Processes and Landforms*, *43*(15), 3057–3073. https://doi.org/10.1002/esp.4469

Bogaard, T., & Greco, R. (2018). Invited perspectives: Hydrological perspectives on precipitation intensity-duration thresholds for landslide initiation: Proposing hydro-meteorological thresholds. *Natural Hazards and Earth System Sciences*, *18*(1), 31–39. https://doi.org/10.5194/nhess-18-31-2018

Bout, B., Lombardo, L., van Westen, C. J., & Jetten, V. G. (2018a). Integration of two-phase solid fluid equations in a catchment model for flashfloods, debris flows and shallow slope failures. *Environmental Modelling and Software*, *105*, 1–16. https://doi.org/10.1016/j.envsoft.2018.03.017

Bout, Bastian, Tang, C., Westen, C., & Jetten, V. (2018b). Simulating multi-stage landslide dam breach flooding in a multi-hazard model. *Geophysical Research Abstracts*, *20*, 9252.

Bout, Bastian, Tang, C., Westen, C., Jetten, V., & Tang, C. (n.d.). *Physically-based Spatial Modelling of Cascading Landslide Hazards*.

Caine, N. (1980). The Rainfall Intensity - Duration Control of Shallow Landslides and Debris Flows. *Geografiska Annaler: Series A, Physical Geography*, *62*(1–2), 23–27. https://doi.org/10.1080/04353676.1980.11879996

Capparelli, G., & Versace, P. (2011). FLaIR and SUSHI: Two mathematical models for early warning of landslides induced by rainfall. *Landslides*, *8*(1), 67–79. https://doi.org/10.1007/s10346-010-0228-6

Chae, B. G., Park, H. J., Catani, F., Simoni, A., & Berti, M. (2017). Landslide prediction, monitoring and early warning: a concise review of state-of-the-art. *Geosciences Journal*, *21*(6), 1033–1070. https://doi.org/10.1007/s12303-017-0034-4

Chen, J., Liang, C., & Chen, L. (2011). Parameter sensitivity analysis of SWAT model—Case study of small watersheds with differentland cover types in Hailuogou Valley (in Chinese). *South-to-North Water Diversion and Water Science & Technology*, *9*(2), 41.

Chen, H. X., & Zhang, L. M. (2015). EDDA 1.0: Integrated simulation of debris flow erosion, deposition and property changes. *Geoscientific Model Development*, *8*(3), 829–844. https://doi.org/10.5194/gmd-8-829-2015

Cho, C. Y., Chou, P. H., Chung, Y. C., King, C. T., Tsai, M. J., Lee, B. J., & Chou, T. Y. (2008). Wireless sensor networks for debris flow observation. *2008 5th Annual IEEE Communications Society Conference on Sensor, Mesh and Ad Hoc Communications and Networks, SECON*, 615–617. https://doi.org/10.1109/SAHCN.2008.88

Christen, B., Robles, V., Raya, M., Paramonov, I., & Belmonte, J. (2010). Regeneration and reprogramming compared. *BMC Biology*, *8*(1), 5. https://doi.org/10.1186/1741-7007-8-5

Christen, M., Bühler, Y., Bartelt, P., Leine, R., Glover, J., Schweizer, A., … Feistl, T. (2012). Integral Hazard Management Using a Unified Software Environment Numerical Simulation Tool "RAMMS." *Congress Interpraevent*, 77–86.

Cornelis;, W. M., & D. Gabriels. (2003). The effect of surface moisture on the entrainment of dune sandby wind: an evaluation of selected models. *Sedimentology*, *50*(4), 771. https://doi.org/10.1046/j.1365-3091.2003.00577.x

Cui, P., Chen, X. Q., Zhu, Y. Y., Su, F. H., Wei, F. Q., Han, Y. S., Zhuang, J. Q. (2011). The Wenchuan Earthquake (May 12, 2008), Sichuan Province, China, and resulting geohazards. *Natural Hazards*, *56*(1), 19–36. https://doi.org/10.1007/s11069-009-9392-1

De Roo, A. P. J. (1996). THE LISEM PROJECT: AN INTRODUCTION. *Hydrological Processes*, *10*(8), 1021–1025. https://doi.org/10.1002/(SICI)1099-1085(199608)10:8<1021::AID-HYP407>3.0.CO;2-I

Domènech, G., Fan, X., Scaringi, G., van Asch, T. W. J., Xu, Q., Huang, R., & Hales, T. C. (2019). Modelling the role of material depletion, grain coarsening and revegetation in debris flow occurrences after the 2008 Wenchuan earthquake. *Engineering Geology*, *250*, 34–44. https://doi.org/10.1016/J.ENGGEO.2019.01.010

Fan, X., Domènech, G., Scaringi, G., Huang, R., Xu, Q., Hales, T. C., … Francis, O. (2018). Spatio-temporal evolution of mass wasting after the 2008 M w 7.9 Wenchuan earthquake revealed by a detailed multi-temporal inventory. *Landslides*, *15*(12), 2325–2341. https://doi.org/10.1007/s10346-018-1054-5

Fan, X., Juang, C. H., Wasowski, J., Huang, R., Xu, Q., Scaringi, G., Havenith, H. B. (2018). What we have learned from the 2008 Wenchuan Earthquake and its aftermath: A decade of research and challenges. *Engineering Geology*, *241*, 25–32. https://doi.org/10.1016/j.enggeo.2018.05.004

Fan, X., Scaringi, G., Domènech, G., Yang, F., Guo, X., Dai, L., Huang, R. (2019). Two multi-temporal datasets that track the enhanced landsliding after the 2008 Wenchuan earthquake. *Earth System Science Data*, *11*(1), 35–55. https://doi.org/10.5194/essd-11-35-2019

Franzi, L., & Bianco, G. (2001). A statistical method to predict debris flow deposited volumes on a debris fan. *Physics and Chemistry of the Earth, Part C: Solar, Terrestrial and Planetary Science*, *26*(9), 683–688. https://doi.org/10.1016/S1464-1917(01)00067-8

Glade, T., Crozier, M., & Smith, P. (2000). Applying probability determination to refine landslide-triggering rainfall thresholds using an empirical "Antecedent Daily Rainfall Model." *Pure and Applied Geophysics*, *157*(6–8), 1059–1079. https://doi.org/10.1007/s000240050017

Godt, J. W., Baum, R. L., & Chleborad, A. F. (2006). Rainfall characteristics for shallow landsliding in Seattle, Washington, USA. *Earth Surface Processes and Landforms*, *31*(1), 97–110. https://doi.org/10.1002/esp.1237

Guimarães, R. F., Montgomery, D. R., Greenberg, H. M., Fernandes, N. F., Trancoso Gomes, R. A., & de Carvalho, O. A. (2003). Parameterization of soil properties for a model of topographic controls on shallow landsliding: application to Rio de Janeiro. *Engineering Geology*, *69*(1–2), 99–108. https://doi.org/10.1016/S0013-7952(02)00263-6

Guo, Xiao-jun, Cui, P., & Li, Y. (2013). Debris flow warning threshold based on antecedent rainfall: A case study in Jiangjia Ravine, Yunnan, China. *Journal of Mountain Science*, *10*(2), 305–314. https://doi.org/10.1007/s11629-013-2521-z

Guo, Xiaojun, Cui, P., Li, Y., Fan, J., Yan, Y., & Ge, Y. (2016). Temporal differentiation of rainfall thresholds for debris flows in Wenchuan earthquake-affected areas. *Environmental Earth Sciences*, *75*(2), 1–12. https://doi.org/10.1007/s12665-015-5031-1

Guo, Xiaojun, Cui, P., Li, Y., Ma, L., Ge, Y., & Mahoney, W. B. (2016a). Intensity-duration threshold of rainfall-triggered debris flows in the Wenchuan Earthquake affected area, China. *Geomorphology*, *253*, 208–216. https://doi.org/10.1016/j.geomorph.2015.10.009

Guo, Xiaojun, Cui, P., Li, Y., Ma, L., Ge, Y., & Mahoney, W. B. (2016b). Intensity–duration threshold of rainfall-triggered debris flows in the Wenchuan Earthquake affected area, China. *Geomorphology*, *253*, 208–216. https://doi.org/10.1016/j.geomorph.2015.10.009

Guzzetti, F., Peruccacci, S., Rossi, M., & Stark, C. P. (2007). Rainfall thresholds for the initiation of landslides in central and southern Europe. *Meteorology and Atmospheric Physics*, *98*(3–4), 239–267. https://doi.org/10.1007/s00703-007-0262-7

Guzzetti, Fausto, Peruccacci, S., Rossi, M., & Stark, C. P. (2008). The rainfall intensity-duration control of shallow landslides and debris flows: An update. *Landslides*, *5*(1), 3–17. https://doi.org/10.1007/s10346-007-0112-1

Hales, T. C. (2018). Modelling biome-scale root reinforcement and slope stability. *Earth Surface Processes and Landforms*, *43*(10), 2157–2166. https://doi.org/10.1002/esp.4381

Han, Z., Chen, G., Li, Y., Zhang, H., & He, Y. (2016). Elementary analysis on the bed-sediment entrainment by debris flow and its application using the TopFlowDF model. *Geomatics, Natural Hazards and Risk*, *7*(2), 764–785. https://doi.org/10.1080/19475705.2014.966868

He, D., Wang, E., Wang, J., & Robertson, M. J. (2017). Data requirement for effective calibration of process-based crop models. *Agricultural and Forest Meteorology*, *234–235*, 136–148. https://doi.org/10.1016/j.agrformet.2016.12.015

Heckmann, T., & Becht, M. (2009). Investigating the transferability of statistical disposition models for slope-type debris flows. *Erdkunde*, *63*(1), 19–33. https://doi.org/10.3112/erdkunde.2009.01.02

Hessel, R., Jetten, V., Liu Baoyuan, Zhang Yan & Stolte, J. (2002). *LISEM CALIBRATION AND VALIDATION Partly* (Vol. 9).

Hessel, R., Jetten, V., Baoyuan, L., Yan, Z., & Stolte, J. (2003). Calibration of the LISEM model for a small Loess Plateau catchment. *Catena*, *54*(1–2), 235–254. https://doi.org/10.1016/S0341-8162(03)00067-5

Hong, Y., & Adler, R. F. (2007). Towards an early-warning system for global landslides triggered by rainfall and earthquake. *International Journal of Remote Sensing*, *28*(16), 3713–3719. https://doi.org/10.1080/01431160701311242

Hsu, Y.-C., Chang, Y.-L., Chang, C.-H., Yang, J.-C., & Tung, Y.-K. (2018). Physical-based rainfall-triggered shallow landslide forecasting. *Smart Water*, *3*(1). https://doi.org/10.1186/s40713-018-0011-8

Hu, W., Scaringi, G., Xu, Q., Pei, Z., Van Asch, T. W. J., & Hicher, P. Y. (2017). Sensitivity of the initiation and runout of flowslides in loose granular deposits to the content of small particles: An insight from flume tests. *Engineering Geology*, *231*, 34–44. https://doi.org/10.1016/j.enggeo.2017.10.001

Huang, J., Wen, J., Wang, B., & Hinokidani, O. (2020). Parameter sensitivity analysis for a physically based distributed hydrological model based on Morris' screening method. *Journal of Flood Risk Management*, *13*(1). https://doi.org/10.1111/jfr3.12589

Huang, R., & Fan, X. (2013). The landslide story. *Nature Geoscience*, *6*(5), 325–326. https://doi.org/10.1038/ngeo1806

ISDR. (2004). *Terminology Basic Terms of Disaster Risk Reduction.* Retrieved from http://www.unisdr.org/eng/library/lib-terminology- eng home.htm.

Itakura, Y., Inaba, H., & Sawada, T. (2005). A debris-flow monitoring devices and methods bibliography. *Natural Hazards and Earth System Science*, *5*(6), 971–977. https://doi.org/10.5194/nhess-5-971-2005

Itakura, Yasumasa, Fujii, N., & Sawada, T. (2000). Basic characteristics of ground vibration sensors for the detection of debris flow. *Physics and Chemistry of the Earth, Part B: Hydrology, Oceans and Atmosphere*, *25*(9), 717–720. https://doi.org/10.1016/S1464-1909(00)00091-5

Iverson, R. M. (2000). Landslide triggering by rain infiltration. *Water Resources Research*, *36*(7), 1897–1910. https://doi.org/10.1029/2000WR900090

Iverson, R. M., Reid, M. E., Logan, M., LaHusen, R. G., Godt, J. W., & Griswold, J. P. (2011). Positive feedback and momentum growth during debris-flow entrainment of wet bed sediment. *Nature Geoscience*, *4*(2), 116–121. https://doi.org/10.1038/ngeo1040

Jin, Y. Q., & Xu, F. (2011). Monitoring and early warning the debris flow and landslides using VHF radar pulse echoes from layering land media. *IEEE Geoscience and Remote Sensing Letters*, *8*(3), 575–579. https://doi.org/10.1109/LGRS.2010.2093598

Kamphorst, E. C., Jetten, V., Guérif, J., Pitk a ¨ nen, J., Iversen, B. V., Douglas, J. T., & Paz, A. (2000). Predicting Depressional Storage from Soil Surface Roughness. *Soil Science Society of America Journal*, *64*(5), 1749–1758. https://doi.org/10.2136/sssaj2000.6451749x

Keeefr, D. K., WILSON, R. C., MARK, R. K., BRABB, E. E., BROWN, W. M., ELLEN, S. D., … ZATKIN, R. S. (1987). Real-Time Landslide Warning During Heavy Rainfall. *Science*, *238*(4829), 921–925. https://doi.org/10.1126/science.238.4829.921

Keisuke SAITO, Susumu OGAWA, M. A. and K. O. (2001). Estimates of lai for forest management in okutama. *Area*, (November), 5–9. Retrieved from https://crisp.nus.edu.sg/~acrs2001/pdf/155SAITO.PDF

Kuriakose, S. L., van Beek, L. P. H., & van Westen, C. J. (2009). Parameterizing a physically based shallow landslide model in a data poor region. *Earth Surface Processes and Landforms*. https://doi.org/10.1002/esp.1794

LaHusen, R. (2005). Debris-flow instrumentation. In *Debris-flow Hazards and Related Phenomena* (pp. 291–304). https://doi.org/10.1007/3-540-27129-5_12

Li, Z., Jiao, Q., Liu, L., Tang, H., & Liu, T. (2014). Monitoring Geologic Hazards and Vegetation Recovery in the Wenchuan Earthquake Region Using Aerial Photography. *ISPRS International Journal of Geo-Information*, *3*(1), 368–390. https://doi.org/10.3390/ijgi3010368

Lu, T., Zeng, H., Luo, Y., Wang, Q., Shi, F., Sun, G., … Wu, N. (2012). Monitoring vegetation recovery after China's May 2008 Wenchuan earthquake using Landsat TM time-series data: A case study in Mao County. *Ecological Research*, *27*(5), 955–966. https://doi.org/10.1007/s11284-012-0976-y

Ma, Y., & Li, C. (2017). Research on the Debris Flow Hazards after the Wenchuan Earthquake in Bayi Gully, Longchi, Dujiangyan, Sichuan Province, China. *Proceedings of the 2017 International Conference on Advanced Materials Science and Civil Engineering (AMSCE 2017)*. https://doi.org/10.2991/amsce-17.2017.36

Ma, Y., Yu, B., Wu, Y., Zhang, J., & Qi, X. (2011). Research on the Disaster of Debris Flow of Bayi Gully，Longchi，Dujiangyan，Sichuan on August 13， 2010 (in chinese). *JOURNAL OF SICHUAN UNIVERSITY*, *43*. https://doi.org/10.15961/j.jsuese.2011.s1.005

MacDougall, A. H., & Flowers, G. E. (2011). Spatial and temporal transferability of a distributed energy-balance glacier melt model. *Journal of Climate*, *24*(5), 1480–1498. https://doi.org/10.1175/2010JCLI3821.1

Marra, F., Destro, E., Nikolopoulos, E. I., Zoccatelli, D., Creutin, J. D., Guzzetti, F., & Borga, M. (2017). Impact of rainfall spatial aggregation on the identification of debris flow occurrence thresholds. *Hydrology and Earth System Sciences*, *21*(9), 4525–4532. https://doi.org/10.5194/hess-21-4525-2017

Mathew, J., Babu, D. G., Kundu, S., Kumar, K. V., & Pant, C. C. (2014). Integrating intensity-duration-based rainfall threshold and antecedent rainfall-based probability estimate towards generating early warning for rainfall-induced landslides in parts of the Garhwal Himalaya, India. *Landslides*, *11*(4), 575–588. https://doi.org/10.1007/s10346-013-0408-2

Medina, V., Hürlimann, M., & Bateman, A. (2008). Application of FLATModel, a 2D finite volume code, to debris flows in the northeastern part of the Iberian Peninsula. *Landslides*, *5*(1), 127–142. https://doi.org/10.1007/s10346-007-0102-3

Melchiorre, C., & Frattini, P. (2012). Modelling probability of rainfall-induced shallow landslides in a changing climate, Otta, Central Norway. *Climatic Change*, *113*(2), 413–436. https://doi.org/10.1007/s10584-011-0325-0

Mergili, M., Fellin, W., Moreiras, S. M., & Stötter, J. (2012). Simulation of debris flows in the Central Andes based on Open Source GIS: Possibilities, limitations, and parameter sensitivity. *Natural Hazards*, *61*(3), 1051–1081. https://doi.org/10.1007/s11069-011-9965-7

Mergili, M., Fischer, J.-T., Krenn, J., & Pudasaini, S. P. (2017). r.avaflow v1, an advanced open-source computational framework for the propagation and interaction of two-phase mass flows. *Geoscientific Model Development*, *10*(2), 553–569. https://doi.org/10.5194/gmd-10-553-2017

Ming, C. (2014). *Quantitative Risk Assessment of Debris Flow in Coseismic Area Based on Remote Sensing and Numerical Simulation* (in chinese) (Doctoral dissertation) (Chengdu University of Technology). Retrieved from https://doi.org/CNKI:CDMD:1.1015.530054

Mroczkowski, M., Raper, G. P., & Kuczera, G. (1997). The quest for more powerful validation of conceptual catchment models. *Water Resources Research*, *33*(10), 2325–2335. https://doi.org/10.1029/97WR01922

Naidu, S., Sajinkumar, K. S., Oommen, T., Anuja, V. J., Samuel, R. A., & Muraleedharan, C. (2018). Early warning system for shallow landslides using rainfall threshold and slope stability analysis. *Geoscience Frontiers*, *9*(6), 1871–1882. https://doi.org/10.1016/j.gsf.2017.10.008

O'Brien, J. S., Julien, P. Y., & Fullerton, W. T. (1993). Two-Dimensional Water Flood and Mudflow Simulation. *Journal of Hydraulic Engineering*, *119*(2), 244–261. https://doi.org/10.1061/(ASCE)0733-9429(1993)119:2(244)

Pan, H., Huang, J., Wang, R., & Ou, G. (2013). Rainfall threshold calculation method for debris flow pre-warning in data-poor areas. *Journal of Earth Science*, *24*(5), 854–862. https://doi.org/10.1007/s12583-

013-0377-3
Pan, H. L., Jiang, Y. J., Wang, J., & Ou, G. Q. (2018). Rainfall threshold calculation for debris flow early warning in areas with scarcity of data. *Natural Hazards and Earth System Sciences*, *18*(5), 1395–1409. https://doi.org/10.5194/nhess-18-1395-2018
Pudasaini, S. P. (2012). A general two-phase debris flow model. *Journal of Geophysical Research: Earth Surface*, *117*(F3), n/a-n/a. https://doi.org/10.1029/2011JF002186
Raia, S., Alvioli, M., Rossi, M., Baum, R. L., Godt, J. W., & Guzzetti, F. (2014). Improving predictive power of physically based rainfall-induced shallow landslide models: A probabilistic approach. *Geoscientific Model Development*, *7*(2), 495–514. https://doi.org/10.5194/gmd-7-495-2014
Rianna, G., Pagano, L., & Urciuoli, G. (2014). Rainfall patterns triggering shallow flowslides in pyroclastic soils. *Engineering Geology*, *174*, 22–35. https://doi.org/10.1016/j.enggeo.2014.03.004
Salciarini, D., Brocca, L., Camici, S., Ciabatta, L., Volpe, E., Massini, R., & Tamagnini, C. (2019). Physically based approach for rainfall-induced landslide projections in a changing climate. *Proceedings of the Institution of Civil Engineers - Geotechnical Engineering*, *172*(6), 481–495. https://doi.org/10.1680/jgeen.18.00216
Salvatici, T., Tofani, V., Rossi, G., D'Ambrosio, M., Tacconi Stefanelli, C., Benedetta Masi, E., … Casagli, N. (2018). Application of a physically based model to forecast shallow landslides at a regional scale. *Natural Hazards and Earth System Sciences*, *18*(7), 1919–1935. https://doi.org/10.5194/nhess-18-1919-2018
Saulnier, G. M., Beven, K., & Obled, C. (1997). Including spatially variable effective soil depths in TOPMODEL. *Journal of Hydrology*, *202*(1–4), 158–172. https://doi.org/10.1016/S0022-1694(97)00059-0
Schilirò, L., Montrasio, L., & Scarascia Mugnozza, G. (2016). Prediction of shallow landslide occurrence: Validation of a physically-based approach through a real case study. *Science of The Total Environment*, *569–570*, 134–144. https://doi.org/10.1016/j.scitotenv.2016.06.124
Schimmel, A., & Hübl, J. (2015). Approach for an Early Warning System for Debris Flow Based on Acoustic Signals. In *Engineering Geology for Society and Territory - Volume 3* (Vol. 3, pp. 55–58). https://doi.org/10.1007/978-3-319-09054-2_11
Schürch, P., Densmore, A. L., Rosser, N. J., Lim, M., & Mcardell, B. W. (2011). Detection of surface change in complex topography using terrestrial laser scanning: Application to the Illgraben debris-flow channel. *Earth Surface Processes and Landforms*, *36*(14), 1847–1859. https://doi.org/10.1002/esp.2206
Segoni, S., Piciullo, L., & Gariano, S. L. (2018). A review of the recent literature on rainfall thresholds for landslide occurrence. *Landslides*, *15*(8), 1483–1501. https://doi.org/10.1007/s10346-018-0966-4
Sekhar, L., Westen, C.J., Lakhera, R.C., Beek, L.V., Sankar, G., Alkema, D., Asch, T.V., & Jayadev, S. K. (2006). Effect of vegetation on debris flow initiation : conceptualization and parameterization of a dynamic model for debris flow initiation in Tikovil river basin, Kerala, India, using PCRaster. *Geography*, 2–7. Retrieved from https://scholarsarchive.byu.edu/cgi/viewcontent.cgi?article=1134&context=iemssconference
Shen, P., Zhang, L. M., Chen, H. X., & Gao, L. (2017). Role of vegetation restoration in mitigating hillslope erosion and debris flows. *Engineering Geology*, *216*, 122–133. https://doi.org/10.1016/j.enggeo.2016.11.019
Shen, Ping, Zhang, L., Chen, H., & Fan, R. (2018). EDDA 2.0: integrated simulation of debris flow initiation and dynamics considering two initiation mechanisms. *Geoscientific Model Development*, *11*(7), 2841–2856. https://doi.org/10.5194/gmd-11-2841-2018
Shieh, C. L., Chen, Y. S., Tsai, Y. J., & Wu, J. H. (2009). Variability in rainfall threshold for debris flow after the Chi-Chi earthquake in central Taiwan, China. *International Journal of Sediment Research*, *24*(2), 177–188. https://doi.org/10.1016/S1001-6279(09)60025-1
Shrestha, S., Bastola, S., Babel, M. S., Dulal, K. N., Magome, J., Hapuarachchi, H. A. P., … Takeuchi, K. (2007). The assessment of spatial and temporal transferability of a physically based distributed hydrological model parameters in different physiographic regions of Nepal. *Journal of Hydrology*, *347*(1–2), 153–172. https://doi.org/10.1016/j.jhydrol.2007.09.016
Takahashi, T., Nakagawa, H., Harada, T., & Yamashiki, Y. (1992). Routing Debris Flows with Particle Segregation. *Journal of Hydraulic Engineering*, *118*(11), 1490–1507. https://doi.org/10.1061/(ASCE)0733-9429(1992)118:11(1490)
Tang, Chenxiao. (2019). *Monitoring landslide risk dynamics after a major earthquake in a mountainous environment* (Dotoral dissertation) (ITC Printing Department). https://doi.org/10.3990/1.9789036547925

Tang, Chenxiao, Tanyas, H., van Westen, C. J., Tang, C., Fan, X., & Jetten, V. G. (2019). Analysing post-earthquake mass movement volume dynamics with multi-source DEMs. *Engineering Geology*, *248*, 89–101. https://doi.org/10.1016/J.ENGGEO.2018.11.010

Tang, Chenxiao, Van Westen, C. J., Tanyas, H., & Jetten, V. G. (2016). Analysing post-earthquake landslide activity using multi-temporal landslide inventories near the epicentral area of the 2008 Wenchuan earthquake. *Natural Hazards and Earth System Sciences*, *16*(12), 2641–2655. https://doi.org/10.5194/nhess-16-2641-2016

Tang, Chuan, Zhu, J., Ding, J., Cui, X. F., Chen, L., & Zhang, J. S. (2011). Catastrophic debris flows triggered by a 14 August 2010 rainfall at the epicenter of the Wenchuan earthquake. *Landslides*, *8*(4), 485–497. https://doi.org/10.1007/s10346-011-0269-5

Tofani, V., Bicocchi, G., Rossi, G., Segoni, S., D'Ambrosio, M., Casagli, N., & Catani, F. (2017). Soil characterization for shallow landslides modeling: a case study in the Northern Apennines (Central Italy). *Landslides*, *14*(2), 755–770. https://doi.org/10.1007/s10346-017-0809-8

UNDRR. (2019). *Global assessment report on disater risk reduction*. Retrieved from https://gar.undrr.org/sites/default/files/chapter/2019-05/Chapter_3.pdf

van Westen, C. J. (2004). Geo-Information tools for landslide risk assessment: an overview of recent developments. In A. S. F. S. W. Lacerda, M. Erlich, S.A.B. Fontoura (Ed.), *Landslides : evaluation and stabilization - glissement de terrain: Evaluation et Stabilisation : proceedings of the 9th international symposium on landslides* (pp. 39–56). https://doi.org/10.1201/b16816-6

Wieczorek, G. F., & Glade, T. (2005). Climatic factors influencing occurrence of debris flows. In *Debris-flow Hazards and Related Phenomena* (pp. 325–362). https://doi.org/10.1007/3-540-27129-5_14

Wu, Y.-H., Liu, K.-F., & Chen, Y.-C. (2013). Comparison between FLO-2D and Debris-2D on the application of assessment of granular debris flow hazards with case study. *Journal of Mountain Science*, *10*(2), 293–304. https://doi.org/10.1007/s11629-013-2511-1

Xu, C., Xu, X., Yao, X., & Dai, F. (2014). Three (nearly) complete inventories of landslides triggered by the May 12, 2008 Wenchuan Mw 7.9 earthquake of China and their spatial distribution statistical analysis. *Landslides*, *11*(3), 441–461. https://doi.org/10.1007/s10346-013-0404-6

Xu, Q., Zhang, S., Li, W. L., & Van Asch, T. W. J. (2012). The 13 August 2010 catastrophic debris flows after the 2008 Wenchuan earthquake, China. *Natural Hazards and Earth System Science*, *12*(1), 201–216. https://doi.org/10.5194/nhess-12-201-2012

Yang, F., He, C., Huang, R., Domènech, G., Xu, Q., Dai, L., … Scaringi, G. (2019). Two multi-temporal datasets that track the enhanced landsliding after the 2008 Wenchuan earthquake. *Earth System Science Data*, *11*(1), 35–55. https://doi.org/10.5194/essd-11-35-2019

Yinping, N., & Xiuzhen, L. (2019). Hazard assessment of Bayi Gully debris flow based on Flow-R model. *Journal of Natural Disasters*, *28*(1), 157. https://doi.org/CNKI:SUN:ZRZH.0.2019-01-019

Young, P. C., McCabe, A. P., & Chotai, A. (2002). STATE-DEPENDENT PARAMETER NONLINEAR SYSTEMS: IDENTIFICATION, ESTIMATION AND CONTROL. *IFAC Proceedings Volumes*, *35*(1), 441–446. https://doi.org/10.3182/20020721-6-ES-1901.00235

Zhang, S., & Zhang, L. M. (2017). Impact of the 2008 Wenchuan earthquake in China on subsequent long-term debris flow activities in the epicentral area. *Geomorphology*, *276*, 86–103. https://doi.org/10.1016/j.geomorph.2016.10.009

Zhang, S, & Zhang, L. M. (2017). Impact of the 2008 Wenchuan earthquake in China on subsequent long-term debris flow activities in the epicentral area. *Geomorphology*, *276*(276), 86–103. https://doi.org/10.1016/j.geomorph.2016.10.009

Zhang, Shaojie, Yang, H., Wei, F., Jiang, Y., & Liu, D. (2014). A model of debris flow forecast based on the water-soil coupling mechanism. *Journal of Earth Science*, *25*(4), 757–763. https://doi.org/10.1007/s12583-014-0463-1

Zhang, Shucheng. (1993). A Comprehensive Approach to the Observation and Prevention of Debris Flows in China. *Natural Hazards*, *7*(1), 1–23. https://doi.org/10.1007/BF00595676

Zhang Ziguang, Zhang Zhiming, Z. S. (2010). Formation conditions and dynamics features of the debris flow in Bayi Gully in Dujiangyan County. *The Chinese Journal of Geological Hazard and Control*, *21*, 642. https://doi.org/10.16031/j.cnki.issn.1003-8035.2010.01.022

Zhou, J., Wang, Y., & Liu, Y. (2004). a Review of an Early-Warning Technique of Flash Flood and Debris. *ISCO 2004 - 13th International Soil Conservation Organisation Conference – Brisbane, July 2004*, (340), 1–5. Retrieved from https://www.tucson.ars.ag.gov/isco/isco13/PAPERS F-L/JINXING.pdf

Zhou, W., Tang, C., Van Asch, T. W. J., & Zhou, C. (2014). Rainfall-triggering response patterns of post-seismic debris flows in the Wenchuan earthquake area. *Natural Hazards*, *70*(2), 1417–1435.

https://doi.org/10.1007/s11069-013-0883-8
Zieher, T., Rutzinger, M., Schneider-Muntau, B., Perzl, F., Leidinger, D., Formayer, H., & Geitner, C. (2017). Sensitivity analysis and calibration of a dynamic physically based slope stability model. *Natural Hazards and Earth System Sciences*, *17*(6), 971–992. https://doi.org/10.5194/nhess-17-971-2017